# GENETICS AND ENVIRONMENTAL FACTORS SHAPING CANNABIS PHENOTYPES: A STUDY ON TEMPERATURE EFFECTS AND GENETIC REGULATION OF ANTHOCYANIN ACCUMULATION IN *CANNABIS SATIVA*

Sean Kim

A thesis submitted in partial fulfillment of

the requirements for the degree of

Master of Science

(Plant Breeding and Plant Genetics)

At the

UNIVERSITY OF WISCONSIN-MADISON

2024

Committee members:

Dr. Shelby Ellison, Assistant Professor, Horticulture

Dr. Irwin Goldman, Professor, Horticulture

Dr. Hiroshi Maeda, Professor, Botany

## DEDICATION

It is with profound gratitude that I dedicate this thesis to Cannabis. Cannabis, you have been more than just a plant in my life; you have been a source of inspiration, healing, and profound transformation. Thanks to you, I've had the privilege of meeting many remarkable individuals with diverse backgrounds and experiences. These connections, through a shared appreciation of Cannabis, have enriched my life and broadened my perspectives in profound ways. Your therapeutic properties have brought solace and relief to those in need, including myself, fostering a deeper appreciation for the complexities of nature's remedies. You have shaped my academic endeavors and ignited a passion within me to pursue a career in this field in hopes of sharing your gifts with the world. May this work stand as a testament to the significance and potential of Cannabis in scientific inquiry and societal well-being.

## ACKNOWLEDGMENTS

I want to start by thanking Dr. Brian Barringer for all the support, encouragement, and experiences we shared while learning about cannabis during the last two years of my undergraduate degree. Brian helped build my confidence in academia and made me feel like my research was worthwhile. Brian helped refine my research techniques and guided me towards success during my time at UW-Stevens Point and beyond. The connections and opportunities I have gained from our relationship have been invaluable and lifechanging. Brian has become an excellent mentor to look up to and I'm grateful we had the opportunity to meet.

I am very grateful to Dr. Robert Michitsch for his guidance and mentorship during my academic journey at UW-Stevens Point. Although not a member of my thesis committee, Dr. Michitsch played a pivotal role in shaping my understanding of soil science and guiding me through my undergrad project. His open-door policy and willingness to collaborate fostered an environment of learning and growth. I feel fortunate to have had the opportunity to work alongside Dr. Michitsch, and I am sincerely appreciative of his support and expertise.

I would like to thank my advisor Dr. Shelby Ellison who has been supporting me throughout this journey. I was fortunate to work with Shelby for a semester out in the field before I got started with my master's degree. Working in a cannabis field has always been a dream of mine and it became a reality thanks to Shelby. Learning how to build a cannabis program from the ground up has been an extremely useful experience that I will take with me moving forward in my career. Shelby has been a great advisor who provided me with a stress-free work environment. I have enjoyed my time here at UW-Madison learning about cannabis alongside Shelby. I'd like to give a special thanks to her for giving me this opportunity!

I would like to extend my sincere appreciation to Dr. Hiroshi Maeda for his valuable assistance in understanding anthocyanin quantification methods. Dr. Maeda's expertise and guidance were instrumental in navigating experimental protocols and making informed decisions regarding methodological approaches. His support significantly enhanced the quality and accuracy of this research.

I would like to express my sincere appreciation to Dr. Irwin Goldman for his all-important contributions to my thesis. Dr. Goldman's expertise in plant breeding and genetics provided valuable insights that significantly enhanced the quality my research. With Dr. Goldman's seasoned guidance on my committee, I felt assured that my project was on the correct path. I have been lucky to have him on my committee.

I extend my deepest gratitude to Professor Al Kovaleski whose unwavering support and guidance have been instrumental in the success of one of my projects. Dr. Kovaleski generously provided me access to growth chambers, enabling me to conduct experiments central to my research. His expertise and assistance with data analysis were important in ensuring the accuracy and integrity of my findings. Beyond logistical support, Dr. Kovaleski served as an exceptional mentor, offering valuable insights that significantly enhanced my understanding of certain topics. I am immensely thankful for his wisdom and encouragement, which have undoubtedly played a pivotal role in my academic journey. I would also like to thank Francisco Campos Arguedas for showing me how to operate the growth chambers for my experiments and providing me assistance when needed. I am sincerely grateful for your help.

I am immensely grateful to Phillip Alberti, our dedicated lab manager, who has significantly enhanced my academic experience. Phil's unwavering commitment to ensuring the smooth operation of our laboratory has been invaluable. His proactive approach to problem-solving and continuous efforts to streamline our workflow have greatly facilitated my research endeavors. Phil's supportive demeanor and willingness to offer assistance whenever needed have made him an indispensable member of the team. I am deeply appreciative of Phil's contributions, which have undoubtedly contributed to the success of our lab and enriched my overall experience.

I extend my sincere gratitude to members of Philipp Simon’s Lab, particularly Erin Lalor and Michael Paulsmeyer, for assisting in our attempt to identify the specific anthocyanins in our samples using HPLC. Michael played a crucial role by providing the protocol for quantifying total monomeric anthocyanins in our samples and guiding us toward developing our own protocol. Erin's expertise and support were instrumental in running samples on HPLC, providing insights into the compounds present in our samples. I want to thank Philipp Simons Lab for providing the necessary instruments and resources to conduct these analyses. Their collective efforts have significantly contributed to the progress and success of my research endeavors.

I would like to extend my appreciation to my fellow grad students, Autumn Brown, Grace Connelly, Carter Prillaman, Jillian Abendroth, and Rebecca Olivia Arias. Your support, camaraderie, and collaborative spirit have made my journey through this master's program truly memorable and rewarding. I am grateful for the opportunity to have worked alongside such talented individuals.

I would like to extend a thank you to my fellow lab members, Robert Witherell, Ademola Aina, Pawan Basnet (especially for assistance with data analysis), Derrick Grunwald, and Eliot Stanton. Working alongside these individuals has been a great experience, as they consistently offered support and guidance whenever needed. Their collaborative spirit and willingness to provide feedback on presentations and research have greatly contributed to my growth and success in the lab. I am immensely thankful for their dedication, expertise, and support.

Thank you to the dedicated undergraduates who provided assistance throughout my academic journey: Azura Jorda, Tylor Savage, Logan Gartman, Cheyanne Mattie, Chloe Zimmer, Mataya Duncan, Maria Soutor, Renee Watson, Sydney Stroschein, Bella Firnstahl, Dylan Mahant, Miguel Mares, and Kairo Pullum. Their support and dedication have been instrumental in the progress of my research endeavors.

Lastly, I want to thank both of my parents for supporting me my whole life. I have changed directions a lot in life, and my parents have been in my corner the entire time. I never thought that my parents would support my change in career paths with expirations to grow cannabis. Thank both of you for all the love.

## ABSTRACT

Purple pigments found in the inflorescence of cannabis plants are a desired trait in the cannabis flower industry, contributing to market appeal, cultivar differentiation, and potentially providing added therapeutic and health benefits to consumers. Anthocyanins, the compounds responsible for purple pigments in *C. sativa*, provide plants with protection against various environmental stressors. The mechanisms underlying this trait in *C. sativa* are poorly understood and warrant investigation to facilitate the development of new cultivars with diverse pigmentation patterns, increased levels of anthocyanins, and enhanced resilience to environmental stressors. To better understand how environmental temperatures affect anthocyanin accumulation in *C. sativa*, temperature treatments were conducted and data on anthocyanin content, CBD percentages, and biomass yield were collected. Anthocyanin biosynthesis in the inflorescence was significantly affected by temperature, with plants grown in 8 and 15°C accumulating the highest levels of anthocyanins. Temperature treatments were also shown to effect CBD percentages and biomass yield, but contrary to anthocyanin biosynthesis, differences in these traits were likely due to differences in maturity. To better understand the genetic mechanism governing anthocyanin accumulation in *C. sativa*, a mapping population and an open-pollinated population were used to help identify qualitative trait loci (QTL) associated with this trait. Significant single nucleotide polymorphisms (SNPs) for flower and leaf color were found on chromosome 6 while significant SNPs for stem color were found on chromosome 8. Investigating randomly selected SNPs within the QTL regions to further elucidate the mode of inheritance of anthocyanin accumulation in C. sativa revealed both complete and incomplete dominance patterns. To achieve a comprehensive understanding of the environmental factors, genetic mechanisms, and mode of inheritance governing anthocyanin accumulation in *C. sativa*, it is imperative that further studies are

conducted. These studies should involve expanding temperature treatments to cover wider ranges with smaller intervals, allowing for a more nuanced exploration of temperature's impact on anthocyanin accumulation. Also, creating additional mapping populations with various cultivars can provide a more comprehensive view of the genetic landscape. Furthermore, evaluating a greater number of SNPs can enhance resolution and facilitate a deeper understanding of the underlying genetic mechanisms. By integrating these approaches, researchers can advance our knowledge of the complex interplay between environmental factors and genetic traits in *C. sativa*.

## Table of Contents

# LIST OF TABLES

## LIST OF FIGURES

## LIST OF PICTURES

# LIST OF ABBREVIATIONS

CSA: Controlled Substances Act

THC: Tetrahydrocannabinol

CBD: Cannabidiol

THCA: Tetrahydrocannabinolic acid

CBDA: Cannabidiolic acid

CBG: Cannabigerol

CBGA: Cannabigerolic acid

PCoA: Principal coordinate analysis

Busco: Benchmarking universal single-copy orthologs

NCBI: National Center for Biotechnology Information

PAL**:** Phenylalanine ammonia lyase

C4H: Cinnamate 4-hydroxylase

4CL**:** Cinnamic acid-4-hydroxylase

CHS: Chalcone synthase

CHI: Chalcone isomerase

F3H: Flavanone-3-hydroxylase

F3’H**:** Flavanone 3′-hydroxylase

F3’5’H**:** Flavanone 3′5′-hydroxylase

DFR: Dihydroflavonol 4-reductase

ANS: Anthocyanidin synthetase

VSC: Volatile-sulfur-compounds

HPLC: High Performance Liquid Chromatography

QTL: quantitative trait loci

MBW: MYB-bHLH-WDR

GDD: Growing degree days

GABA: Gamma-aminobutyric acid

THCVA: Tetrahydrocannabivarin acid

UV: Ultraviolet

EBGs: Early biosynthesis anthocyanin genes

LBGs: Late anthocyanin biosynthesis genes

UPLC: Ultra Performance Liquid Chromatography

CBCA: Cannabichromenic acid

CBC: Cannabichromene

CBN: Cannabinol

D.I.: Deionized

RCBD: Randomized complete block design

TDW: Total dry weight

TCBD: Total CBD

TMA: Total monomeric anthocyanins

TAS: Total anthocyanin score

OP: Open-pollinated

TAL: Tyrosine ammonia lyase

UGT/UFGT: Uridine diphosphate-dependent glucosyltransferase

GT: Glucosyltransferase

RT: rhamnosyltransferase

MT: methyltransferase

AT: Acyltransferase

ROS: Reactive oxygen species

C3R: Cyanidin-3-rutinoside

CW: Cherry Wine 307

118: 118 Early Harvest

GBS: Genotyping-by-Sequencing

## List of Supplemental Tables and Figures

# CHAPTER 1: LITERATURE REVIEW OF CANNABIS AND ANTHOCYANIN ACCUMULATION

## Cannabis history and regulation

*Cannabis sativa* (*C. sativa*) is believed to have originated in Central, South and East Asia, but the exact origin is unclear (Clarke & Merlin, 2013). Proposed locations of origin include the area between the Caucasus and Altai Mountains, the foothills of the Himalayan and Hindu Kush Mountains, the mountainous Hengduan region, or along the Yangzi and Huang He River of present-day China (Clarke & Merlin, 2013). Cannabis is one of the oldest plants cultivated by humans in recorded history (Clarke & Merlin, 2013). The earliest recorded uses of *C. sativa* date back over 5,000 years to ancient China (Li, 1974). Archaeological evidence suggests that the plant was first cultivated for its fibers, which were used in the production of textiles and ropes (Clarke & Merlin, 2013). Before the use of cotton, cannabis was the dominant textile in Northern China (Li, 1974). These early applications laid the foundation for the plant's role in the development of human civilization. As human societies expanded and interacted, the use of cannabis did as well and knowledge about the plant spread throughout the world. Humans have discovered a multitude of uses for almost every part of the cannabis plant, with primary foci on fibers from the stalks, cannabinoids from the female flowers, and deriving nutrients and oils from the seeds. In ancient civilizations, cannabinoids were used medicinally and for ritualistic purposes (Booth, 2005). In China, the common name for cannabis is Má(麻), a character that can be found in textual examples meaning numbness or anesthesia and most likely dates to the Han Dynasty (206 B.C. -220 A.D.) (Crocq, M. A. 2020). In addition to medicinal use, the psychoactive properties of cannabis were recognized and consumed during religious ceremonies in China 1980). Similarly, in India, there is evidence that cannabis was integrated into religious practices around 1500 BCE (Aldrich, 1980).

Looking further West, *C. sativa* unveiled its historical importance in medicinal applications and recreation documented on Assyrian tablets and Egyptian Eber Papyrus (Bonini et al., 2018, Scurlock & Andersen, 2010). In the Middle East, cannabis was embraced for its medicinal properties, while in Africa, they found use for the plant in traditional healing practices (Booth, 2005). Central Italy saw a rise in *C. sativa* cultivation during the Roman era, with evidence dating back to the 1st century A.D., as indicated by pollen analysis (Mercuri et al., 2002). Additionally, one of the earliest references to the medicinal application of cannabis roots was provided by the Roman historian Pliny the Elder (Ryz et al., 2017). The first extensive cultivation and commercialization of the plant in the Mediterranean region was spearheaded by Italians (Bonini et al., 2018). In Europe, cannabis became valued for its fibers, contributing to the production of sails, ropes, and clothing (Aldrich, 1980).

*C. sativa* remained unknown in the Americas until the first European colonists arrived and settled (Bonini et al., 2018). Humans played a pivotal role in the extensive and fairly recent global spread of cannabis, particularly outside of Eurasia (Clarke & Merlin, 2013). European settlers are thought to have introduced cannabis to the Americas during the 16th century, primarily using routes through Mexico and Chile (Clarke & Merlin, 2013). In North America, the introduction and cultivation of cannabis is attributed to Louis Hebert, a Canadian apothecary, who is thought to have practiced growing cannabis in Nova Scotia around 1606 (Clarke & Merlin, 2013). Cannabis production did not begin in the United States until 1611 in Jamestown, Virginia, before spreading to Massachusetts in 1632, Kentucky in 1775, and Missouri in 1835 (Mikos & Kam, 2019). Not long after in 1848 a Scottish physician, Robert A. Christison, mentioned the medicinal value of cannabis in his publication "*A dispensatory of commentary on the pharmacopoeias of Great Britain and the United States"*. During the U.S. Civil War (1861-1865), military doctors utilized cannabis as a pain reliever when treating combat injuries (Mikos & Kam, 2019). Notably, in 1891, an important paper was published by American physician J.B. Mattison in the St. Louis Medical and Surgical Journal where he discussed the use of cannabis for treating cocaine and opiate addiction as well as treating migraines and headaches (Mikos & Kam, 2019). These early publications played key roles in the United States embarking on a short-lived exploration of cannabis for its medical potential. In 1922, cannabis was eventually labeled as a narcotic (Mikos & Kam, 2019), which inevitably led to the plant being portrayed as potentially harmful and dangerous. In 1937, the first regulations on cannabis began with the Marihuana Tax Act of 1937. This new Act placed a tax on the sale of cannabis and regulated the importation, cultivation, possession and/or distribution of the crop. Due to the Marihuana Tax Act, the exploration of medicinal cannabis nearly disappeared in the United States, making it a federal offense to possess and distribute cannabis.

In 1970, Congress intended to replace the Marihuana Tax Act and modernize the American drug policy by enacting the Comprehensive Drug Abuse Prevention and Control Act and the Controlled Substances Act (CSA) (Mikos & Kam, 2019). The CSA created a five-tier Schedule system for all substances previously under federal regulation, with cannabis being categorized as a Schedule I drug. Schedule I drugs are defined as drugs or other substances that have high potential for abuse, no currently accepted medical use in treatment in the United States, and there is a lack of accepted safety for use of the drugs or other substances under medical supervision (DEA, 2018). In the US, *Cannabis sativa* has been an ongoing subject of legal and cultural debate which has played a vital role in shaping the nation's drug policies and societal attitudes about this plant. Advocates in favor of cannabis typically prefer the term "cannabis" over "marihuana" because the latter is connected to anti-cannabis propaganda from the early 20th century, designed to classify the substance as foreign and, consequently, dangerous while also targeting Mexican immigrants (Gettman, 2015). Despite the ongoing disputes surrounding the plant, States began legalizing cannabis for medical use in 1996 with California being the first.

The Agricultural Act of 2014, commonly referred to as the 2014 Farm Bill, had substantial consequences for the growth and exploration of cannabis within the United States. This legislation authorized the controlled growth of industrial hemp (cannabis with tetrahydrocannabinol (THC) levels lower than 0.3% on a dry weight basis), provided it was conducted for research purposes. The 2014 Farm Bill served as the initial step toward the more profound changes brought about by the 2018 Farm Bill. This latter legislation effectively eliminated industrial hemp from the controlled substances list, reclassifying it as an agricultural commodity. This reclassification allowed for expanded commercial hemp cultivation and the nationwide production of products derived from hemp. Additionally, the 2018 Farm Bill provided legal clarity regarding cannabidiol (CBD) sourced from hemp, spurring the rapid growth of the industry in the United States. In 2022, the estimated value of industrial hemp in the United States totaled $238 million (National Hemp Report, 2023), while the states that have legalized high THC, or drug-type, cannabis generated more than $3.7 billion in 2021 (Marijuana Policy Project, 2022). Over the last decade, the legal cannabis market has grown into a billion-dollar industry and the innovation of new cannabis-based products has been on the rise.

## Plant Biology and Physiology

*Cannabis sativa,* a member of the cannabaceae family, is an annual, diploid ($2n = 20$) plant characterized by its strong fibers, palmate leaves, and distinctive serrated leaflets (Russo, 2007). Cannabis is an outcrossing species that utilizes the wind to disperse pollen. In Canada, regulations require a minimum isolation distance of five kilometers for hemp producers to prevent the inadvertent cross-contamination of pollen from external sources (Small & Antle, 2003). Cannabis is an erect, herbaceous plant that is mostly dioecious but can also be monoecious and/or hermaphroditic. Male cannabis plants will have a sex chromosome pair of XY, while female and monoecious cannabis plants have XX (Divashuk et al., 2014, Razumova et al., 2016). In general, female cannabis plants tend to flower later than males, and they exhibit a notable accumulation of glandular trichomes surrounding their floral structures, a feature less prominent in male flowers (Figure 1.1). Environmental stressors can cause hormonal changes in plants which can result in dioecious plants becoming monoecious which has been utilized in breeding programs and the production of feminized seeds (Golenberg & West, 2013). This phenomenon has enabled cannabis growers to investigate the utilization of exogenous compounds like silver thiosulfate, gibberellic acid, and colloidal silver to control sex expression in *C. sativa* (Flajšman et al., 2021, Lubell & Brand, 2018).

*Cannabis sativa* is a short-day plant that typically requires more than 12 hours of uninterrupted darkness a day to trigger flowering. Researchers are currently exploring optimal photoperiods for cultivating cannabis, questioning whether the conventional 12-hour light and 12-hour dark cycle is the most effective (Ahrens et al., 2023, Peterswald et al., 2023). Cannabis plants can also be day-neutral, which means the plant will not require a certain photoperiod to induce flowering, but instead flowering is triggered based on maturity. These plants are often referred to as autoflowers. Cannabis can be heavily impacted by the latitude at which it is grown. A study conducted in China revealed that cannabis plants cultivated at high latitudes (north of approximately 40° N) tend to produce shorter plants with reduced branching, thinner stems, and shorter life cycles while plants grown at lower latitudes (south of about 30° N) exhibit opposite traits, with day length being the most influential factor (Zhang et al. 2018).

Cannabis can be propagated clonally via stem cuttings and can also be grown under tissue culture. These techniques are favored over seed production in many cases because of the tremendous amount of heterozygosity that exists in modern-day cannabis populations. Because cannabis does not tolerate inbreeding well, it can be useful to have genetically identical individuals created through clonal propagation. In the cannabis industry, the use of clones is favored in many cases, with breeders and growers making use of this technique to protect the valuable genetic characteristics of their carefully selected mother plants. Utilizing clones also proves to be a valuable resource for researchers aiming to characterize sources of environmental variation in their experiments.

Techniques in cannabis cultivation differ depending on its intended end use. Hemp cultivated for grain and fiber typically involves mechanized farming practices, whereas cannabis grown for cannabinoids demands a more hands-on approach. The production of grain and fiber involves the use of a grain combine and haying equipment, along with the necessary step of retting for fiber separation; in contrast, for cannabinoid production, plants are carefully cultivated, commonly transplanted into rows with precise irrigation, spaced at wider intervals and are manually harvested (Alberti et al., 2024). There are also observable differences in plant structure when comparing cannabis grown for seed, fiber, and flower. Outdoor cultivation is common for both fiber and seed crops, with fiber plants often towering at 2 meters or more and displaying limited branching, while seed plants, resembling fiber crops in their unbranched structure, have seen a development of shorter modern cultivars, sometimes around 1 meter or less in height (Zheng & Small, 2022). Cultivars with dual purposes are also available, allowing for the harvesting of both grain and fibers. Cannabis cultivars employed for medicinal benefits are often identified by their need for a short photoperiod to induce flowering (Spitzer-Rimon et al., 2019), and are commonly cultivated in controlled environments. Drug-type cannabis cultivars are grown for the secondary metabolites found on the female flowers which are used for medicinal and recreational purposes. Selection on flower morphology and increased levels of cannabinoids such as tetrahydrocannabinolic acid (THCA) and cannabidiolic acid (CBDA) have led to drug-type cultivars becoming renowned for their robust inflorescences densely covered in glandular trichomes (Figure 1.1). Glandular trichomes, most abundant on the calyces of female flowers, serve as the primary site for synthesizing specialized metabolites such as cannabinoids (e.g., CBDA and THCA) and terpenes (Livingston et al., 2020). Cannabis plants possess the capability to produce over 100 different cannabinoids (Tanney et al., 2021). The cannabinoids that have received the most attention include THC, CBD, and cannabigerol (CBG), with CBD emerging as the focal point of heightened interest in product development across the United States.

Through principal coordinate analysis (PCoA), drug-type cannabis and hemp have been shown to be genetically different, but indica, sativa, and hybrid cultivars were not significantly different from one another (Schwabe et al., 2021). Hemp has been grown and selected for both seed and fiber quality. Optimal geographic locations for growing specific cannabis varieties have been investigated, revealing that lower latitudes are favorable for seed production, whereas higher latitudes are preferable for fiber production, within a latitude range spanning from 19 to 58 degrees (de Meijer & Keizer, 1994). The majority of drug-type cannabis cultivation takes place in controlled environments where variables such as climate and photoperiod can be manipulated, though outdoor cultivation remains widespread globally.

## Cannabis genetics and breeding

Two subspecies, *C. sativa* subsp. *sativa*, and *C. sativa* subsp. *indica*, have been recognized and are correlated to their geographical origin, with “sativa” having Indian heritage with descendants carried into Southeast Asia, South- and East Africa, and the Americas, while “indica” plants have origins from Pakistan and regions around Afghanistan (Chandra et al., 2017). Variations in phenotypes and chemical compositions are noticeable when contrasting "indica" and "sativa" cannabis plants (Chandra et al., 2017). Varieties classified as "sativa" are known for their heightened production of Δ9-tetrahydrocannabinol (THC) relative to cannabidiol (CBD), "herbal" or "sweet" terpene profiles, and psychoactive effects that are stimulating, uplifting, and energizing (Chandra et al., 2017). "Indica" varieties, known for promoting relaxation, sedation, and pain relief, yield a THC-to-CBD ratio that is nearly balanced, along with a terpenoid profile contributing to a pungent or "skunky" scent (Chandra et al., 2017).

When buying cannabis seeds, most “cultivars” in the market resemble open-pollinated varieties. It is challenging to find uniform cultivars that can be grown from seed. There are breeders across the world who have worked hard to stabilize cannabis lines, but a tremendous amount of variation exists. Most cannabis varieties available on the market are hybrids, and genuine landraces have become increasingly scarce. Unfortunately, many of the landrace varieties grown by farmers in regions around the world are becoming progressively harder to find due to the potential economic gain of growing the new, higher-yielding, better-performing varieties on the market. For drug-type cannabis, underground breeding programs and the collaborative sharing of genetic resources within cannabis communities have spurred the evolution of the high cannabinoid varieties we see today. Popular traits that breeders and farmers may prioritize include yield, sex, photoperiod, disease resistance, cannabinoid content, terpene profile, volatile secondary metabolites, flavor/taste, and overall aesthetics.

## Genomic resources for cannabis

A high-quality reference genome for *C. sativa* has been assembled using a high CBD variety, CBDRx, and was validated by a benchmarking universal single-copy orthologs (Busco) completeness score of 97.2% and a genome size (736Mb) which matched predictions from k-mer frequencies (Grassa et al., 2021). The National Center for Biotechnology Information (NCBI) has selected the CBDRx (cs10) genome as the reference genome for *Cannabis sativa* and produced a high-quality gene prediction set that is available for users while the raw data can be found at NCBI under project PRJEB29284, GenBank assembly accession GCA_900626175.2 (Grassa et al., 2021). This valuable resource is the most complete reference genome to date and is being used by many to help better understand the genetics of *C. sativa.*

## Flavonoids and Anthocyanins

Polyphenols are the largest, most widely distributed group of phytochemicals and are mostly comprised of flavonoids (King & Young, 1999). The molecular structure of flavonoids consists of a 15-carbon skeleton, which consists of two phenyl rings (A and B) and a heterocyclic ring (C) as shown in Figure 1.2. Flavonoids can be classified into several subclasses based on the degree of oxidation and the presence of various functional groups (Harborne, 1993). One such subgroup contains anthocyanins, which are responsible for the red, blue, pink, and purple pigments we see in plants (King and Young 1999). Pelargonidin, cyanidin, and delphinidin are three major types of anthocyanins and are responsible for producing orange-red, red-magenta, and magenta-purple colors, respectively (Falcone Ferreyra et al., 2012). Anthocyanins can be seen in many modern cannabis varieties and have become a desired trait in many breeding programs and among cannabis consumers. In a recent study, Bassolino and colleagues detected cyanidin 3-glucoside, cyanidin 3-rutinoside, and peonidin 3-glucoside as the anthocyanins present in a subset of purple cannabis samples (Bassolino et al., 2023). Identifying the specific anthocyanins found in cannabis allows for more accurate quantification of cannabis-derived products and contributes to a deeper comprehension of how these substances might enhance the well-being of both plants and humans.

## Anthocyanin biosynthesis and regulation

In 1835, Ludwig Clamor Marquart, a German pharmacist, was the first to call the blue flower pigments, anthocyanins (Shibata et al., 1919). Anthocyanins are widely distributed throughout the plant kingdom and are water soluble. These molecules, mostly accumulating in the epidermal layer (Chaves et al., 2018), benefit plants by targeting free radicals and protecting against environmental stresses such as intense UV-light, cold temperatures, wounding, herbivory, heavy-metal contamination, and nutrient deficiencies (Gould, 2004; Albert et al., 2014). There is evidence that crops with higher anthocyanin content may experience a significantly prolonged shelf life and exhibit enhanced resistance to pathogens (Bassolino et al., 2013; Zhang et al., 2013).

The biosynthesis of anthocyanins in plants is a complex process that involves a series of enzymatic reactions and transcriptional genes that are relatively conserved across plant species. The pathway is regulated by several factors, including light, nutrient availability, temperature, pH, and the developmental stage of the plant (Zhang & Zhu, 2023). The anthocyanin biosynthetic pathway can be divided into two main stages: the early biosynthetic pathway and the late biosynthetic pathway. The early biosynthetic pathway involves the synthesis of the anthocyanin precursor, flavonoids, while the late biosynthetic pathway involves the modification of flavonoids to form anthocyanins (Shi & Xie, 2014; Zhang & Zhu, 2023). The early biosynthetic pathway starts with phenylalanine which undergoes a series of enzymatic reactions involving phenylalanine ammonia lyase (PAL), cinnamate 4-hydroxylase (C4H), and cinnamic acid-4-hydroxylase (4CL) which ultimately results in the formation of coumaroyl-CoA (Figure 1.2A) (Zhang & Zhu, 2023). Coumaroyl-CoA is then transformed into dihydroflavonols via enzymes including chalcone synthase (CHS), chalcone isomerase (CHI), flavanone-3-hydroxylase (F3H), flavanone 3′-hydroxylase (F3′H), and flavanone 3′5′-hydroxylase (F3′5′H) (Figure 1.2) (Zhang & Zhu 2023). In the late biosynthetic pathway, dihydroflavonol 4-reductase (DFR) catalyzes the production of various leucoanthocyanidins, and anthocyanidin synthetase (ANS) further transforms the colorless leucoanthocyanidins into anthocyanidins. (Figure 1.2) (Zhang & Zhu 2023).

The amount and activity of each enzyme in the biosynthetic pathway is carefully regulated so that a cell produces only as much of any compound as is needed. Transcriptional genes encode transcription factors that regulate the expression of the structural pathway genes. These transcription factors include R2R3 MYBs, bHLHs, and WD40s that together form an entity known as the MYB-bHLH-WD40 (MBW) complex, which binds to specific DNA sequences in the promoters of the structural genes and activates their transcription (Figure 1.2B) (Jaakola, 2013; Albert et al., 2014; Xu, et al., 2015; Chaves-Silva et al., 2018; Zhang & Zhu, 2023).

Post-transcriptional genes regulate the stability and processing of mRNA molecules, which are the intermediates between DNA and protein synthesis (Corbett, 2018). For example, RNA-binding proteins and microRNAs can regulate the expression of structural genes involved in anthocyanin biosynthesis by modulating mRNA stability or translation. Signal transduction genes encode proteins involved in signal transduction pathways, which transmit information from the environment to the plant cell (Chen & Heidari, 2020). Signal transduction pathways can modulate the expression of transcriptional genes involved in anthocyanin biosynthesis in response to environmental cues such as light, temperature, and stress (Chaves-Silva et al., 2018; Khusnutdinov et al., 2021). Other types of genes involved in anthocyanin accumulation include genes encoding enzymes involved in the production of precursors for anthocyanin biosynthesis, such as shikimate pathway enzymes and isoprenoid biosynthesis enzymes (Albert et al., 2014). While genetics are a key factor in deciding which compounds a plant can produce, the stress experienced by the plant also plays a crucial role in shaping the specific anthocyanin homolog it synthesizes (Kovinich et al., 2014; Ponder et al., 2021). A more thorough understanding of the impacts of distinct stressors on anthocyanin accumulation in *C. sativa* may lead to increased plant resilience and the discovery of innovative product possibilities.

## Anthocyanins in cannabis

Anthocyanins are expressed in many modern cannabis cultivars and have become a desired trait in breeding programs and among consumers. Researching purple pigments in cannabis can provide insight into genetic control, environmental adaptation, antioxidant properties, consumer preferences, medicinal potential, market differentiation, and aesthetic values of this crop. Apart from protecting the plant against various biotic and abiotic stresses, purple pigments can present a distinctive visual feature that sets certain cultivars apart, giving growers and producers a marketing advantage. In addition to marketability, anthocyanins could also play a role in the medicinal/therapeutic effects of *C. sativa*. In recent studies, researchers have begun to explore the "entourage effect" (Christensen et al., 2023), which refers to the idea that the combination of various compounds found in *C. sativa*, including cannabinoids, terpenes, esters, volatile-sulfur-compounds (VSC) and other phytochemicals, may produce a more significant therapeutic effect than individual compounds in isolation. Ben-Shabat et al. (1998) were the pioneers in identifying this phenomenon, illustrating that the presence of specific esters significantly enhanced cannabinoid activity (Ben-Shabat et al., 1998). In the pursuit of unraveling the full therapeutic potential of cannabis, it is imperative to extend our focus beyond cannabinoids and terpenes to include anthocyanins. These colorful compounds, often overlooked in the entourage effect, could be crucial in discovering new dimensions of medicinal efficacy, paving the way for more nuanced and personalized approaches to cannabis-based medicine. Exploring anthocyanins in cannabis not only offers the potential to enhance medical cannabis research but also contributes to a comprehensive understanding of *C. sativa's* physiology. Strengthening our understanding of the mechanisms behind anthocyanin biosynthesis will greatly improve the way we cultivate cannabis with increased anthocyanin levels.

## Genetic regulation of anthocyanin accumulation in *C. sativa*

Bassolino et al. (2020) provided the first genome-wide analysis of bHLHs and MYBs families in *C. sativa* and further classified these families into subfamilies through comparative phylogenetic analysis with *Arabidopsis thaliana* (Bassolino et al., 2020). More recently Kundan et al. (2022) described 99 R2R3-MYB genes in the *C. sativa* genome and two candidate anthocyanin regulators were identified, *CsMYB33* and *CsMYB78*. Activation of anthocyanin biosynthesis and accumulation was verified by overexpressing candidates in *Nicotiana benthamiana* leaves (Kundan et al., 2022).

## Anthocyanin quantification

There are different methods for quantifying anthocyanins which depend on tissue type, the molecular structure of the compounds being extracted, and the instrument being used.

Spectroscopy is one of the most common methods for quantifying anthocyanins and involves measuring the absorbance of extracted anthocyanins at a specific wavelength. Typically, the wavelength used for measuring anthocyanin absorbance is approximately 520 nm. Another method used for quantifying anthocyanins is High Performance Liquid Chromatography (HPLC). HPLC is a highly accurate method that separates compounds based on their chemical properties which can be especially useful when identifying and quantifying anthocyanins in each sample.

The pH differential method, first introduced by Ernest Sondheimer and Z.I. Kertesz in 1948, utilizes the fact that anthocyanins will change color depending on the acidity of their surroundings (Sondheimer, E., & Kertesz, Z.I., 1948). When performing the pH differential method, different pH conditions are intentionally created, and the absorbance is measured in each environment. The two most commonly used pH values are pH 1.0 (acidic) and pH 4.5 (slightly acidic). The absorbance readings at both pH 1.0 and pH 4.5 are then used to calculate the concentration of anthocyanins in the sample. Despite its accuracy, the existing method for quantifying anthocyanin levels in plants presents significant challenges, including laborious procedures, time constraints, the use of dangerous chemicals, and prohibitive costs. It is imperative to develop a non-destructive assay capable of efficiently and accurately characterizing anthocyanin phenotypes. Developing this assay holds great promise for facilitating future research endeavors and providing valuable assistance to breeders and growers in the cannabis industry.

## Current research

Our research aims to provide a better understanding of the environmental and genetic factors influencing anthocyanin accumulation in *Cannabis sativa*, which will have implications for breeding and the production of cannabis-based products. These compounds benefit plant health by protecting against environmental stresses such as UV radiation and extreme temperatures. With an unpredictable climate ahead, being able to produce these compounds will benefit plants tremendously by providing greater resilience to stressful conditions. A better understanding of the environmental stresses that cause anthocyanin expression will be paramount to developing varieties that can overcome and adapt these challenges. To investigate the role of anthocyanins in plants under stress, we developed a stable, day-neutral, purple cannabis population. We grew these populations under various cold treatments, without UV exposure, in two replicated studies, to see how temperature affects anthocyanin accumulation, biomass yield, and total CBD percentage in the inflorescence. This study aimed to offer suggestions for optimizing these traits and elucidate the physiological mechanisms governing them. Anthocyanins were extracted from tissue samples and a high-throughput assay was developed to quantify the levels of anthocyanins via spectroscopy. Spectroscopy was utilized to compute total monomeric anthocyanin levels, which were then compared with a visual rating score established by the Ellison lab and colleagues. This visual rating score provides a quick and cost-effective method for phenotyping and estimating anthocyanin levels in cannabis plants.

To better understand the genetic control of anthocyanin accumulation, 7 $BC_2F_2$ mapping populations, and an open pollinated population were phenotyped and genotyped to identify quantitative trait loci (QTL) associated with this trait. By identifying the QTL associated with anthocyanins in cannabis, breeders will be able to develop cultivars more efficiently with techniques such as marker-assisted selection.  Creating new cultivars with higher concentrations of anthocyanins will lead to plants being more resistant to disease, stressful environments, and has the potential to enhance medicinal properties and consumer appeal.

**Chapter 1 Figures**


**Figure 1.1.** Three day-neutral *C. sativa* cultivars. The bottom section of the A, B, and C panels illustrate the entire plant, while the top shows their respective inflorescences. (A) Green pigmented cultivar ($F_2$ generation of MXU x 118 Early Harvest) exhibiting both pollinated and unpollinated female flowers. (B) Ruby cultivar, developed by High Alpine Genetics, characterized by its purple pigmentation, showing pollinated female flowers densely covered with glandular trichomes containing specialized secondary metabolites. (C) Male cannabis plant specifically highlighting male cannabis inflorescences displaying both opened and unopened pollen sacs, demonstrating comparatively lesser accumulation of glandular trichomes than the females.

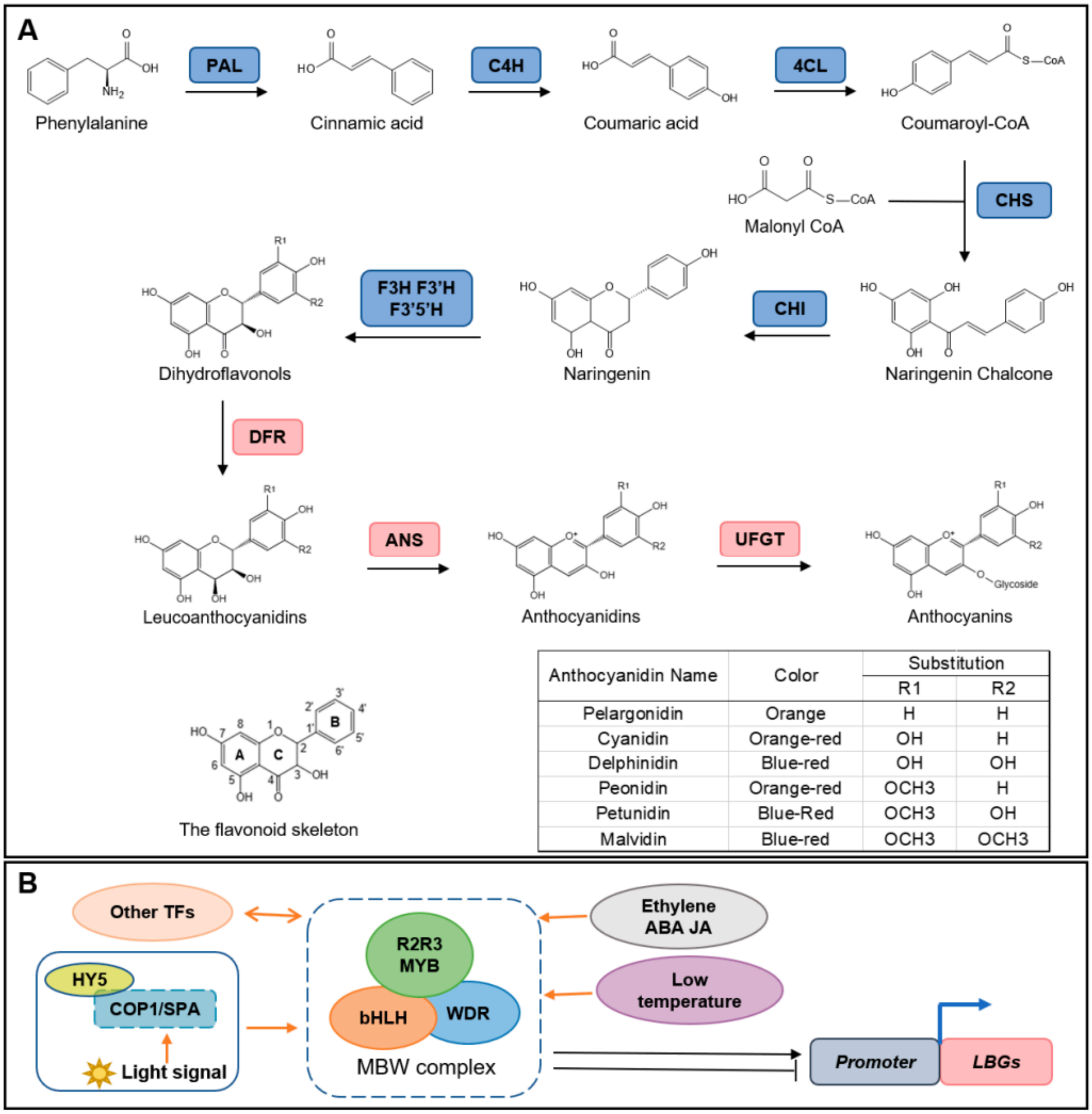


**Figure 1.2.** Anthocyanin biosynthesis pathway and the regulation factors. (**A**) Schematic pathway of anthocyanin biosynthesis in plants and the chemical structure of anthocyanins. Blue and light-red boxes represent early biosynthetic genes (*EBGs)* and late biosynthetic genes (*LBGs)* respectively. (**B**) Other factors regulate anthocyanin accumulation in plants through affecting the MBW complex. The key *LBGs DFR*, *ANS* and *UFGT* are mainly regulated by a conserved MYB-bHLH-WDR (MBW) complex. The MBW complex interacts with other transcriptional factors and is regulated by phytohormones including ethylene, ABA (abscisic acid) and JA (jasmonic acid). The environment factors temperature and light signal affect the activity of the MBW complex. PAL, phenylalanine ammonia lyase; C4H, cinnamate 4-hydroxylase; 4CL, cinnamic acid-4-hydroxylase; CHS, Chalcone synthase; CHI, chalcone isomerase; F3H, flavanone-3-hydroxylase; F3′H, flavanone 3′-hydroxylase; F3′5′H, flavanone 3′5′-hydroxylase; DFR, dihydroflavonol 4-reductase; ANS, anthocyanidin synthetase; UFGT, flavonoid 3-O-glucosyltransferase. (Figure adapted from Zhang & Zhu, 2023).

**Chapter 1 References**

Ahrens, A., Llewellyn, D., & Zheng, Y. (2023). Is Twelve Hours Really the Optimum Photoperiod for Promoting Flowering in Indoor-Grown Cultivars of Cannabis sativa? Plants, 12(14). https://doi.org/10.3390/plants12142605

Albert, N. W., Davies, K. M., Lewis, D. H., Zhang, H., Montefiori, M., Brendolise, C., ... & Schwinn, K. E. (2014). A conserved network of transcriptional activators and repressors regulates anthocyanin pigmentation in eudicots. The Plant Cell, 26(3), 962-980.

Alberti, P., Ellison, S., & Mirsky, S. (2024). Crops and Soils Division of Extension (Hemp). Retrieved March 17, 2024, from https://cropsandsoils.extension.wisc.edu/hemp/

Aldrich, M. R. (1980). Origins of psychopharmacology: From CPZ to LSD.

Bassolino, L., Buti, M., Fulvio, F., Pennesi, A., Mandolino, G., Milc, J., Francia, E., & Paris, R. (2020). In silico identification of myb and bhlh families reveals candidate transcription factors for secondary metabolic pathways in cannabis sativa L. *Plants*, *9*(11), 1–19. https://doi.org/10.3390/plants9111540

Bassolino, L., Fulvio, F., Pastore, C., Pasini, F., Gallina Toschi, T., Filippetti, I., & Paris, R. (2023). When Cannabis sativa L. Turns Purple: Biosynthesis and Accumulation of Anthocyanins. *Antioxidants*, *12*(7). https://doi.org/10.3390/antiox12071393

Bassolino, L., Zhang, Y., Schoonbeek, H. J., Kiferle, C., Perata, P., & Martin, C. (2013). Accumulation of anthocyanins in tomato skin extends shelf life. *New Phytologist*, *200*(3), 650–655. https://doi.org/10.1111/nph.12524

Bonini, S. A., Premoli, M., Tambaro, S., Kumar, A., Maccarinelli, G., Memo, M., & Mastinu, A. (2018). Cannabis sativa: A comprehensive ethnopharmacological review of a medicinal plant with a long history. In Journal of Ethnopharmacology (Vol. 227, pp. 300–315). Elsevier Ireland Ltd. https://doi.org/10.1016/j.jep.2018.09.004

Booth, M. (2005). *Cannabis: a history.* 1st Picador ed. New York, Picador.

Chandra, S., Lata, H., & ElSohly, M. A. (2017). Cannabis sativa L. - botany and biotechnology. In *Cannabis sativa L. - Botany and Biotechnology*. Springer International Publishing. https://doi.org/10.1007/978-3-319-54564-6

Chaves-Silva, S., Santos, A. L. dos, Chalfun-Júnior, A., Zhao, J., Peres, L. E. P., & Benedito, V. A. (2018). Understanding the genetic regulation of anthocyanin biosynthesis in plants – Tools for breeding purple varieties of fruits and vegetables. In *Phytochemistry* (Vol. 153, pp. 11–27). Elsevier Ltd. https://doi.org/10.1016/j.phytochem.2018.05.013

Chen, J. T., & Heidari, P. (2020). Cell signaling in model plants. In *International Journal of Molecular Sciences* (Vol. 21, Issue 17, pp. 1–4). MDPI AG. https://doi.org/10.3390/ijms21176062

Crocq, M. A. (2020). History of cannabis and the endocannabinoid system. Dialogues in Clinical Neuroscience, 22(3), 223–228. https://doi.org/10.31887/DCNS.2020.22.3/MCROCQ

Corbett, A. H. (2018). Post-transcriptional regulation of gene expression and human disease. In *Current Opinion in Cell Biology* (Vol. 52, pp. 96–104). Elsevier Ltd. https://doi.org/10.1016/j.ceb.2018.02.011

de Meijer, E. P. M., & Keizer, L. C. P. (1994). Field Crops Research Variation of Cannabis for phenological development and stem elongation in relation to stem production. In Field Crops Research (Vol. 38).

DEA. 10 July, 2018. Drug Scheduling. Retrieved from https://www.dea.gov/drug-information/drug-scheduling on 25 March, 2024

Dias, M. C., Pinto, D. C. G. A., & Silva, A. M. S. (2021). Plant flavonoids: Chemical characteristics and biological activity. In *Molecules* (Vol. 26, Issue 17). MDPI. https://doi.org/10.3390/molecules26175377

Divashuk, M. G., Alexandrov, O. S., Razumova, O. v., Kirov, I. v., & Karlov, G. I. (2014). Molecular cytogenetic characterization of the dioecious Cannabis sativa with an XY chromosome sex determination system. PLoS ONE, 9(1). https://doi.org/10.1371/journal.pone.0085118

Falcone Ferreyra, M. L., Rius, S. P., & Casati, P. (2012). Flavonoids: Biosynthesis, biological functions, and biotechnological applications. In *Frontiers in Plant Science* (Vol. 3, Issue SEP). Frontiers Research Foundation. https://doi.org/10.3389/fpls.2012.00222

Flajšman, M., Slapnik, M., & Murovec, J. (2021). Production of Feminized Seeds of High CBD Cannabis sativa L. by Manipulation of Sex Expression and Its Application to Breeding. Frontiers in Plant Science, 12. https://doi.org/10.3389/fpls.2021.718092

Gettman, J. (2015). Marijuana V. Cannabis: Pot-Related Terms to Use and Words We Should Lose. *High Times*. https://hightimes.com/culture/marijuana-vs-cannabis-pot-related-terms-to-use-and-words-we-should-lose/

Golenberg, E. M., & West, N. W. (2013). Hormonal interactions and gene regulation can link monoecy and environmental plasticity to the evolution of dioecy in plants. *American Journal of Botany*, *100*(6), 1022–1037. https://doi.org/10.3732/ajb.1200544

Gould, K. S. (2004). Nature's Swiss Army Knife: The Diverse Protective Roles of Anthocyanins in Leaves. In *Journal of Biomedicine and Biotechnology* • (Issue 5). http://jbb.hindawi.com

Grassa, C. J., Weiblen, G. D., Wenger, J. P., Dabney, C., Poplawski, S. G., Timothy Motley, S., Michael, T. P., & Schwartz, C. J. (2021). A new Cannabis genome assembly associates elevated cannabidiol (CBD) with hemp introgressed into marijuana. *New Phytologist*, *230*(4), 1665–1679. https://doi.org/10.1111/nph.17243

Jaakola, L. (2013). New insights into the regulation of anthocyanin biosynthesis in fruits. Trends in Plant Science, 18(9), 477-483.

King, A and Young, G. (1999). Characteristics and Occurrence of Phenolic Phytochemicals. Journal of the American Dietetic Association, Vol.99 (2), p.213-218

Kundan, M., Gani, U., Fayaz, M., Angmo, T., Kesari, R., Rahul, V. P., Gairola, S., & Misra, P. (2022). Two R2R3-MYB transcription factors, CsMYB33 and CsMYB78 are involved in the regulation of anthocyanin biosynthesis in Cannabis sativa L. *Industrial Crops and Products*, *188*. https://doi.org/10.1016/j.indcrop.2022.115546

Lee, J., Durst, R. W., Wrolstad, R. E., Barnes, K. W., Eisele, ; T, Giusti, ; M M, Haché, ; J, Hofsommer, ; H, Koswig, ; S, Krueger, D. A., Kupina, ; S, Martin, ; S K, Martinsen, ; B K, Miller, T. C., Paquette, ; F, Ryabkova, ; A, Skrede, ; G, Trenn, ; U, & Wightman, J. D. (2005). *Determination of Total Monomeric Anthocyanin Pigment Content of Fruit Juices, Beverages, Natural Colorants, and Wines by the pH Differential Method: Collaborative Study*. https://academic.oup.com/jaoac/article/88/5/1269/5657437

Li, H.-L. (1974). An Archaeological and Historical Account of Cannabis in China. *Economic Botany*, *28*(4), 437–448. http://www.jstor.org/stable/4253540

Lin-Wang, K., Micheletti, D., Palmer, J., Volz, R., Lozano, L., Espley, R., Hellens, R. P., Chagnè, D., Rowan, D. D., Troggio, M., Iglesias, I., & Allan, A. C. (2011). High temperature reduces apple fruit colour via modulation of the anthocyanin regulatory complex. *Plant, Cell and Environment*, *34*(7), 1176–1190. https://doi.org/10.1111/j.1365-3040.2011.02316.x

Livingston, S. J., Quilichini, T. D., Booth, J. K., Wong, D. C. J., Rensing, K. H., Laflamme-Yonkman, J., Castellarin, S. D., Bohlmann, J., Page, J. E., & Samuels, A. L. (2020). Cannabis glandular trichomes alter morphology and metabolite content during flower maturation. Plant Journal, 101(1), 37–56. https://doi.org/10.1111/tpj.14516

Lubell, J. D., & Brand, M. H. (2018). Foliar sprays of silver thiosulfate produce male flowers on female hemp plants. HortTechnology, 28(6), 743–747. https://doi.org/10.21273/HORTTECH04188-18

Marijuana Policy Project (2022) Cannabis Tax Revenue in States that Regulate Cannabis for Adult Use. Marijuana Policy Project (MPP).

Mercuri, A., Accorsi, C. & Bandini Mazzanti, M. (2002) The long history of *Cannabis* and its cultivation by the Romans in central Italy, shown by pollen records from Lago Albano and Lago di Nemi. *Veget Hist Archaeobot* **11**, 263–276. https://doi.org/10.1007/s003340200039

Mikos, R. A., & Kam, C. D. (2019). Has the "M" word been framed? Marijuana, cannabis, and public opinion. *PLoS ONE*, *14*(10). https://doi.org/10.1371/journal.pone.0224289

National Hemp Report. (2023). https://downloads.usda.library.cornell.edu/usda-esmis/files/gf06h2430/76538f824/w9506f61g/hempan23.pdf

Panche, A. N., Diwan, A. D., & Chandra, S. R. (2016). Flavonoids: An overview. In *Journal of Nutritional Science* (Vol. 5). Cambridge University Press. https://doi.org/10.1017/jns.2016.41

Peterswald, T. J., Mieog, J. C., Azman Halimi, R., Magner, N. J., Trebilco, A., Kretzschmar, T., & Purdy, S. J. (2023). Moving Away from 12:12; the Effect of Different Photoperiods on Biomass Yield and Cannabinoids in Medicinal Cannabis. Plants, 12(5). https://doi.org/10.3390/plants12051061

Razumova, O. v., Alexandrov, O. S., Divashuk, M. G., Sukhorada, T. I., & Karlov, G. I. (2016). Molecular cytogenetic analysis of monoecious hemp (Cannabis sativa L.) cultivars reveals its karyotype variations and sex chromosomes constitution. Protoplasma, 253(3), 895–901. https://doi.org/10.1007/s00709-015-0851-0

Russo, E. B. (2007). History of cannabis and its preparations in saga, science, and sobriquet. In *Chemistry and Biodiversity* (Vol. 4, Issue 8, pp. 1614–1648). https://doi.org/10.1002/cbdv.200790144

Ryz, N. R., Remillard, D. J., & Russo, E. B. (2017). Cannabis Roots: A Traditional Therapy with Future Potential for Treating Inflammation and Pain. In Cannabis and cannabinoid research (Vol. 2, Issue 1, pp. 210–216). NLM (Medline). https://doi.org/10.1089/can.2017.0028

Schwabe, A. L., Hansen, C. J., Hyslop, R. M., & McGlaughlin, M. E. (2021). Comparative Genetic Structure of Cannabis sativa Including Federally Produced, Wild Collected, and Cultivated Samples. Frontiers in Plant Science, 12. https://doi.org/10.3389/fpls.2021.675770

Scurlock, J. A., & Andersen, B. (2010). *Diagnoses in Assyrian and Babylonian Medicine: Ancient Sources, Translations, and Modern Medical Analyses*. University of Illinois Press.

Small, E., & Antle, T. (2003). A preliminary study of pollen dispersal in cannabis sativa in relation to wind direction. *Journal of Industrial Hemp*, *8*(2), 37–50. https://doi.org/10.1300/J237v08n02_03

Shibata, K., Shibata, Y., & Kasiwagi, I. (1913). ). STUDIES ON ANTHOCYANINS- COLOR VARIATION IN ANTHOCYANINS. In *Sitzb. Akad. Wiss* (Vol. 401, Issue 8). https://pubs.acs.org/sharingguidelines

Shi, M.-Z., & Xie, D.-Y. (2014). reprints@benthamscience.net Recent Patents Biosynthesis and Metabolic Engineering of Anthocyanins in Arabidopsis thaliana. In *Biotechnology* (Vol. 8). http://dx.doi.org/10.2174/1872208307666131218123538

Sondheimer, E., & Kertesz, Z.I. (1948) Anthocyanin Pigments. *Anal. Chem.* **20**, 245–248

Spitzer-Rimon, B., Duchin, S., Bernstein, N., & Kamenetsky, R. (2019). Architecture and florogenesis in female Cannabis sativa plants. Frontiers in Plant Science, 10. https://doi.org/10.3389/fpls.2019.00350

Tanney, C. A. S., Backer, R., Geitmann, A., & Smith, D. L. (2021). Cannabis Glandular Trichomes: A Cellular Metabolite Factory. In Frontiers in Plant Science (Vol. 12). Frontiers Media S.A. https://doi.org/10.3389/fpls.2021.721986

Xu, W., Dubos, C., & Lepiniec, L. (2015). Transcriptional control of flavonoid biosynthesis by MYB-bHLH-WDR complexes. In *Trends in Plant Science* (Vol. 20, Issue 3, pp. 176–185). Elsevier Ltd. https://doi.org/10.1016/j.tplants.2014.12.001

Zhang, P., & Zhu, H. (2023). Anthocyanins in Plant Food: Current Status, Genetic Modification, and Future Perspectives. In *Molecules* (Vol. 28, Issue 2). MDPI. https://doi.org/10.3390/molecules28020866

Zhang, Y., Butelli, E., de Stefano, R., Schoonbeek, H. J., Magusin, A., Pagliarani, C., Wellner, N., Hill, L., Orzaez, D., Granell, A., Jones, J. D. G., & Martin, C. (2013). Anthocyanins double the shelf life of tomatoes by delaying overripening and reducing susceptibility to gray mold. *Current Biology*, *23*(12), 1094–1100. https://doi.org/10.1016/j.cub.2013.04.072

Zhang, Q., Chen, X., Guo, H., Trindade, L. M., Salentijn, E. M. J., Guo, R., Guo, M., Xu, Y., & Yang, M. (2018). Latitudinal adaptation and genetic insights into the origins of cannabis sativa L. *Frontiers in Plant Science*, *871*. https://doi.org/10.3389/fpls.2018.01876

Zheng, Y., & Small, E. (2022). Introduction. In Handbook of Cannabis Production in Controlled Environments (pp. 1–11). CRC Press. https://doi.org/10.1201/9781003150442-1

# CHAPTER 2: THE EFFECT OF TEMPERATURE ON *CANNABIS SATIVA* YIELD, CBD CONTENT, AND ANTHOCYANIN ACCUMULATION

Sean Kim, Pawan Basnet, Al Kovaleski, Shelby Ellison

## Abstract

Limited information exists on how temperature affects the yield, cannabidiol (CBD) content, and accumulation of anthocyanins in the inflorescence of *Cannabis sativa*. Understanding how temperature influences these traits will be essential for advancing cultivation practices, meeting market demands, and developing novel cannabis cultivars with improved agronomic, medicinal, and aesthetic attributes. In this study, a day-neutral population with uniform expression of purple pigmentation on the leaves and flowers was used to explore how low temperatures (≤ 22°C) impact floral biomass yields, cannabinoid content, and anthocyanin accumulation in *C. sativa*. Growth chambers, each maintained at a photoperiod of 16 h of light and 8 h of darkness, were used to expose plants to five constant temperature treatments ranging from 0.5°C to 22°C, and two fluctuating temperature treatments between 4°C and 22°C. Data on floral biomass (g), CBD (%), and anthocyanin content (mg/L) in the primary inflorescence of each plant were collected. Total CBD and floral biomass yield exhibited a positive association with increasing temperatures, which is likely associated with an increase of growing degree days (GDD) rather than temperature stimuli. Anthocyanin accumulation was found to be significantly affected by temperature stimuli, exhibiting peak production levels at constant temperatures of 8°C and 15°C. This study proposes that total CBD and floral biomass yield predominantly correlate with plant maturity, whereas anthocyanin accumulation is responsive to variations in environmental temperature. Through modeling anthocyanin concentration, cannabinoid levels, and dry biomass

yield across various temperature treatments, our goal is to provide insights that will help guide strategies to optimize these traits and reveal the physiological mechanisms involved.

## Introduction

*Cannabis sativa* cultivation and breeding efforts, for the floral market class, revolve around focal areas including yield, vigor, disease resistance, cannabinoid content, aroma, flavor, medicinal effects, psychoactive effects, and aesthetic appeal. Understanding the mechanisms governing these traits in *C. sativa* is fundamental for the improvement of existing cannabis cultivars, the development of new cultivars, and optimizing production practices. Cannabis cultivars showcase considerable phenotypic plasticity in response to various environmental factors. Plants in the field encounter diverse biotic and abiotic stresses, leading them to rely on secondary metabolites as defense mechanisms. Various combinations of secondary metabolites create unique chemical profiles and help shape cannabinoid content (Maioli et al., 2022/ Livingston et al., 2020), aroma and flavor (Dias et al., 2021), medicinal effects (Grof, 2018), and aesthetics. Many sought-after compounds (e.g. cannabinoids, terpenes, anthocyanins) in *C. sativa* accumulate in glandular trichomes which are most abundant on and around the inflorescences (Hammond and Mahlberg, 1977; Livingston et al., 2020). Three types of glandular trichomes, capitate-stalked, capitate-sessile, and bulbous can be found on cannabis plants (Hammond and Mahlberg, 1977). The glandular trichomes, containing the desired compounds, are most densely concentrated on the calyces and bracts, however, trichomes can also be present on the sugar leaves (reduced leaves found within the inflorescences), as well as on the larger leaves and stems, although they are typically less abundant in these areas (Hammond and Mahlberg, 1977; Tanney et al., 2021; Maioli et al., 2022). Cannabis produced for the floral market class is typically cultivated in controlled environments such as hoop houses, greenhouses, and indoor facilities. Manipulating these environments to optimize desired traits is a common practice in cannabis cultivation and the focus of many research endeavors. Cannabis inflorescences are harvested and processed into various products such as smokeable flower, concentrates, edibles, drinks, and various forms of consumables. Designing strategies to increase the concentrations of these compounds in cannabis plants offers the possibility of achieving greater yields, while also providing the plant with increased levels of defensive compounds. Optimal growth conditions for cannabis, particularly temperature, are suggested to range between 25-35°C, though this varies significantly based on genetic factors (Chandra et al., 2011). Further investigation into how *C. sativa* responds to environmental stressors, such as shifts in cold temperatures, will be necessary for further elucidating the plant defense mechanisms in this species.

The harvested yield from a cannabis plant will vary greatly depending on the genotype, the environment, and the interaction between the two. When cultivating cannabis for the inflorescence, yield may be quantified by the amount of harvested floral biomass, harvested trichome heads, and/or extracted compounds such as cannabidiol (CBD). The evaluation of these metrics varies based on the intended end product. Current investigations to improve cannabis yields include grafting methods (Purdy et al., 2022), pruning techniques (Gaudreau et al., 2020; Massuela et al., 2022), planting dates (Coolong et al., 2023), harvesting times (Massuela et al., 2022), changes in light spectra (Mitchell et al., 2021; Reichel et al., 2021), changes in photoperiod (Peterswald et al., 2023 ), direct seeding versus transplanting (Zheljazkov et al., 2022), and the use of plant growth promoting rhizobacteria (Lyu et al., 2023). Temperature ranges for optimal growing conditions have been investigated (Jin et al., 2019), yet the relationship between temperature stimuli and cannabis yields is still poorly understood.

Secreting glandular plant trichomes produce and store many secondary metabolites and act as the first line of defense against predators (Wagner, 1991). Cannabinoids are stored in these secreting glandular trichomes and there has been longstanding interest in creating methods to manipulate and enhance cannabinoid levels. Studies exploring how cannabinoid synthesis can be influenced include using exogenous hormone treatments such as methyl jasmonate, salicylic acid, and gamma-aminobutyric acid (GABA) which were found to increase CBD and THC accumulation levels (Garrido et al., 2022). Other methods have included inducing polyploidization to increase CBD content (Parsons et al., 2019), using mevinolin to reduce THC content (Mansouri & Salari, 2014), and changing light conditions to influence cannabinoid synthesis in *C. sativa* (Islam et al., 2021; Xie et al., 2023). Galic et al. (2022) found a decrease in total CBD and THC content when plants are exposed to cold-acclimated conditions Other findings include a link between herbicides and decreased cannabinoid content (Toth et al., 2021) and increases in Δ9-tetrahydrocannabinol with the use of rock phosphate dust (De Prato et al., 2023). Kotiranta *et al.* (2024) found high red:far red ratio treatments increase CBD, tetrahydrocannabivarin acid (THCVA), and cannabigerolic acid (CBGA) when compared with low red:far red ratio treatments (Kotiranta et al., 2024). Increasing our understanding of this subject by examining the influence of low temperatures on CBD concentration in *C. sativa* will improve our insight into the mechanisms regulating cannabinoid synthesis, thereby assisting in the refinement of production strategies for cultivating these compounds.

Anthocyanins, widely distributed throughout the plant kingdom, are water-soluble compounds that benefit both plant and human health (Castañeda-Ovando et al., 2009; Robinson and Robinson, 1933; Khoo et al., 2017). These molecules, mostly accumulate in the epidermal layer (Chaves et al., 2018), and benefit plants by targeting free radicals and protecting against environmental stresses such as intense ultraviolet (UV) light, cold temperatures, wounding, herbivory, heavy-metal contamination, and nutrient deficiencies (Gould, 2004; Albert et al., 2014). There is also evidence that crops with higher anthocyanin content may experience a significantly prolonged shelf life and exhibit enhanced resistance to pathogens (Bassolino et al., 2013; Zhang et al., 2013). When consumed in large amounts, these compounds have been shown to benefit cardiovascular health (Krga & Milenkovic 2019), act as anti-diabetic agents (Oliveira et al., 2020), manage memory deficits, protect against oxidative damage in the brain (Pacheco et al., 2018), exhibit nephroprotective effects (Popović et al., 2019), and have antimicrobial, anticancer, and anti-inflammatory properties (Smeriglio et al., 2016). While numerous anthocyanins exist in nature, only six common aglycone groups; delphinidin, cyanidin, petunidin, pelargonidin, peonidin, and malvidin are found in foods regularly consumed in the US diet (Wu et al., 2006; Gonçalves et al., 2021). Stronger anticancer effects have been observed in cyanidins and peonidins when compared to malvidins, and cyanidins exhibit heightened hepatoprotective and antidiabetic effects when compared to peonidins (He et al., 2021).

The effects of temperature on anthocyanin concentration in plants have been investigated across various plant species. After exposure to low temperatures (12°C), an increase in the expression of early biosynthesis anthocyanin genes (EBGs) and a notable rise in the expression levels of late anthocyanin biosynthesis genes (LBGs) has been observed in purple head Chinese cabbage (He et al., 2020). Exposure to low temperatures (12°C) also results in noticeable up-regulation of the R2R3-MYB transcription factor gene *BrMYB2* and the basic-helix-loop-helix regulatory gene *BrTT8* (He et al., 2020). At temperatures of 12°C, 15°C, and 16°C, parsley, 35S:PAP1 *Arabidopsis*, and crabapple plants exhibit elevated levels of anthocyanin accumulation, respectively (Hasegawa et al., 2001; Rowan et al., 2009; Tian et al., 2015). In contrast, it has been observed that temperatures above 20°C can downregulate the expression of *MYB10*, which in turn reduces anthocyanin accumulation in apples (Lin-Wang et al., 2011). It has also been shown that high temperatures, 26/22 °C day/night, can decrease anthocyanin accumulation by enhancing the expression of *StMYB44* and downregulating the activity of the *DFR* promoter in potatoes (Liu et al., 2019). A consistent finding is that lower temperatures, approximately 20°C or lower, tend to increase anthocyanin production, while higher temperatures, usually above 20°C, can reduce or impede anthocyanin production. This pattern is seen in grapes (Gao-Takai et al., 2019), red oranges (lo Piero et al., 2005), *Mikania micrantha* (Zhang et al., 2019), *Zoysia japonica* (Jin et al., 2022), apple (Lin-Wang et al., 2011), snapdragon (Ichimura et al., 2021), cabbage (He et al., 2020), kale (Zhang et al., 2012) and *Plantago lanceolata* (Stiles et al., 2007). While it is common for anthocyanin levels to increase with decreasing temperatures, this is not universally true, as seen in strawberries, where low temperatures can inhibit the accumulation of anthocyanins (Mao et al., 2022). It is important to recognize that the correlation between temperature and the accumulation of anthocyanins is complex and can be affected by additional factors such as light, nutrient availability, and developmental stage.

The ability to produce anthocyanins increases cannabis' ability to respond effectively to adverse conditions and can provide enhanced protection against environmental stressors. Plants grown in temperate zones and high-altitude areas require the ability to withstand a variety of stressors including extreme temperature changes. While genetics are a key factor, the environment also significantly influences the phenotype and phytochemical composition of a cannabis plant. When using genetically identical plants (clones), *C. sativa* cultivated at high altitudes exhibit a notably higher accumulation of secondary metabolites, particularly terpenes, cannabinoids, and flavonoids, compared to those grown in lowland regions, perhaps due to increased environmental stressors such as UV radiation (Giupponi et al., 2020). Current knowledge surrounding plant secondary metabolite responses to environmental changes in *C. sativa* is scarce and research usually targets cannabinoids, terpenes, and specific flavanols. Further exploration of how temperature influences anthocyanin accumulation in *C. sativa* has the potential to enhance the resilience of emerging cultivars and optimize the yield of these beneficial compounds, thereby contributing to the well-being of both humans and the plant itself.

In this study, we aimed to explore how low temperatures affect the floral biomass yield, cannabidiol (CBD) content, and anthocyanin accumulation in the inflorescence of *C. sativa.* To better understand the effects of temperature on floral biomass yield, cannabinoid production, and anthocyanin accumulation, plants were cultivated under various temperature treatments (0.5°C, 4°C, 8°C, 15°C, 22°C, 8°C fluctuating, 15°C fluctuating), and data on biomass yield (g), CBD (%), and anthocyanin levels (mg/L) in the primary inflorescence of each plant were collected. Employing growth chambers enabled for the evaluation of temperature effects on each trait, without the influence of UV radiation. By modeling anthocyanin concentration, cannabinoid levels, and yield at different temperatures, our goal is to offer recommendations for optimization and provide insight into the physiological mechanisms governing these processes.

## Material and Methods

<u>Plant materials</u>

The cultivar used in all studies was created from crossing a purple female phenotype of 118 Early Harvest, a high cannabidiol (CBD), day-neutral cultivar (7-Mile Farms) to a green male phenotype of Cherry Wine 307, a high CBD, day-neutral cultivar (HempLogic). From this initial cross, two more generations of selection of the intercrossed offspring were made to create a day-neutral population with a uniform expression of purple pigment on the leaves and flowers. For the first experiment, 180 plants were grown in cone-tainers at the Walnut Street Greenhouse at The University of Wisconsin - Madison (Madison, WI, USA) from February 20$^{th}$ – April 3$^{rd}$, 2023, with an average temperature of 24.4°C and an average humidity of 26.8%. Subsequently, for the second experiment, 200 plants were grown in cone-tainers at the same location from April 3rd – May 15th, 2023, with an average temperature of 25.5°C and an average humidity of 28.1%. All male plants were removed during this process. The remaining female plants were grown in the greenhouse for 42 days, until approximately 15 days after female flower initiation, before entering their respective treatments. At this point, the plants showed no sign of purple pigmentation.

Experimental design

A randomized complete block design (RCBD) was used, where individual plants were randomly distributed in the growth chamber to minimize the influence of temperature and light on localized plant response, and blocks consisted of two replications over time. An experimental unit within each replicate consisted of a single plant grown inside a cone-tainer, with ten (or more) plants per treatment. Reported means in tables and figures represent the means of two repeated temperature experiments. From each replicated experiment, floral biomass yield, cannabinoid content, and anthocyanin content was measured and recorded (Supplementary Table 2.1). The first experiment consisted of 75 plants randomized across five temperature treatments (15 plants per treatment) of 0.5°, 4°, 8°, 15°, and 22°C, each maintained at a photoperiod of 16 h of light and 8 h of darkness. The second experiment mirrored the first except for 13 plants per treatment and the inclusion of two fluctuating temperature treatments. One fluctuating temperature treatment was 22°C for 5 h and 4°C for 19 h, averaging 7.75°C (hereon referred to as 8°C fluctuating), while the other was 22°C for 15 h and 4°C for 9 h, averaging 15.25°C (hereon referred to as 15°C fluctuating). Plants were grown in their respective growth chamber using LED lights for 30 days before data collection.

<u>Biomass analysis</u>

To calculate the floral biomass of each sample, the top 6cm of each plant was harvested, lyophilized, and weighed. Subsequently, the remaining flower and leaf tissue from each plant was dried at 30°C, and floral and leaf tissue was removed from stems, and weighed. The two weights were summed and the total biomass weight (g) for each plant was determined.

<u>Cannabinoid analysis</u>

At harvest, tissue from the top 6cm of the primary inflorescence was processed for total CBD content analysis using Ultra Performance Liquid Chromatography (UPLC) by the University of Wisconsin, Madison, Wisconsin Crop Innovation Center (Madison, WI, USA). For each sample, 20 mg of dried, milled tissue was mixed with 1.0 mL extraction solvent (8:2 acetonitrile to methanol) in a 1.5 mL centrifuge tube, containing a ceramic homogenizer, by high-speed shaking at room temperature with a vortex for 10 min. Each sample was then centrifuged for 10 min at 3000 Relative Centrifugal Force (RCF) and 125 µL was transferred to an amber microcentrifuge vial containing 875 µL of extraction solvent (a 1:8 dilution). Samples were filtered using a 0.45 µm regenerated cellulose filter vial and subjected to UPLC analysis (Agilent 1290 Infinity II) using an InfinityLab Poroshell 120 EC-C18 3 x 100 mm column heated at 35 °C. Samples were injected and eluted at a flow rate of 1.0 mL/minute with a changing gradient to match elution: 30:70 water:acetonitrile (0.05% formic acid in both) to 28:72 water:acetonitrile at 1.95 min then an immediate switch to 22:78 water:acetonitrile to 18:82 water:acetonitrile at 4.00 min, ending with 100% acetonitrile at 5.00 min. Absorbance was measured at 220 nm. The following standards were used as calibrants: Tetrahydrocannabinolic acid (THCA), Δ9-THC, cannabidiolic acid (CBDA), CBD, cannabichromenic acid (CBCA), cannabichromene (CBC), cannabigerolic acid (CBGA), cannabigerol (CBG), cannabinol (CBN), and Δ8-THC (Sigma

Aldrich, St. Louis, MO, USA). Cannabinoid content was calculated as Total CBD = CBD + (CBDA × 0.877) in accordance with the USDA Hemp Final Rule.

Total anthocyanin score

Leaf and floral tissue from each plant were visually assessed and given a score of 0 (green/no pigmentation), 1 (lilac/pink), 2 (magenta/reddish), and 3 (purple/dark purple) (Picture 1.1), depending on the shade of the tissue. A total percent anthocyanin coverage of the entire plant was also recorded. These scores were used together to calculate the total anthocyanin score for each plant using the following equation:

Total Anthocyanin Score = (Leaf score + Flower score) x Percent coverage

<u>Total monomeric anthocyanin quantification</u>

The top 6 cm of the terminal inflorescence was excised, placed in a plastic bag, and subsequently lyophilized. Once dried, stems were removed, samples were ground into a fine powder, and 0.1g of ground tissue was weighed into an amber vial. Total anthocyanins were extracted by adding 2 ml of a 2% formic acid in methanol solution to each amber vial, which was then left overnight at 3°C. After the overnight extraction, the amber vials underwent centrifugation to separate particulate matter from the extracted solution. The supernatant from each sample was subjected to a 4-fold dilution using 2% formic acid dissolved in methanol before being analyzed via spectroscopy. The total monomeric anthocyanin content was determined using the pH differential method (Lee et al., 2005) with some modifications. An aliquot (50ul) of the 4-fold diluted anthocyanin sample was mixed with 150ul of pH 1.0 buffer (potassium chloride, 0.025M) and pH 4.5 buffer (sodium acetate, 0.4M) solutions, respectively, and equilibrated for 30 min at room temperature. An Agilent BioTek 800 TS Absorbance reader was used to measure the absorbance of 96-well plates at 515nm and 690nm, using deionized (D.I.) water as a blank. Total monomeric anthocyanin content was calculated as cyanidin-3-glucoside equivalents using the following equation:

Anthocyanin pigment (cyanidin-3-glucoside equivalents mg/L) = $\frac{A\ x\ MW\ x\ DF\ x\ 10^3}{\varepsilon\ x\ l}$

Where A = (A515nm – A690nm) at pH 1.0 – (A515nm – A690nm) at pH 4.5; MW (molecular weight) = 449.2 g/mol for cyanidin-3-glucoside; DF = dilution factor; l = pathlength in cm; ε = 26900 molar extinction coefficient, in L & mol$^{-1}$ & cm$^{-1}$, for cyd-3-glu, and $10^3$ = factor for conversion from g to mg.

Statistical analysis

All statistical analyses were conducted in R (R 4.1.1). The effects of treatments on total dry weight (TDW), total CBD (TCBD), and total monomeric anthocyanins (TMA) were evaluated as inflorescence dry weight (g), CBD percentage on a dry weight basis, and cyanidin-3-glucoside equivalents (mg/L), respectively. An outlier test was conducted using Rosner's generalized extreme studentized deviate test in the EnvStats package, and outliers were removed manually (Millard 2014). Correlation analyses were performed using the Pearson's correlation test and a 2-tailed significance level of 5%. Data visualization for correlation plots was conducted using the 'ggplot2' package (Wickham 2009).

For each response variable, TDW, TCBD, and TMA, a two-way ANOVA was used to look at the effect of two factors – Temperature (0.5°C, 4°C, 8°, 8°fluctuating, 15°C, 15°C fluctuating, 22°C) and Condition (fluctuating or constant) – as well as the interaction. For TDW and TCBD, there were no significant effects attributed to Condition or the interaction of Temperature and

Condition (Table 2.1), so average temperatures were used as descriptors for fluctuating treatments, and Condition was removed from the model. Regressions were analyzed as linear-mixed-effect models using the lmer function in lme4 (Bates et al. 2015). When effects were found to be significant, pairwise comparisons for the slope coefficients were run using Fisher's Least Significant Difference (lsmeans, emmeans package, Lenth et al. 2023).

Both TDW and TCBD were analyzed with a generalized linear-mixed effect model with temperature as a fixed effect and Repeat as a random effect. Regressions for TDW and TCBD were analyzed using the lme model in the 'car' package (Fox & Weisberg, 2019). A one-way ANOVA was used to assess the overall significance of Temperature on TDW and TCBD while accounting for the variability introduced by the random effect of Repeat. The anova function in R was used to conduct hypothesis tests for the coefficients in the TDW and TCBD models.

A one-way ANOVA was used to analyze the effect of temperature on TMA. Temperature and Temperature2 (representing temperature squared values) were treated as continuous predictors in the model. Incorporating Temperature2 in the model addresses the nonlinear effects of anthocyanin accumulation in response to temperature, ensuring accurate analysis and correction for temperature dynamics. Condition is a binary variable, representing whether the environmental temperature was constant or fluctuating. No significant effects were detected for the interaction between Temperature and Condition, resulting in its removal from the model. When the condition is fluctuating, we include the Condition variable as a predictor in our model. Conversely, when the condition remains constant, we do not include Condition in the model. This approach allows us to account for the influence of fluctuating conditions on TMA while maintaining model simplicity in instances where the condition remains constant. Coefficients were obtained using the summary function in R. For each ANOVA, the significance level was set to 5%. If the ANOVA showed significance between treatments, pairwise comparisons for treatment means were run using a Tukey's post-hoc test ($p \leq 0.05$).

## Results

The effect of temperature on biomass yield

Average total dry weight ranged from 1.01g to 2.07g with 0.5°C resulting in the lowest dry weight and 22°C resulting in the highest dry weight (Table 2.1). Temperature had a significant effect on biomass yield (p-value < .0001) (Table 2.2). Plants exposed to fluctuating temperature treatments exhibited no significant differences in TDW when compared to plants exposed to equivalent constant temperature conditions of 8°C and 15°C (Figure 2.1). Total dry weight exhibited a positive correlation with increasing temperatures ranging from 0.5°C to 22°C, and there was an observed increase in 0.048g dried flower per degree increase of temperature.

The effect of temperature on cannabidiol

Average total CBD percentage ranged from 3.42% to 5.16% with 8°C resulting in the lowest concentration of CBD and 22°C resulting in the highest concentration (Table 2.1). CBD percentage was significantly affected by temperature (p-value < .0001) (Table 2.2). Plants exposed to fluctuating temperature treatments with an average temperature of 8°C and 15°C displayed total CBD percentages comparable to those recorded in plants cultivated under constant temperature conditions of 8°C and 15°C (Figure 2.2 and Table 2.2). Total CBD exhibited a positive correlation with increasing temperatures ranging from 0.5°C to 22°C and there was an observed increase of 0.0879% in total CBD with every degree C increase in temperature.

The effect of temperature on anthocyanins

Total anthocyanin score

Plants grown in constant temperatures of 8°C and 15°C expressed the highest levels of purple pigmentation with scores of 534.1 and 532.5 respectively, while plants subject to a constant 0.5°C expressed the lowest amount of pigmentation with an average score of 19.4 (Table 2.1 and Figure 2.3). The visual rating for anthocyanin accumulation was significantly influenced by the temperature treatments (p-value < 0.001) (Table 2.2 and Figure 2.3). Both temperature and fluctuating conditions had a significant effect on visual pigment scores (p-value < 0.001) (Table 2.2).

Total monomeric anthocyanins

Total monomeric anthocyanin (TMA) levels ranged from 0 mg/L to 150 mg/L. Plants grown at constant temperatures of 8°C and 15°C had the highest levels of total monomeric anthocyanins with an average of 67.86 mg/L and 57.71 mg/L respectively (Table 2.1). Plants grown in constant temperatures of 0.5°C and 22°C accumulated the least amount of anthocyanins when compared to all other treatments. Plants grown in fluctuating temperature treatments averaging 8°C and 15°C, were significantly different from the 0.5°C, 8°C and 15°C treatments when comparing total monomeric anthocyanin levels (Table 2.2 and Figure 2.4). The prediction model that was derived for total monomeric anthocyanins is as follows:

$$TMA = -2.7 + 12.33(Temperature) - 0.528(Temperature^2) - 32.53(if\ fluctuating)$$

Correlations between Traits

A strong correlation was found between our visual score (TAS) and spectroscopy results (TMA) in both repeated studies (Figure 2.5.). The strong positive correlation between total anthocyanin score (TAS) and total monomeric anthocyanins (TMA) was 0.7 for repeat 1 (p-value < 0.001) and 0.8 for repeat 2 (p-value <0.001) (Figure 2.5). A positive correlation between TAS and TDW was observed in repeat 1 and 2 with correlation coefficients of 0.40 and 0.47 respectively (p-value < 0.001) (Figure 2.5). A correlation between TCBD and TDW was observed in repeat 1 and 2 with correlation coefficients of 0.61 (p-value < 0.001) and 0.26 (p-value < 0.05) respectively (Figure 2.5). No other strong correlations were found when comparing TDW, TCBD, TMA, and TAS (Figure 2.5)

## Discussion

Growing degree days influence biomass and cannabinoid content but not anthocyanins

Both extreme low and extreme high temperatures have been shown to negatively affect the growth of *C. sativa* with an optimal growing temperature falling between 25°C – 35°C (Chandra et al., 2011; Jin et al., 2019 ). The optimal temperature ranges for growth can vary between drug-type cannabis and fiber types, with cultivar selection being a key determinant (Chandra et al., 2011). In our study, temperature increases, in a range from 0.5°C to 22°C, appear to have a positive influence on both biomass and CBD concentrations in the primary inflorescence. Past studies have demonstrated that temperature increases, to an extent, have been shown to increase photosynthetic assimilation and biomass production (Chandra et al., 2008; Werf et al., 1995; Jin et al., 2019). Field observations suggest that temperature variation does not significantly affect THC and CBD percentages, whereas growing degree days (GDD) exhibit a positive correlation with these traits (Sikora et al., 2011). Our observations align with this phenomenon as demonstrated by the inclusion of two fluctuating temperature treatments. Plants subjected to fluctuating temperature treatments, reaching maturity equal to those in constant temperature treatments, exhibited no significant differences in CBD percentages. CBD content remained consistent among plants reaching equivalent maturity, suggesting that the cold temperature stimulus of 4°C did not influence CBD synthesis. A similar trend was observed with total dry weight (biomass), and plants exposed to fluctuating temperature treatments exhibited no significant differences compared to those cultivated under constant temperature conditions. These findings suggest that plant maturity plays a predominant role in shaping CBD content and total biomass, rather than environmental temperatures. If equal GDD was achieved for all plants in this study, we hypothesize that individuals from each treatment would exhibit no significant differences in total CBD concentration and floral biomass yield. To test this hypothesis, it is essential that plants from all treatments achieve equal maturity (equal GDD) before being assessed to elucidate any influence of temperature on biomass and cannabinoid concentration.

Anthocyanin production peaks before biomass and cannabinoids

The optimal temperature range for anthocyanin production was found to be distinct from that required for the growth of the inflorescence and the synthesis of cannabinoids (Figure 2.6). Observing maximum anthocyanin levels at 8°C and 15°C, along with declines at 0.5°C and 22°C, and consistent increases in total CBD and total dry weight across these temperatures, suggests distinct temperature-dependent regulatory pathways for anthocyanin biosynthesis in *C. sativa*, separate from those influencing biomass and CBD biosynthesis (Figure 2.6). If the desired goal is to obtain the highest amount of anthocyanin concentration per gram of dried flower, exposing cannabis plants to temperatures between 8°C - 15°C may be an appropriate range. Additional research incorporating a broader span of temperatures with narrower intervals will enhance the efficiency of addressing this subject. Examining the minimal stimulus required to induce heightened anthocyanin levels in *C. sativa* will also aid in developing strategies to maximize the amount of purple pigments in the inflorescence without any significant trade-offs in yield or cannabinoid percentages. To grasp the full extent of the mechanisms governing anthocyanin accumulation in response to temperature changes, it is necessary to investigate a broader range of genotypes as well.

Temperature stimuli influences anthocyanin accumulation in *C. sativa*

Two fluctuating growth chambers were introduced in the second experiment, with average temperatures of 8°C and 15°C, fluctuating between 4°C and 22°C, to investigate whether temperature stimuli or maturity has the most significant effect on anthocyanin accumulation. Plants in the fluctuating treatments, exposed to an average temperature of approximately 8°C (22°C for 5 h & 4°C for 19 h) and 15°C (22°C for 15 h & 4°C for 9 h), exhibited biomass levels similar to plants exposed to constant temperatures of 8°C and 15°C (Figure 2.1), while exhibiting total monomeric anthocyanin levels similar to plants exposed to constant 4°C (Figure 2.4). This indicates that fluctuating temperature conditions did not impede the maturity of the plants when compared to constant temperature conditions, suggesting that the reduction in anthocyanin accumulation in plants grown at 4°C, relative to those at 8°C or 15°C, is likely due to temperature stimuli rather than a lack of growing degree days (GDD). The experimental groups subjected to fluctuating temperature conditions between 4°C and 22°C, showed no significant differences in total anthocyanin content when compared to specimens cultivated under the constant 4°C conditions; however, there was a significant difference in total anthocyanin content when comparing with plants subjected to constant 8°C and 15°C conditions (Figure 2.4). These results revealed that the observed effects were attributable to temperature stimuli rather than the maturity of the plants.

Strong correlation between visual scores and calculated total monomeric anthocyanins

The strong correlation between our visual score and total monomeric anthocyanins shows promise for an affordable visual assessment of anthocyanin accumulation in *C. sativa,* eliminating the necessity for specialized equipment or costly instruments. Developing a protocol for quick and accurate phenotyping of purple pigmented cannabis cultivars, along with predictive assessments of anthocyanin content, will offer significant utility to breeders, farmers, and researchers. The positive correlation (0.7-0.8) observed between our visual ratings and the values obtained via spectrophotometry indicates potential for establishing such a protocol. Visual scores, when compared to spectroscopy results, were shown to have inflated values. The visual anthocyanin score may be somewhat inflated due to the limitation of visually assessing anthocyanins, which predominantly exist in the epidermal layer of plants. This method solely evaluates the exterior appearance of the plant, neglecting the anthocyanin content present throughout the entire plant. Additionally, it should be acknowledged that the correlation between visual scores and spectroscopy readings may become less accurate as the plant starts to senesce, highlighting the importance of assessing plants at equivalent stages of maturity.

<u>The interactions and implications of this data</u>

Our results demonstrate how anthocyanin accumulation, total biomass, and total CBD respond to relatively cold temperatures (compared to the industry standard) in *C. sativa*. Optimal growing temperatures for photosynthesis and cannabinoid production do not align with optimal temperatures for anthocyanin production. Our findings suggest that there are distinct physiological mechanisms governing anthocyanin accumulation when compared to those regulating inflorescence biomass and the synthesis of CBD in *C. sativa*. While increasing temperatures may promote floral yield and CBD production due to enhanced metabolic activity, they may also suppress anthocyanin production. Depending on the overall goal, maximizing one or a combination of these traits may be desired. Understanding the plants' response to temperature stimuli allows indoor and greenhouse growers to manipulate their environment to optimize these traits, while also equipping outdoor growers with insights to effectively oversee their operations, such as determining optimal harvest times or adjusting environments to regulate temperatures. To assess the potential protective role of anthocyanins in *C. sativa*, plants with both high and low anthocyanin content should be subjected to varying stressors and responses should be compared to investigate whether anthocyanins confer any protective benefits, as hypothesized.

## Conclusions

Understanding the effects of temperature stimuli on secondary metabolite production and overall metabolic processes in *C. sativa* is essential for improving cultivation practices in both controlled environments and field conditions. To better understand the influence of temperature-related effects on anthocyanin accumulation in *C. sativa*, a wider range of temperatures with narrower temperature intervals should be tested. Anthocyanin biosynthesis can be complex due to the involvement of multiple genes and regulatory factors, intricate metabolic pathways, and sensitivity to various environmental cues. Further investigation is necessary to elucidate how the interaction of environmental stimuli influences anthocyanin biosynthesis in *C. sativa*. For example, the accumulation of anthocyanins in "Fuji" apple is influenced by the interaction between low nighttime temperatures and sunlight intensity, with low sunlight intensity and low nighttime temperatures promoting anthocyanin accumulation, while higher sunlight intensity in conjunction with low nighttime temperatures resulted in a significant decrease in anthocyanin concentration (Xue et al., 2021). Optimizing temperatures for anthocyanin accumulation without sacrificing yield or cannabinoid content will also require a better understanding of the minimum stimulus needed to induce anthocyanin biosynthesis. While the base temperature for *C. sativa* remains largely unexplored, observations reported it to be 1°C in the field and 5.7°C in growth chambers (Werf et al., 1995). Comparing temperature treatments of 0.5°C and 4°C revealed elevated levels of biomass and anthocyanin accumulation, implying ongoing activity of metabolic processes. Our results indicate that metabolic processes persisted at 4°C, suggesting that the base temperature for *C. sativa*, in growth chamber conditions, is lower than what has been previously documented. It is important to acknowledge that the outcomes we observed are likely influenced by the genotype used in our experiments and different cultivars may exhibit distinct responses due to genetic variation. Our findings suggest that anthocyanin biosynthesis operates independently from cannabinoid biosynthesis and other metabolic processes. This research starts to uncover the temperature stimuli needed to induce anthocyanin accumulation in *C. sativa.* Our data offers preliminary prediction models of how these traits may interact when subject to various temperature treatments.

**Figures**

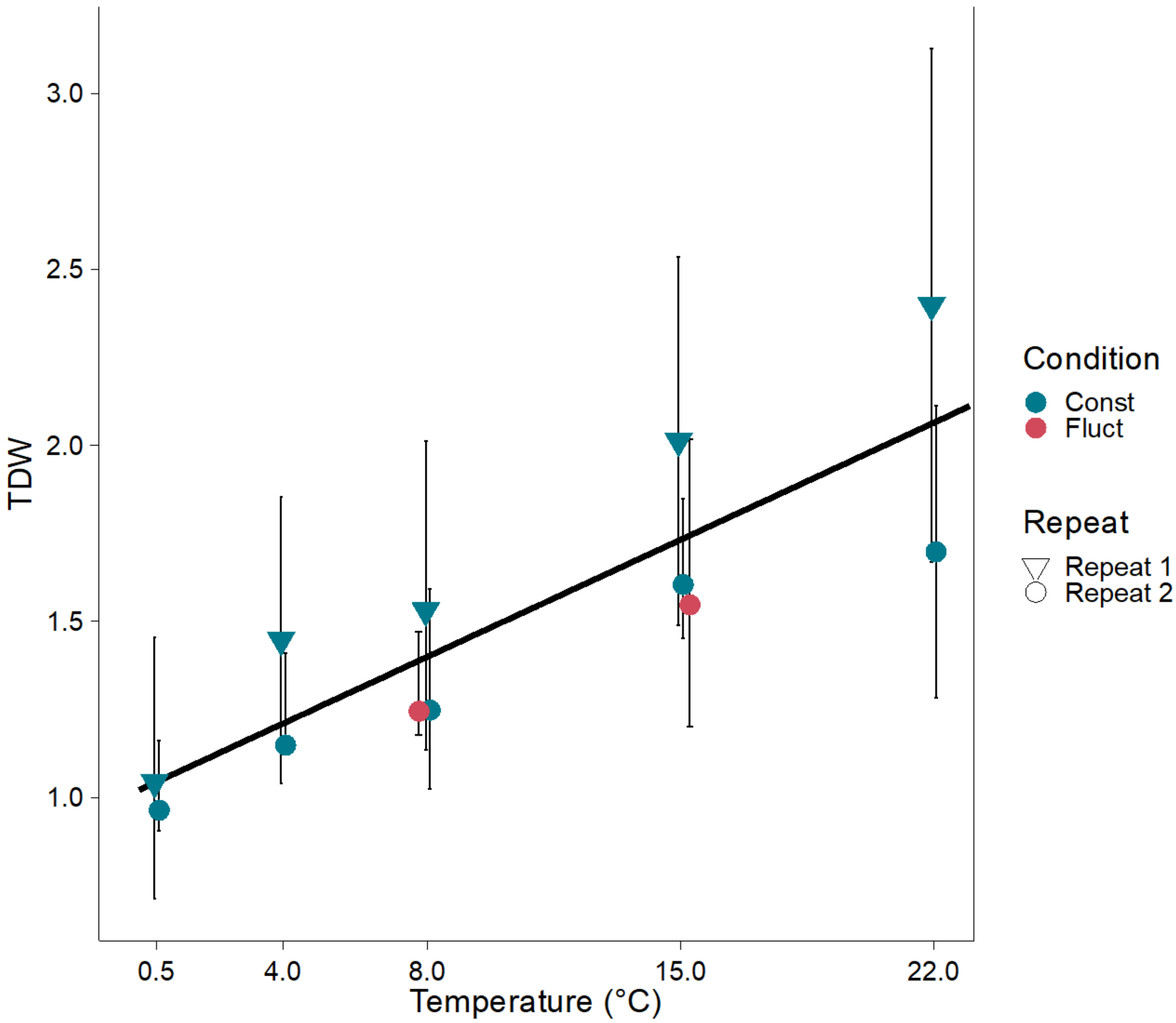


**Figure. 2.1**. Total dry weight (TDW) for two repeated experimental runs (1 and 2). Repeat 2 includes two fluctuating temperatures: 22°C for 5 h and 4°C for 19 h = average temperature of 8°C, and 22°C for 15 h and 4°C for 9 h which = average temperature of 15°C. The trend line represents the linear relationship between temperature and TDW. Error bars show the variation around the mean TDW at different temperatures, while grey shading indicates the confidence interval (95%) for the linear regression line.

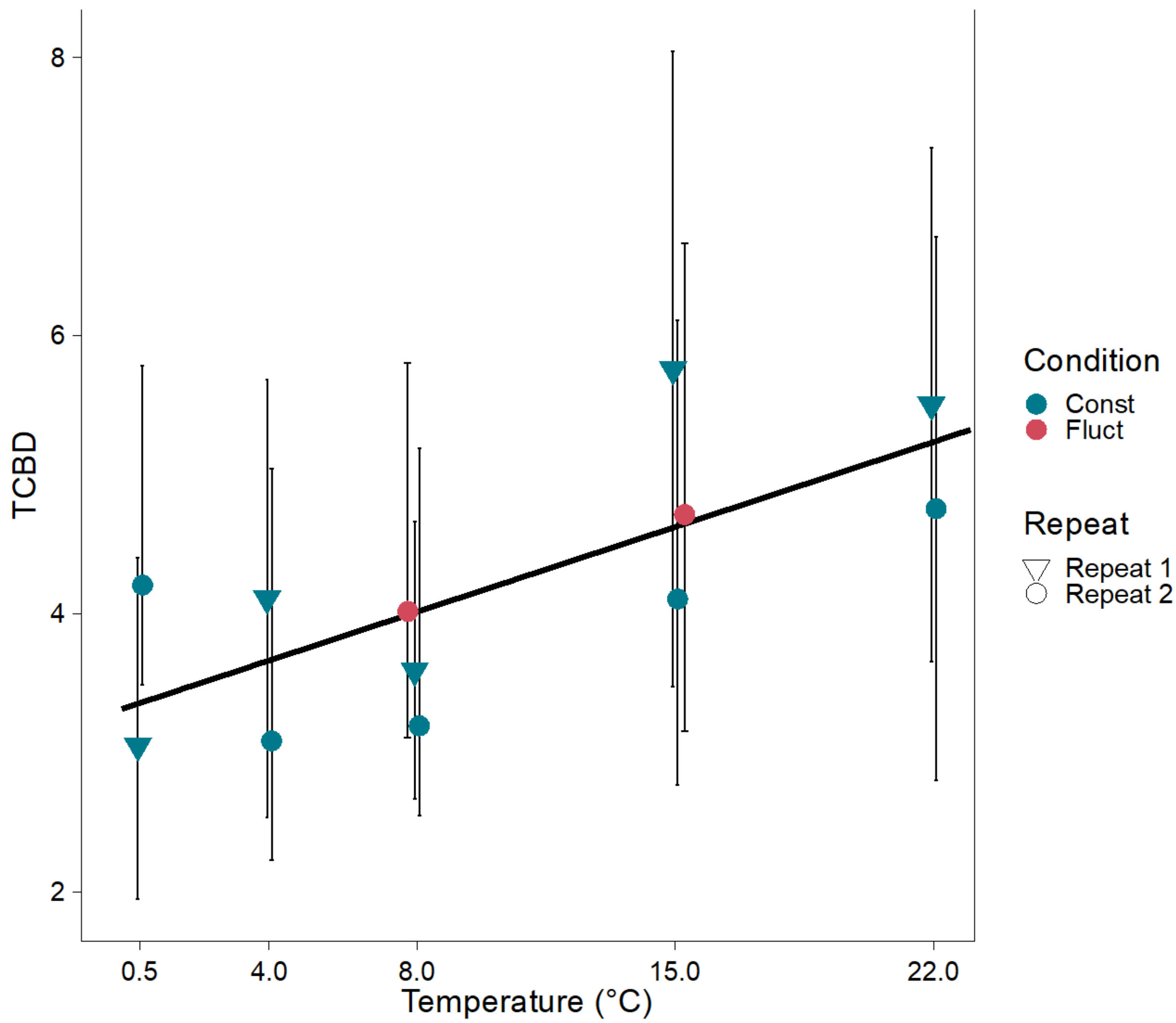


**Figure. 2.2.** Total CBD calculated using HPLC for two repeated experimental runs (1 and 2). Repeat 2 includes 2 fluctuating temperatures: 22°C for 5 h & 4°C for 19 h = average temperature of 8°C, and 22°C for 15 h & 4°C for 9 h which = average temperature of 15°C. The trend line shows the relationship between temperature and TCBD. Error bars show the variation around the mean TDW at different temperatures, while grey shading indicates the confidence interval (95%) for the linear regression line.

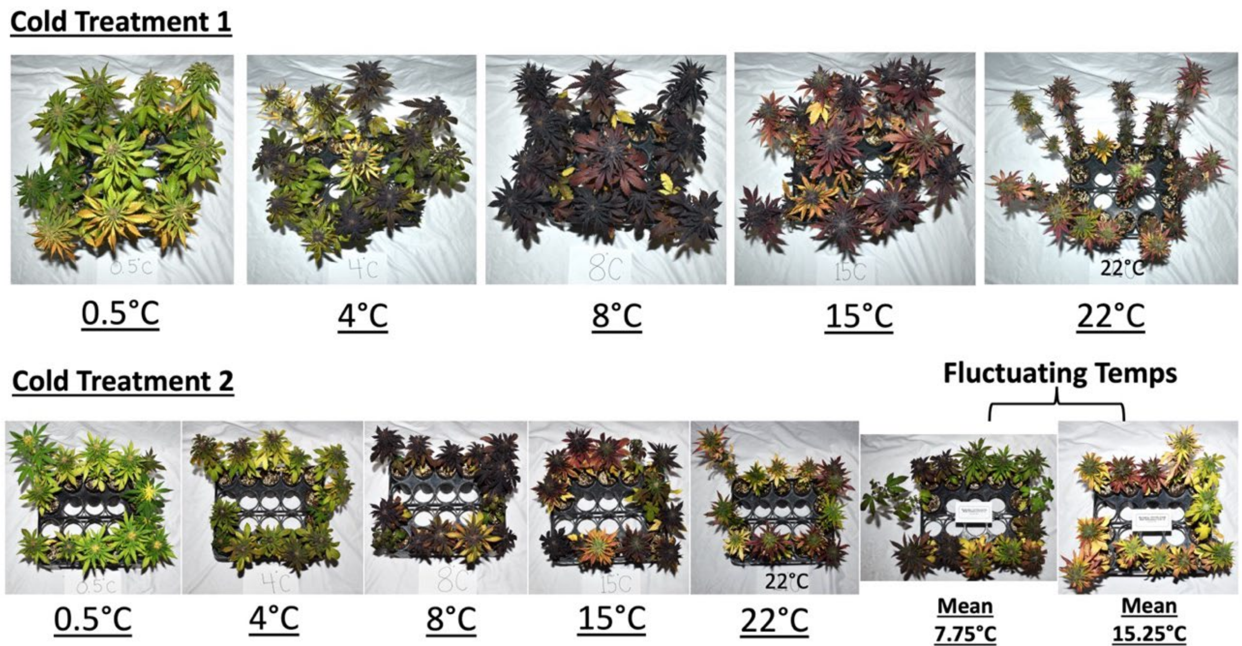


**Figure 2.3**. Photographs of plants after cold temperature treatments. Repeat 1 (top) and repeat 2 (bottom) plants were removed from their respective growth chambers and photographed 23 and 30 days into their treatments, respectively. Each photo represents 13-15 plants.

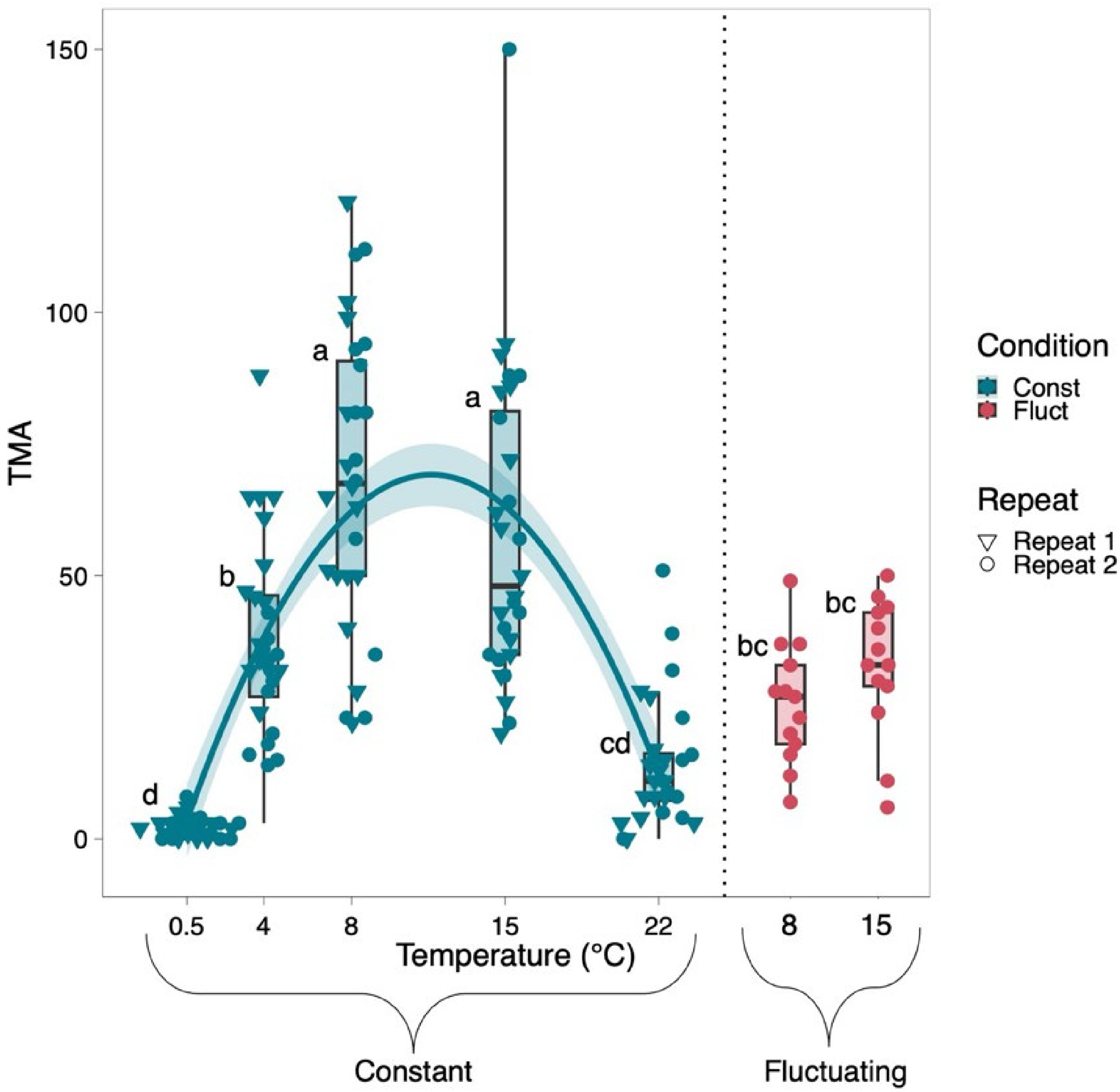


**Figure. 2.4.** Total Monomeric Anthocyanins (TMA) calculated using the pH differential method for two repeated experimental runs (1 & 2). Repeat 2 includes 2 fluctuating temperatures: 22°C for 5 h & 4°C for 19 h = average temp. of 8°C, and 22°C for 15 h & 4°C for 9 h which = average temp. of 15°C. Boxplots display the distribution of TMA levels among individuals exposed to various temperature treatments. Boxplots are colored based on experimental conditions (constant or fluctuating). The trend line represents the quadratic relationship between temperature and TMA while the light blue shading represents the confidence interval (95%) for the trendline.

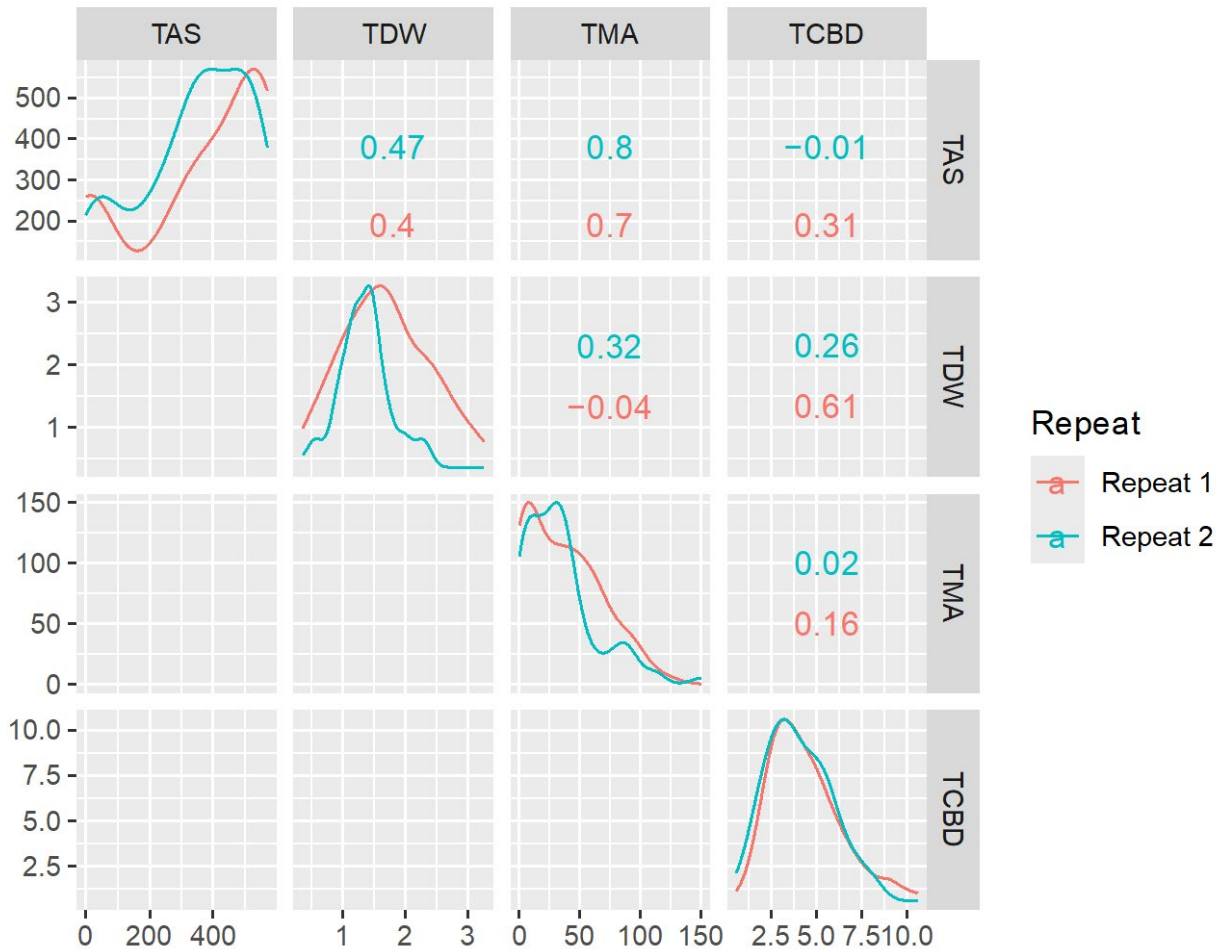


**Figure. 2.5**. Correlation between traits for two repeated cold treatment experiments. TDW: Total Dry Weight (g), TAS: Total Anthocyanin Score, TMA: Total Monomeric Anthocyanins (mg/L), TCBD: Total CBD (%). Significant positive correlations were observed for TAS and TMA ($p < 0.001$), TAS and TDW ($p < 0.001$), and TCBD and TDW ($p < 0.05$).

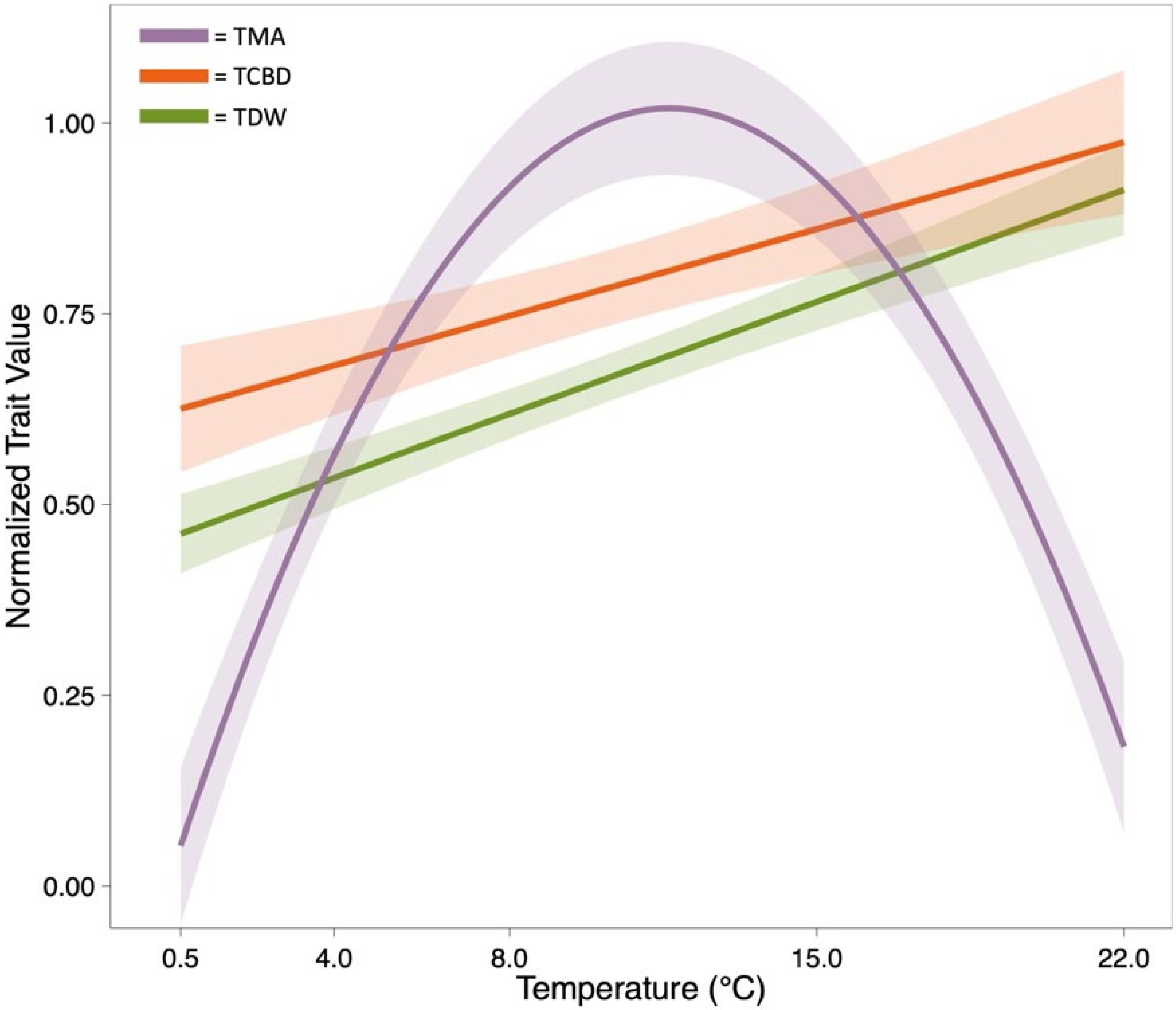


**Figure 2.6.** Normalized trait values for total dry weight (g) (TDW) (Green), total CBD (%) (TCBD) (Orange), and total monomeric anthocyanins (mg/L) (TMA) (Purple) for *C. sativa* plants grown in various temperature treatments. The trendlines represent the overall modeled relationship between temperature and TDW, TCBD, and TMA.

## Tables

**Table 2.1.** Average values of total dry weight (TDW), total CBD (TCBD), total monomeric anthocyanins (TMA), and total anthocyanin score (TAS) for each temperature treatment across two repeated studies. Note: 8°C fluctuating and 15°C fluctuating treatments were only included in the second study.

| *Treatment* | *Total Dry Weight (g) (TDW)* | *Total CBD (%) (TCBD)* | *Total Monomeric Anthocyanins (mg/L) (TMA)* | *Total Anthocyanin Score (TAS)* |
|---|---|---|---|---|
| *0.5°C* | 1.01 | 3.59 | 2.21 | 19.4 |
| *4°C* | 1.31 | 3.65 | 25.8 | 333.2 |
| *8°C* | 1.40 | 3.42 | 67.9 | 532.5 |
| *15°C* | 1.82 | 4.99 | 57.7 | 534.1 |
| *22°C* | 2.07 | 5.16 | 14.2 | 324.3 |
| *8°C fluctuating* | 1.24 | 4.02 | 25.8 | 286.2 |
| *15°C fluctuating* | 1.55 | 4.71 | 32.7 | 400.4 |

**Table 2.2.** Summary of Analysis of Variance (ANOVA) results evaluating the effects of Temperature, Temperature$^2$, Condition, and the interaction of Temperature and Condition on total dry weight (TDW), total CBD (TCBD), total monomeric anthocyanins (TMA), and total anthocyanin score (TAS).

| | *P-value* | | | |
|---|---|---|---|---|
| *Effect* | TDW | TCBD | TMA | TAS |
| *Temperature* | **<0.0001** | **<0.0001** | **<0.0001** | **<0.0001** |
| *Temperature$^2$* | - | - | **<0.0001** | **<0.0001** |
| *Condition* | 0.9340 | 0.8834 | **<0.0001** | **<0.0001** |
| *Temperature: Condition* | 0.7746 | 0.9483 | 0.4688 | 0.2624 |

**Pictures**

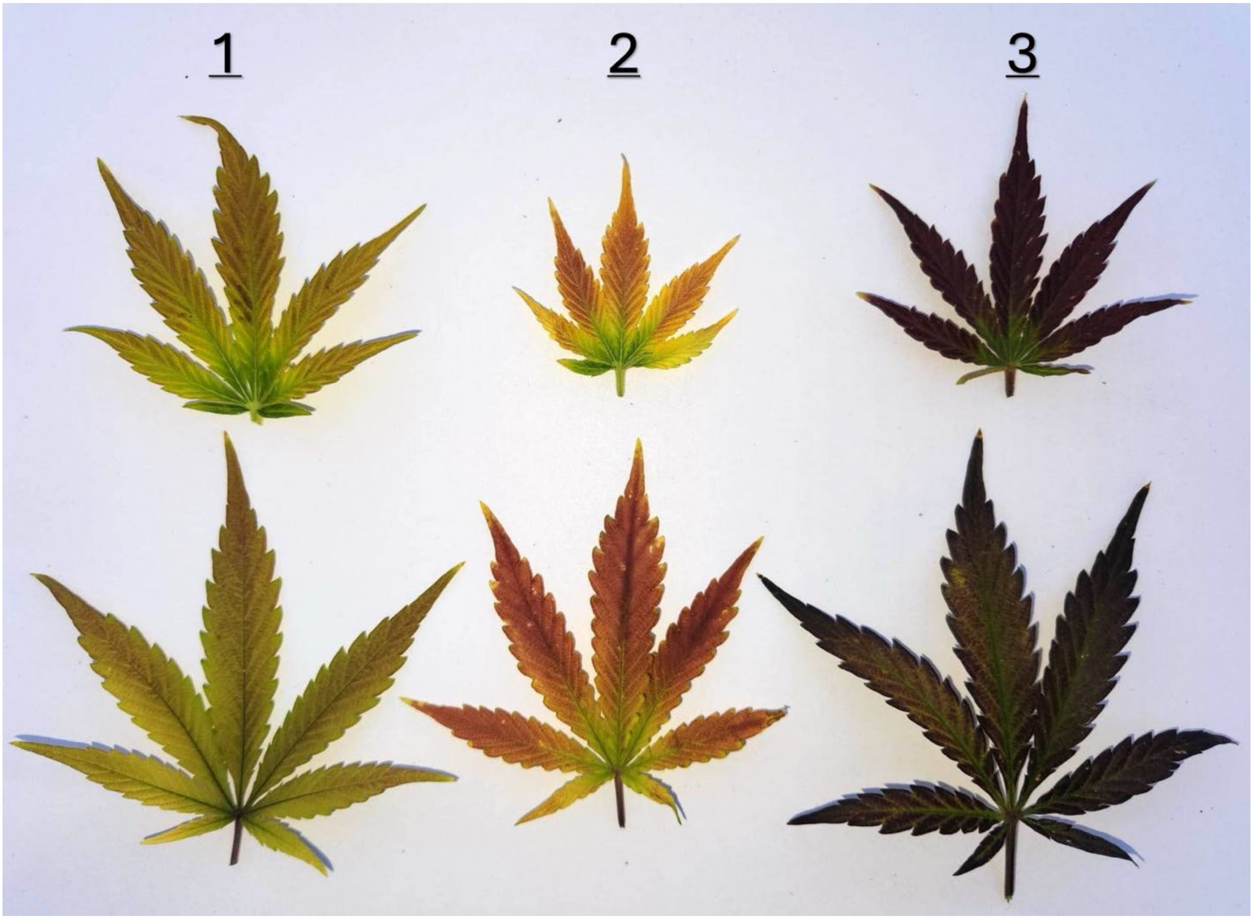


**Picture 2.1.** Leaf tissue representations of the color grade used to obtain visual scores of plants subject to cold treatments. Color hue descriptions are as follows: 1 (lilac/pink), 2 (magenta/reddish), and 3 (purple/dark purple). The total anthocyanin coverage (%) across the entire plant was also quantified. These combined scores facilitated the calculation of the total anthocyanin score (TAS) for each plant.

## Supplemental Tables

**Supplemental Table 2.1.** Raw data from two repeated cold treatment studies. Condition represents whether the environmental temperature was constant or fluctuating. Data was collected on the following traits: total anthocyanin score (TAS), total dry weight (g) (TDW), total monomeric anthocyanins (TMA) evaluated as cyanidin-3-glucoside equivalents (mg/L), and total CBD (%) (TCBD).

| Plant ID | Repeat | Condition | Temperature | TAS | TDW | TMA | TCBD |
|---|---|---|---|---|---|---|---|
| **16** | Repeat 1 | Const | 0.5 | 20 | 1.18 | 3 | 5.84 |
| **17** | Repeat 1 | Const | 0.5 | 10 | 1.52 | 5 | 1.84 |
| **19** | Repeat 1 | Const | 0.5 | 3 | 1.24 | 2 | 2.66 |
| **20** | Repeat 1 | Const | 0.5 | 20 | 1.43 | 6 | 3.4 |
| **22** | Repeat 1 | Const | 0.5 | 15 | 1.37 | 3 | 4.63 |
| **25** | Repeat 1 | Const | 0.5 | 15 | 1.59 | 4 | 3.24 |
| **26** | Repeat 1 | Const | 0.5 | 10 | 1.21 | 1 | 4.97 |
| **32** | Repeat 1 | Const | 0.5 | 3 | 1.05 | 0 | 3.01 |
| **36** | Repeat 1 | Const | 0.5 | 6 | 1.26 | 0 | 3.63 |
| **43** | Repeat 1 | Const | 0.5 | 6 | 0.83 | 2 | 2.53 |
| **58** | Repeat 1 | Const | 0.5 | 4 | 0.93 | 3 | 2.37 |
| **64** | Repeat 1 | Const | 0.5 | 2 | 0.46 | 3 | 1.28 |
| **78** | Repeat 1 | Const | 0.5 | 2 | 0.63 | 1 | 1.97 |
| **79** | Repeat 1 | Const | 0.5 | 2 | 0.38 | 2 | 2.63 |
| **85** | Repeat 1 | Const | 0.5 | 2 | 0.56 | 0 | 1.76 |
| **4** | Repeat 1 | Const | 4 | 160 | 1.6 | 32 | 6.57 |
| **10** | Repeat 1 | Const | 4 | 375 | 1.62 | 37 | 2.8 |
| **27** | Repeat 1 | Const | 4 | 350 | 1.76 | 88 | 6.05 |
| **42** | Repeat 1 | Const | 4 | 325 | 1.72 | 45 | 3.13 |
| **44** | Repeat 1 | Const | 4 | 325 | 1.32 | 32 | 4.72 |
| **48** | Repeat 1 | Const | 4 | 375 | 1.57 | 52 | 5.17 |
| **50** | Repeat 1 | Const | 4 | 250 | 1.2 | 46 | 2.66 |
| **51** | Repeat 1 | Const | 4 | 375 | 1.23 | 65 | 2.55 |
| **52** | Repeat 1 | Const | 4 | 450 | 2.07 | 61 | 6.56 |
| **54** | Repeat 1 | Const | 4 | 250 | 1.29 | 32 | 2.13 |
| **56** | Repeat 1 | Const | 4 | 375 | 1.59 | 47 | 3.79 |
| **57** | Repeat 1 | Const | 4 | 200 | 1.71 | 34 | 4.63 |
| **59** | Repeat 1 | Const | 4 | 375 | 1.74 | 65 | 5.22 |
| **63** | Repeat 1 | Const | 4 | 450 | 0.48 | 24 | 3.65 |

| | | | | | | | |
|---|---|---|---|---|---|---|---|
| **66** | Repeat 1 | Const | 4 | 480 | 0.8 | 65 | 2 |
| **15** | Repeat 1 | Const | 8 | 540 | 1.67 | 40 | 3.67 |
| **23** | Repeat 1 | Const | 8 | 540 | 1.84 | 67 | 2.87 |
| **29** | Repeat 1 | Const | 8 | 570 | 1.55 | 71 | 4.53 |
| **33** | Repeat 1 | Const | 8 | 510 | 1.82 | 50 | 4.68 |
| **34** | Repeat 1 | Const | 8 | 570 | 1.87 | 50 | 6.24 |
| **37** | Repeat 1 | Const | 8 | 510 | 1.59 | 50 | 2.49 |
| **38** | Repeat 1 | Const | 8 | 540 | 1.81 | 22 | 3.7 |
| **39** | Repeat 1 | Const | 8 | 540 | 1.59 | 28 | 3.16 |
| **40** | Repeat 1 | Const | 8 | 510 | 1.88 | 65 | 2.47 |
| **41** | Repeat 1 | Const | 8 | 570 | 1.78 | 81 | 4.1 |
| **46** | Repeat 1 | Const | 8 | 540 | 2.16 | 51 | 3.7 |
| **67** | Repeat 1 | Const | 8 | 540 | 0.93 | 63 | 2.53 |
| **80** | Repeat 1 | Const | 8 | 570 | 0.67 | 121 | 3.33 |
| **81** | Repeat 1 | Const | 8 | 570 | 0.92 | 102 | 3.24 |
| **82** | Repeat 1 | Const | 8 | 570 | 0.88 | 99 | 3.14 |
| **2** | Repeat 1 | Const | 15 | 570 | 2.39 | 35 | 4.16 |
| **3** | Repeat 1 | Const | 15 | 540 | 2.37 | 62 | 10.59 |
| **5** | Repeat 1 | Const | 15 | 540 | 1.86 | 72 | 5.92 |
| **7** | Repeat 1 | Const | 15 | 570 | 2.61 | 26 | 3.49 |
| **9** | Repeat 1 | Const | 15 | 570 | 2.47 | 85 | 4.79 |
| **11** | Repeat 1 | Const | 15 | 570 | 1.94 | 43 | 2.65 |
| **13** | Repeat 1 | Const | 15 | 510 | 2.12 | 20 | 5.06 |
| **14** | Repeat 1 | Const | 15 | 540 | 2.34 | 38 | 4.66 |
| **24** | Repeat 1 | Const | 15 | 570 | 2.5 | 59 | 8.86 |
| **31** | Repeat 1 | Const | 15 | 540 | 1.69 | 50 | 4.53 |
| **47** | Repeat 1 | Const | 15 | 540 | 2.18 | 86 | 7.6 |
| **60** | Repeat 1 | Const | 15 | 570 | 2.31 | 94 | 9.23 |
| **61** | Repeat 1 | Const | 15 | 540 | 1.05 | 46 | 5.46 |
| **76** | Repeat 1 | Const | 15 | 570 | 1.36 | 31 | 4.08 |
| **77** | Repeat 1 | Const | 15 | 540 | 0.99 | 92 | 5.27 |
| **1** | Repeat 1 | Const | 22 | 375 | 3.26 | 8 | 5.75 |
| **6** | Repeat 1 | Const | 22 | 425 | 2.88 | 28 | 7.16 |
| **8** | Repeat 1 | Const | 22 | 375 | 2.8 | 4 | 3.58 |
| **12** | Repeat 1 | Const | 22 | 400 | 2.39 | 27 | 3.37 |

| | | | | | | | |
|---|---|---|---|---|---|---|---|
| **18** | Repeat 1 | Const | 22 | 480 | 2.85 | 13 | 7.45 |
| **21** | Repeat 1 | Const | 22 | 425 | 3.05 | 8 | 8.97 |
| **28** | Repeat 1 | Const | 22 | 400 | 2.53 | 11 | 7.7 |
| **30** | Repeat 1 | Const | 22 | 320 | 2.27 | 14 | 4.04 |
| **35** | Repeat 1 | Const | 22 | 510 | 2.1 | 17 | 3.91 |
| **49** | Repeat 1 | Const | 22 | 260 | 3.17 | 0 | 6.6 |
| **53** | Repeat 1 | Const | 22 | 280 | 2.49 | 3 | 5.36 |
| **55** | Repeat 1 | Const | 22 | 300 | 2.75 | 8 | 6.28 |
| **62** | Repeat 1 | Const | 22 | 350 | 1.24 | 11 | 2.6 |
| **83** | Repeat 1 | Const | 22 | 70 | 0.93 | 3 | 4.44 |
| **86** | Repeat 1 | Const | 22 | 300 | 1.25 | 15 | 5.34 |
| **CT2 1** | Repeat 2 | Const | 0.5 | 60 | 0.89 | 4 | 3.73 |
| **CT2 10** | Repeat 2 | Const | 0.5 | 28 | 1.16 | 0 | 5.93 |
| **CT2 11** | Repeat 2 | Const | 0.5 | 40 | 1.18 | 4 | 6.97 |
| **CT2 12** | Repeat 2 | Const | 0.5 | 5 | 0.98 | 1 | 3.87 |
| **CT2 13** | Repeat 2 | Const | 0.5 | 40 | 1.01 | 3 | 3.96 |
| **CT2 2** | Repeat 2 | Const | 0.5 | 60 | 0.96 | 8 | 4.23 |
| **CT2 3** | Repeat 2 | Const | 0.5 | 0 | 0.94 | 0 | 4.74 |
| **CT2 4** | Repeat 2 | Const | 0.5 | 10 | 1.25 | 1 | 4.39 |
| **CT2 5** | Repeat 2 | Const | 0.5 | 10 | 0.91 | 0 | 5.58 |
| **CT2 6** | Repeat 2 | Const | 0.5 | 0 | 0.59 | 1 | 1.63 |
| **CT2 7** | Repeat 2 | Const | 0.5 | 60 | 0.57 | 2 | 2.04 |
| **CT2 8** | Repeat 2 | Const | 0.5 | 100 | 0.93 | 3 | 4.71 |
| **CT2 9** | Repeat 2 | Const | 0.5 | 10 | 1.16 | 0 | 2.89 |
| **CT2 14** | Repeat 2 | Const | 4 | 360 | 0.5 | 15 | 0.59 |
| **CT2 15** | Repeat 2 | Const | 4 | 330 | 1.13 | 20 | 3.39 |
| **CT2 16** | Repeat 2 | Const | 4 | 360 | 1.2 | 43 | 3.05 |
| **CT2 17** | Repeat 2 | Const | 4 | 390 | 1.37 | 36 | 2.35 |
| **CT2 18** | Repeat 2 | Const | 4 | 360 | 1.29 | 35 | 5.24 |
| **CT2 19** | Repeat 2 | Const | 4 | 75 | 0.36 | 3 | NA |
| **CT2 20** | Repeat 2 | Const | 4 | 300 | 1.27 | 18 | 2.85 |
| **CT2 21** | Repeat 2 | Const | 4 | 270 | 1.39 | 16 | 6.01 |
| **CT2 22** | Repeat 2 | Const | 4 | 300 | 1.02 | 14 | 1.73 |
| **CT2 23** | Repeat 2 | Const | 4 | 330 | 1.47 | 38 | 4.76 |
| **CT2 24** | Repeat 2 | Const | 4 | 360 | 1.3 | 28 | 3.35 |

| | | | | | | | |
|---|---|---|---|---|---|---|---|
| **CT2 25** | Repeat 2 | Const | 4 | 360 | 1.48 | 34 | 1.55 |
| **CT2 26** | Repeat 2 | Const | 4 | 420 | 1.15 | 30 | 2.15 |
| **CT2 27** | Repeat 2 | Const | 8 | 540 | 0.93 | 112 | 4.06 |
| **CT2 28** | Repeat 2 | Const | 8 | 360 | 0.72 | 23 | 1.02 |
| **CT2 29** | Repeat 2 | Const | 8 | 570 | 1.67 | 93 | NA |
| **CT2 30** | Repeat 2 | Const | 8 | 510 | 1.56 | 81 | 1.51 |
| **CT2 31** | Repeat 2 | Const | 8 | 510 | 0.94 | 57 | 1.66 |
| **CT2 32** | Repeat 2 | Const | 8 | 570 | 1.24 | 111 | 5.7 |
| **CT2 33** | Repeat 2 | Const | 8 | 540 | 1.33 | 72 | 5.56 |
| **CT2 34** | Repeat 2 | Const | 8 | 570 | 1.91 | 94 | 2.57 |
| **CT2 35** | Repeat 2 | Const | 8 | 540 | 1.18 | 90 | 1.93 |
| **CT2 36** | Repeat 2 | Const | 8 | 480 | 0.87 | 23 | NA |
| **CT2 37** | Repeat 2 | Const | 8 | 540 | 1.18 | 68 | 3.42 |
| **CT2 38** | Repeat 2 | Const | 8 | 510 | 1.24 | 81 | 3.47 |
| **CT2 39** | Repeat 2 | Const | 8 | 480 | 1.45 | 35 | 4.23 |
| **CT2 40** | Repeat 2 | Const | 15 | 540 | 1.79 | 80 | 4.59 |
| **CT2 41** | Repeat 2 | Const | 15 | 570 | 1.46 | 64 | 3.4 |
| **CT2 42** | Repeat 2 | Const | 15 | 510 | 1.5 | 34 | 2.3 |
| **CT2 43** | Repeat 2 | Const | 15 | 540 | 1.44 | 43 | 5.37 |
| **CT2 44** | Repeat 2 | Const | 15 | 480 | 1.43 | 31 | 1.97 |
| **CT2 45** | Repeat 2 | Const | 15 | 540 | 1.47 | 40 | 5.9 |
| **CT2 46** | Repeat 2 | Const | 15 | 540 | 1.59 | 88 | 8.2 |
| **CT2 47** | Repeat 2 | Const | 15 | 480 | 1.74 | 57 | 2.96 |
| **CT2 48** | Repeat 2 | Const | 15 | 510 | 1.29 | 45 | 2.56 |
| **CT2 49** | Repeat 2 | Const | 15 | 570 | 1.98 | 150 | 3.96 |
| **CT2 50** | Repeat 2 | Const | 15 | 480 | 1.57 | 35 | 5.17 |
| **CT2 51** | Repeat 2 | Const | 15 | 375 | 1.98 | 22 | 3.91 |
| **CT2 52** | Repeat 2 | Const | 15 | 540 | 1.62 | 88 | 3.08 |
| **CT2 79** | Repeat 2 | Const | 22 | 510 | 1.61 | 39 | 2.95 |
| **CT2 80** | Repeat 2 | Const | 22 | 150 | 1.25 | 5 | 5.81 |
| **CT2 81** | Repeat 2 | Const | 22 | 360 | 2 | 23 | 4.09 |
| **CT2 82** | Repeat 2 | Const | 22 | 420 | 1.76 | 51 | 7.29 |
| **CT2 83** | Repeat 2 | Const | 22 | 275 | 1.52 | 15 | 3.4 |
| **CT2 84** | Repeat 2 | Const | 22 | 250 | 1.73 | 0 | 2.13 |
| **CT2 85** | Repeat 2 | Const | 22 | 225 | 1.24 | 8 | 2.95 |

| | | | | | | | |
|---|---|---|---|---|---|---|---|
| **CT2 86** | Repeat 2 | Const | 22 | 480 | 2.23 | 32 | 8.07 |
| **CT2 87** | Repeat 2 | Const | 22 | 300 | 2.28 | 16 | 4.51 |
| **CT2 88** | Repeat 2 | Const | 22 | 160 | 1.54 | 9 | 6.94 |
| **CT2 89** | Repeat 2 | Const | 22 | 275 | 2.38 | 11 | 2.64 |
| **CT2 90** | Repeat 2 | Const | 22 | 180 | 1.12 | 15 | 4.76 |
| **CT2 91** | Repeat 2 | Const | 22 | 225 | 1.41 | 4 | 6.28 |
| **CT2 66** | Repeat 2 | Fluct | 7.75 | 390 | 1.4 | 49 | 3.22116 |
| **CT2 67** | Repeat 2 | Fluct | 7.75 | 420 | 1.44 | 37 | 3.53672 |
| **CT2 68** | Repeat 2 | Fluct | 7.75 | 360 | 1.41 | 23 | 4.58848 |
| **CT2 69** | Repeat 2 | Fluct | 7.75 | 250 | 1.46 | 18 | 4.85773 |
| **CT2 70** | Repeat 2 | Fluct | 7.75 | 360 | 1.37 | 27 | 5.22067 |
| **CT2 71** | Repeat 2 | Fluct | 7.75 | 360 | 1.14 | 28 | 2.70266 |
| **CT2 72** | Repeat 2 | Fluct | 7.75 | 100 | 0.56 | 7 | 1.14561 |
| **CT2 73** | Repeat 2 | Fluct | 7.75 | 250 | 1.42 | 16 | 6.66045 |
| **CT2 74** | Repeat 2 | Fluct | 7.75 | 140 | 1.06 | 12 | 3.34838 |
| **CT2 75** | Repeat 2 | Fluct | 7.75 | 175 | 1.45 | 37 | 3.12207 |
| **CT2 76** | Repeat 2 | Fluct | 7.75 | 330 | 1.26 | 33 | 5.80318 |
| **CT2 77** | Repeat 2 | Fluct | 7.75 | 360 | 1.14 | 28 | 5.95286 |
| **CT2 78** | Repeat 2 | Fluct | 7.75 | 225 | 1.07 | 20 | 2.04828 |
| **CT2 53** | Repeat 2 | Fluct | 15.25 | 480 | 2.33 | 44 | 4.01693 |
| **CT2 54** | Repeat 2 | Fluct | 15.25 | 450 | 2.2 | 33 | 2.52004 |
| **CT2 55** | Repeat 2 | Fluct | 15.25 | 375 | 1.42 | 33 | 7.22905 |
| **CT2 56** | Repeat 2 | Fluct | 15.25 | 450 | 1.24 | 50 | 5.42703 |
| **CT2 57** | Repeat 2 | Fluct | 15.25 | 350 | 1.67 | 24 | 3.85308 |
| **CT2 58** | Repeat 2 | Fluct | 15.25 | 360 | 1.12 | 29 | 6.58943 |
| **CT2 59** | Repeat 2 | Fluct | 15.25 | 220 | 1.07 | 6 | 2.61972 |
| **CT2 60** | Repeat 2 | Fluct | 15.25 | 300 | 0.81 | 11 | 2.36464 |
| **CT2 61** | Repeat 2 | Fluct | 15.25 | 450 | 2.06 | 30 | 5.17596 |
| **CT2 62** | Repeat 2 | Fluct | 15.25 | 450 | 1.52 | 40 | 5.22981 |
| **CT2 63** | Repeat 2 | Fluct | 15.25 | 480 | 1.44 | 46 | 3.23688 |
| **CT2 64** | Repeat 2 | Fluct | 15.25 | 420 | 1.71 | 43 | 4.99056 |
| **CT2 65** | Repeat 2 | Fluct | 15.25 | 420 | 1.52 | 36 | 8.01065 |

## Chapter 2 References

Albert, N. W., Davies, K. M., Lewis, D. H., Zhang, H., Montefiori, M., Brendolise, C., ... & Schwinn, K. E. (2014). A conserved network of transcriptional activators and repressors regulates anthocyanin pigmentation in eudicots. The Plant Cell, 26(3), 962-980.

Bassolino, L., Fulvio, F., Pastore, C., Pasini, F., Gallina Toschi, T., Filippetti, I., & Paris, R. (2023). When Cannabis sativa L. Turns Purple: Biosynthesis and Accumulation of Anthocyanins. *Antioxidants*, *12*(7). https://doi.org/10.3390/antiox12071393

Bates, D., Mächler, M., Bolker, B., & Walker, S. (2015). Fitting Linear Mixed-Effects Models Using lme4. *Journal of Statistical Software*, *67*(1), 1–48. https://doi.org/10.18637/jss.v067.i01

Ben-Shabat, S., Fride, E., Sheskin, T., Tamiri, T., Rhee, M.-H., Vogel, Z., Bisogno, T., de Petrocellis, L., Marzo, V. di, & Mechoulam, R. (1998). An entourage effect: inactive endogenous fatty acid glycerol esters enhance 2-arachidonoyl-glycerol cannabinoid activity. In *European Journal of Pharmacology* (Vol. 353).

Castañeda-Ovando, A., Pacheco-Hernández, M. de L., Páez-Hernández, M. E., Rodríguez, J. A., & Galán-Vidal, C. A. (2009). Chemical studies of anthocyanins: A review. In Food Chemistry (Vol. 113, Issue 4, pp. 859–871). https://doi.org/10.1016/j.foodchem.2008.09.001

Chandra, S., Lata, H., Khan, I. A., & ElSohly, M. A. (2011). Temperature response of photosynthesis in different drug and fiber varieties of Cannabis sativa L. *Physiology and Molecular Biology of Plants*, *17*(3), 297–303. https://doi.org/10.1007/s12298-011-0068-4

Chaves-Silva, S., Santos, A. L. dos, Chalfun-Júnior, A., Zhao, J., Peres, L. E. P., & Benedito, V. A. (2018). Understanding the genetic regulation of anthocyanin biosynthesis in plants – Tools for breeding purple varieties of fruits and vegetables. In Phytochemistry (Vol. 153, pp. 11–27). Elsevier Ltd. https://doi.org/10.1016/j.phytochem.2018.05.013

Choi, K. H., Lee, H. A., Park, M. H., & Han, J. S. (2017). Cyanidin-3-rutinoside increases glucose uptake by activating the PI3K/Akt pathway in 3T3-L1 adipocytes. *Environmental Toxicology and Pharmacology*, *54*, 1–6. https://doi.org/10.1016/j.etap.2017.06.007

Choi, K. H., Park, M. H., Lee, H. A., & Han, J. S. (2018). Cyanidin-3-rutinoside protects INS-1 pancreatic β cells against high glucose-induced glucotoxicity by apoptosis. *Zeitschrift Fur Naturforschung - Section C Journal of Biosciences*, *73*(7–8), 281–289. https://doi.org/10.1515/znc-2017-0172

Christensen, C., Rose, M., Cornett, C., & Allesø, M. (2023). Decoding the Postulated Entourage Effect of Medicinal Cannabis: What It Is and What It Isn't. In *Biomedicines* (Vol. 11, Issue 8). Multidisciplinary Digital Publishing Institute (MDPI). https://doi.org/10.3390/biomedicines11082323

Chandra, S., Lata, H., & ElSohly, M. A. (2017). Cannabis sativa L. - botany and biotechnology. In Cannabis sativa L. - Botany and Biotechnology. Springer International Publishing. https://doi.org/10.1007/978-3-319-54564-6

Chandra, S., Lata, H., Khan, I. A., & Elsohly, M. A. (2008). Photosynthetic response of Cannabis sativa Photosynthetic response of Cannabis sativa L. to variations in photosynthetic photon flux densities, temperature and CO 2 conditions. In Physiol. Mol. Biol. Plants (Vol. 14, Issue 4).

Chandra, S., Lata, H., Khan, I. A., & ElSohly, M. A. (2011). Temperature response of photosynthesis in different drug and fiber varieties of Cannabis sativa L. Physiology and Molecular Biology of Plants, 17(3), 297–303. https://doi.org/10.1007/s12298-011-0068-4

Clarke, R. & Merlin, M. (2013). *Cannabis: Evolution and Ethnobotany*. Berkeley: University of California Press. https://doi-org.ezproxy.library.wisc.edu/10.1525/9780520954571

Coolong, T., Cassity-Duffey, K., & Joy, N. (2023). Role of Planting Date on Yield and Cannabinoid Content of Day-neutral and Photoperiod-sensitive Hemp in Georgia, USA. HortTechnology, 33(1), 138–145. https://doi.org/10.21273/HORTTECH05151-22

De Prato, L., Ansari, O., Hardy, G. E. S. J., Howieson, J., O'Hara, G., & Ruthrof, K. X. (2023). Physiological and cannabinoid responses of hemp (Cannabis sativa) to rock phosphate dust under tropical conditions. *Functional Plant Biology*, *50*(5), 378–389. https://doi.org/10.1071/FP22264

Feng, R., Ni, H. M., Wang, S. Y., Tourkova, I. L., Shurin, M. R., Harada, H., & Yin, X. M. (2007). Cyanidin-3-rutinoside, a natural polyphenol antioxidant, selectively kills leukemic cells by induction of oxidative stress. *Journal of Biological Chemistry*, *282*(18), 13468–13476. https://doi.org/10.1074/jbc.M610616200

Flores-Sanchez, I. J., & Verpoorte, R. (2008). Secondary metabolism in cannabis. *Phytochemistry Reviews*, *7*(3), 615–639. https://doi.org/10.1007/s11101-008-9094-4

Fox J, Weisberg S (2019). *An R Companion to Applied Regression*, Third edition. Sage, Thousand Oaks CA. https://socialsciences.mcmaster.ca/jfox/Books/Companion/.

Galic, A., Grab, H., Kaczmar, N., Maser, K., Miller, W. B., & Smart, L. B. (2022). Effects of Cold Temperature and Acclimation on Cold Tolerance and Cannabinoid Profiles of Cannabis sativa L. (Hemp). Horticulturae, 8(6). https://doi.org/10.3390/horticulturae8060531

Gao-Takai, M., Katayama-Ikegami, A., Matsuda, K., Shindo, H., Uemae, S., & Oyaizu, M. (2019). A low temperature promotes anthocyanin biosynthesis but does not accelerate endogenous abscisic acid accumulation in red-skinned grapes. *Plant Science*, *283*, 165–176. https://doi.org/10.1016/j.plantsci.2019.01.015

Garrido, J., Rico, S., Corral, C., Sánchez, C., Vidal, N., Martínez-Quesada, J. J., & Ferreiro-Vera, C. (2022). Exogenous application of stress-related signaling molecules affect growth and cannabinoid accumulation in medical cannabis (Cannabis sativa L.). Frontiers in Plant Science, 13. https://doi.org/10.3389/fpls.2022.1082554

Gaudreau, S., Missihoun, T., & Germain, H. (2020). Early topping: An alternative to standard topping increases yield in cannabis production. Plant Science Today, 7(4), 627–630. https://doi.org/10.14719/PST.2020.7.4.927

Giupponi, L., Leoni, V., Pavlovic, R., & Giorgi, A. (2020). Influence of altitude on phytochemical composition of hemp inflorescence: A metabolomic approach. Molecules, 25(6). https://doi.org/10.3390/molecules25061381

Gonçalves, A. C., Nunes, A. R., Falcão, A., Alves, G., & Silva, L. R. (2021). Dietary effects of anthocyanins in human health: A comprehensive review. In Pharmaceuticals (Vol. 14, Issue 7). MDPI AG. https://doi.org/10.3390/ph14070690

Gould, K. S. (2004). Nature's Swiss Army Knife: The Diverse Protective Roles of Anthocyanins in Leaves. In *Journal of Biomedicine and Biotechnology* • (Issue 5). http://jbb.hindawi.com

Grof, C. P. L. (2018). Cannabis, from plant to pill. In British Journal of Clinical Pharmacology (Vol. 84, Issue 11, pp. 2463–2467). Blackwell Publishing Ltd. https://doi.org/10.1111/bcp.13618

Hammond, C. T., & Mahlberg, P. G. (1977). Morphogenesis of Capitate Glandular Hairs of Cannabis sativa (Cannabaceae). In Source: American Journal of Botany (Vol. 64, Issue 8). https://about.jstor.org/terms

Hasegawa, H., Fukasawa-Akada, T., Okuno, T., Niizeki, M., & Suzuki, M. (2001). Anthocyanin accumulation and related gene expression in Japanese parsley (Oenanthe stolonifera, DC.) induced by low temperature. In J. Plant Physiol (Vol. 158).

He, L., Kang, Z., Haiqin, J., Liankui, W., Yang, H., Siyan, L., Bixiang, W., & Jia, L. (2021). Current advances in anthocyanins- structure, bioactivity and human health. Journal of Food and Nutrition Research, 60(1336–8672), 203–216.

He, Q., Ren, Y., Zhao, W., Li, R., & Zhang, L. (2020). Low temperature promotes anthocyanin biosynthesis and related gene expression in the seedlings of purple head chinese cabbage (Brassica rapa l.). *Genes*, *11*(1). https://doi.org/10.3390/genes11010081

Ichimura, K., Niki, T., Matoh, M., & Nakayama, M. (2021). High temperature under low light conditions suppresses anthocyanin biosynthesis in snapdragon petals associated with decreased sugar levels. *Scientia Horticulturae*, *290*. https://doi.org/10.1016/j.scienta.2021.110510

Islam, M. J., Ryu, B. R., Azad, M. O. K., Rahman, M. H., Cheong, E. J., Lim, J. D., & Lim, Y. S. (2021). Cannabinoids accumulation in hemp (Cannabis sativa l.) plants under led light spectra and their discrete role as a stress marker. Biology, 10(8). https://doi.org/10.3390/biology10080710

Jiang, T., Mao, Y., Sui, L., Yang, N., Li, S., Zhu, Z., Wang, C., Yin, S., He, J., & He, Y. (2019). Degradation of anthocyanins and polymeric color formation during heat treatment of purple sweet potato extract at different pH. *Food Chemistry*, *274*, 460–470. https://doi.org/10.1016/j.foodchem.2018.07.141

Jin, D., Jin, S., & Chen, J. (2019). Cannabis Indoor Growing Conditions, Management Practices, and Post-Harvest Treatment: A Review. American Journal of Plant Sciences, 10(06), 925–946. https://doi.org/10.4236/ajps.2019.106067

Jin, H. X., Jiang, M., Yang, J. F., Wu, Z. H., Ma, L. L., Wang, C. C., Liang, C., Ning, X. Y., Ge, L. F., & Chen, S. (2022). A Survey of Enhanced Cold Tolerance and Low-Temperature-Induced Anthocyanin Accumulation in a Novel Zoysia japonica Biotype. *Plants*, *11*(3). https://doi.org/10.3390/plants11030429

Khoo, H. E., Azlan, A., Tang, S. T., & Lim, S. M. (2017). Anthocyanidins and anthocyanins: Colored pigments as food, pharmaceutical ingredients, and the potential health benefits. In Food and Nutrition Research (Vol. 61). Swedish Nutrition Foundation. https://doi.org/10.1080/16546628.2017.1361779

Khusnutdinov, E., Sukhareva, A., Panfilova, M., & Mikhaylova, E. (2021). Anthocyanin biosynthesis genes as model genes for genome editing in plants. In International Journal of Molecular Sciences (Vol. 22, Issue 16). MDPI. https://doi.org/10.3390/ijms22168752

Krga, I., & Milenkovic, D. (2019). Anthocyanins: From Sources and Bioavailability to Cardiovascular-Health Benefits and Molecular Mechanisms of Action. Journal of Agricultural and Food Chemistry, 67(7), 1771–1783. https://doi.org/10.1021/acs.jafc.8b06737

Kundan, M., Gani, U., Fayaz, M., Angmo, T., Kesari, R., Rahul, V. P., Gairola, S., & Misra, P. (2022). Two R2R3-MYB transcription factors, CsMYB33 and CsMYB78 are involved in the regulation of anthocyanin biosynthesis in Cannabis sativa L. *Industrial Crops and Products*, *188*. https://doi.org/10.1016/j.indcrop.2022.115546

Kovinich, N., Kayanja, G., Chanoca, A., Riedl, K., Otegui, M. S., & Grotewold, E. (2014). Not all anthocyanins are born equal: distinct patterns induced by stress in Arabidopsis. *Planta*, *240*(5), 931–940. https://doi.org/10.1007/s00425-014-2079-1

Kongthitilerd, P., Thilavech, T., Marnpae, M., Rong, W., Yao, S., Adisakwattana, S., Cheng, H., & Suantawee, T. (2022). Cyanidin-3-rutinoside stimulated insulin secretion through activation of L-type voltage-dependent Ca2+ channels and the PLC-IP3 pathway in pancreatic β-cells. *Biomedicine and Pharmacotherapy*, *146*. https://doi.org/10.1016/j.biopha.2021.112494

Kotiranta, S., Pihlava, J. M., Kotilainen, T., & Palonen, P. (2024). The morphology, inflorescence yield, and secondary metabolite accumulation in hemp type Cannabis sativa can be influenced by the R:FR ratio or the amount of short wavelength radiation in a spectrum. Industrial Crops and Products, 208. https://doi.org/10.1016/j.indcrop.2023.117772

Lee, J., Durst, R. W., Wrolstad, R. E., Barnes, K. W., Eisele, ; T, Giusti, ; M M, Haché, ; J, Hofsommer, ; H, Koswig, ; S, Krueger, D. A., Kupina, ; S, Martin, ; S K, Martinsen, ; B K, Miller, T. C., Paquette, ; F, Ryabkova, ; A, Skrede, ; G, Trenn, ; U, & Wightman, J. D. (2005). *Determination of Total Monomeric Anthocyanin Pigment Content of Fruit Juices, Beverages, Natural Colorants, and Wines by the pH Differential Method: Collaborative Study*. https://academic.oup.com/jaoac/article/88/5/1269/5657437

Lenth, R. (2022). emmeans: Estimated marginal means, aka least-squares means. R package version 1.7. 2.

Li, C., Yu, W., Xu, J., Lu, X., & Liu, Y. (2022). Anthocyanin Biosynthesis Induced by MYB Transcription Factors in Plants. In International Journal of Molecular Sciences (Vol. 23, Issue 19). MDPI. https://doi.org/10.3390/ijms231911701

Lin-Wang, K., Micheletti, D., Palmer, J., Volz, R., Lozano, L., Espley, R., Hellens, R. P., Chagnè, D., Rowan, D. D., Troggio, M., Iglesias, I., & Allan, A. C. (2011). High temperature reduces apple fruit colour via modulation of the anthocyanin regulatory complex. *Plant, Cell and Environment*, *34*(7), 1176–1190. https://doi.org/10.1111/j.1365-3040.2011.02316.x

Liu, Y., Lin-Wang, K., Espley, R. v., Wang, L., Li, Y., Liu, Z., Zhou, P., Zeng, L., Zhang, X., Zhang, J., & Allan, A. C. (2019). StMYB44 negatively regulates anthocyanin biosynthesis at high temperatures in tuber flesh of potato. Journal of Experimental Botany, 70(15), 3809–3824. https://doi.org/10.1093/jxb/erz194

Livingston, S. J., Quilichini, T. D., Booth, J. K., Wong, D. C. J., Rensing, K. H., Laflamme-Yonkman, J., Castellarin, S. D., Bohlmann, J., Page, J. E., & Samuels, A. L. (2020). Cannabis glandular trichomes alter morphology and metabolite content during flower maturation. Plant Journal, 101(1), 37–56. https://doi.org/10.1111/tpj.14516

lo Piero, A. R., Puglisi, I., Rapisarda, P., & Petrone, G. (2005). Anthocyanins accumulation and related gene expression in red orange fruit induced by low temperature storage. *Journal of Agricultural and Food Chemistry*, *53*(23), 9083–9088. https://doi.org/10.1021/jf051609s

Lyu, D., Backer, R., Berrué, F., Martinez-Farina, C., Hui, J. P. M., & Smith, D. L. (2023). Plant Growth-Promoting Rhizobacteria (PGPR) with Microbial Growth Broth Improve Biomass and Secondary Metabolite Accumulation of Cannabis sativa L. Journal of Agricultural and Food Chemistry, 71(19), 7268–7277. https://doi.org/10.1021/acs.jafc.2c06961

Maioli, C., Mattoteia, D., Amin, H. I. M., Minassi, A., & Caprioglio, D. (2022). Cannabinol: History, Syntheses, and Biological Profile of the Greatest "Minor" Cannabinoid. In Plants (Vol. 11, Issue 21). MDPI. https://doi.org/10.3390/plants11212896

Mansouri, H., & Salari, F. (2014). Influence of mevinolin on chloroplast terpenoids in Cannabis sativa. Physiology and Molecular Biology of Plants, 20(2), 273–277. https://doi.org/10.1007/s12298-014-0222-x

Mao, W., Han, Y., Chen, Y., Sun, M., Feng, Q., Li, L., Liu, L., Zhang, K., Wei, L., Han, Z., & Li, B. (2022). Low temperature inhibits anthocyanin accumulation in strawberry fruit by activating FvMAPK3-induced phosphorylation of FvMYB10 and degradation of Chalcone Synthase 1. *Plant Cell*, *34*(4), 1226–1249. https://doi.org/10.1093/plcell/koac006

Massuela, D. C., Hartung, J., Munz, S., Erpenbach, F., & Graeff-Hönninger, S. (2022). Impact of Harvest Time and Pruning Technique on Total CBD Concentration and Yield of Medicinal Cannabis. Plants, 11(1). https://doi.org/10.3390/plants11010140

Mitchell Westmoreland, F., Kusuma, P., & Bugbee, B. (2021). Cannabis lighting: Decreasing blue photon fraction increases yield but efficacy is more important for cost effective production of cannabinoids. PLoS ONE, 16(3 March). https://doi.org/10.1371/journal.pone.0248988

Millard, S.P. (2014). EnvStats, an R Package for Environmental Statistics. In Wiley StatsRef: Statistics Reference Online (eds N. Balakrishnan, T. Colton, B. Everitt, W. Piegorsch, F. Ruggeri and J.L. Teugels). https://doi.org/10.1002/9781118445112.stat07181

Oliveira, H., Fernandes, A., Brás, N. F., Mateus, N., de Freitas, V., & Fernandes, I. (2020). Anthocyanins as antidiabetic agents—in vitro and in silico approaches of preventive and therapeutic effects. In Molecules (Vol. 25, Issue 17). MDPI AG. https://doi.org/10.3390/molecules25173813

Pacheco, S. M., Soares, M. S. P., Gutierres, J. M., Gerzson, M. F. B., Carvalho, F. B., Azambuja, J. H., Schetinger, M. R. C., Stefanello, F. M., & Spanevello, R. M. (2018). Anthocyanins as a potential pharmacological agent to manage memory deficit, oxidative stress and alterations in ion pump activity induced by experimental sporadic dementia of Alzheimer's type. Journal of Nutritional Biochemistry, 56, 193–204. https://doi.org/10.1016/j.jnutbio.2018.02.014

Parsons, J. L., Martin, S. L., James, T., Golenia, G., Boudko, E. A., & Hepworth, S. R. (2019). Polyploidization for the genetic improvement of cannabis sativa. Frontiers in Plant Science, 10. https://doi.org/10.3389/fpls.2019.00476

Peterswald, T. J., Mieog, J. C., Azman Halimi, R., Magner, N. J., Trebilco, A., Kretzschmar, T., & Purdy, S. J. (2023). Moving Away from 12:12; the Effect of Different Photoperiods on

Biomass Yield and Cannabinoids in Medicinal Cannabis. Plants, 12(5). https://doi.org/10.3390/plants12051061

Ponder, A., Hallmann, E., Kwolek, M., Średnicka-Tober, D., & Kazimierczak, R. (2021). Genetic differentiation in anthocyanin content among berry fruits. Current Issues in Molecular Biology, 43(1), 36–51. https://doi.org/10.3390/cimb43010004

Popović, D., Kocić, G., Katić, V., Jović, Z., Zarubica, A., Janković Veličković, L., Nikolić, V., Jović, A., Kundalić, B., Rakić, V., Ulrih, N. P., Skrt, M., Sokolović, D., Dinić, L., Stojanović, M., Milosavljević, A., Veličković, F., & Sokolović, D. (2019). Protective effects of anthocyanins from bilberry extract in rats exposed to nephrotoxic effects of carbon tetrachloride. Chemico-Biological Interactions, 304, 61–72. https://doi.org/10.1016/j.cbi.2019.02.022

Purdy, S. J., Hewavitharana, A. K., Halimi, R. A., Magner, N. J., Peterswald, T. J., Trebilco, A., Kretzschmar, T., & Hailstones, D. (2022). A One-Step Grafting Methodology Can Adjust Stem Morphology and Increase THCA Yield in Medicinal Cannabis. Agronomy, 12(4). https://doi.org/10.3390/agronomy12040852

Reichel, P., Munz, S., Hartung, J., Präger, A., Kotiranta, S., Burgel, L., Schober, T., & Graeff-Hönninger, S. (2021). Impact of three different light spectra on the yield, morphology and growth trajectory of three different cannabis sativa L. strains. Plants, 10(9). https://doi.org/10.3390/plants10091866

Robinson, G. M., & Robinson, R. (1933). A survey of anthocyanins: Notes on the distribution of leuco-anthocyanins. *The Biochemical journal*, *27*(1), 206–212.

Rowan, D. D., Cao, M., Lin-Wang, K., Cooney, J. M., Jensen, D. J., Austin, P. T., Hunt, M. B., Norling, C., Hellens, R. P., Schaffer, R. J., & Allan, A. C. (2009). Environmental regulation of leaf colour in red 35S:PAP1 Arabidopsis thaliana. New Phytologist, 182(1), 102–115. https://doi.org/10.1111/j.1469-8137.2008.02737.x

Schloerke B, Cook D, Larmarange J, Briatte F, Marbach M, Thoen E, Elberg A, Crowley J (2023). *GGally: Extension to 'ggplot2'*. R package version 2.2.0, https://github.com/ggobi/ggally, https://ggobi.github.io/ggally/.

Sikora, V., Berenji, J., & Latković, D. (2011). Influence of agroclimatic conditions on content of main cannabinoids in industrial hemp (Cannabis sativa L.). Genetika, 43(3), 449–456. https://doi.org/10.2298/GENSR1103449S

Smeriglio, A., Barreca, D., Bellocco, E., & Trombetta, D. (2016). Chemistry, Pharmacology and Health Benefits of Anthocyanins. In Phytotherapy Research (pp. 1265–1286). John Wiley and Sons Ltd. https://doi.org/10.1002/ptr.5642

Speer, H., D’Cunha, N. M., Alexopoulos, N. I., McKune, A. J., & Naumovski, N. (2020). Anthocyanins and human health—a focus on oxidative stress, inflammation and disease. In Antioxidants (Vol. 9, Issue 5). MDPI. https://doi.org/10.3390/antiox9050366

Spitzer-Rimon, B., Duchin, S., Bernstein, N., & Kamenetsky, R. (2019). Architecture and florogenesis in female Cannabis sativa plants. Frontiers in Plant Science, 10. https://doi.org/10.3389/fpls.2019.00350

Stiles, E. A., Cech, N. B., Dee, S. M., & Lacey, E. P. (2007). Temperature-sensitive anthocyanin production in flowers of Plantago lanceolata. *Physiologia Plantarum*, *129*(4), 756–765. https://doi.org/10.1111/j.1399-3054.2007.00855.x

Tanney, C. A. S., Backer, R., Geitmann, A., & Smith, D. L. (2021). Cannabis Glandular Trichomes: A Cellular Metabolite Factory. In Frontiers in Plant Science (Vol. 12). Frontiers Media S.A. https://doi.org/10.3389/fpls.2021.721986

Thilavech, T., Abeywardena, M. Y., Adams, M., Dallimore, J., & Adisakwattana, S. (2017). Naturally occurring anthocyanin cyanidin-3-rutinoside possesses inherent vasorelaxant actions and prevents methylglyoxal-induced vascular dysfunction in rat aorta and mesenteric arterial bed. *Biomedicine and Pharmacotherapy*, *95*, 1251–1259. https://doi.org/10.1016/j.biopha.2017.09.053

Thilavech, T., Abeywardena, M. Y., Dallimore, J., Adams, M., & Adisakwattana, S. (2018). Cyanidin-3-rutinoside alleviates methylglyoxal-induced cardiovascular abnormalities in the rats. *Journal of Functional Foods*, *49*, 258–266. https://doi.org/10.1016/j.jff.2018.08.034

Tian, J., Han, Z.-Y., Zhang, L.-R., Song, T.-T., Zhang, J., Li, J.-Y., & Yao, Y. (2015). Induction of Anthocyanin Accumulation in Crabapple (Malus cv.) Leaves by Low Temperatures. In HORTSCIENCE (Vol. 50, Issue 5). www.ncbi.nlm.nih.gov/tools/primer-blast

Toth, J. A., Smart, L. B., Smart, C. D., Stack, G. M., Carlson, C. H., Philippe, G., & Rose, J. K. C. (2021). Limited effect of environmental stress on cannabinoid profiles in high-cannabidiol hemp (Cannabis sativa L.). GCB Bioenergy, 13(10), 1666–1674. https://doi.org/10.1111/gcbb.12880

Wagner, G. J. (1991). Secreting Glandular Trichomes: More than Just Hairs. In *Plant Physiology* (Vol. 96). https://academic.oup.com/plphys/article/96/3/675/6087979

Wallace, T. C., & Giusti, M. M. (2015). Anthocyanins. Advances in Nutrition, 6(5), 619–622. https://doi.org/10.3945/an.115.009233

Werf, H. M. G. V. der, Brouwer, K., Wijlhuizen, M., & Withagen, J. C. M. (1995). The effect of temperature on leaf appearance and canopy establishment in fibre hemp (Cannabis sativa L.). Annals of Applied Biology, 126(3), 551–561. https://doi.org/10.1111/j.1744-7348.1995.tb05389.x

Wickham H (2009). Ggplot2, Elegant Graphics for Data Analysis,177–82. doi: 10.1007/978-0-387-98141-3_10.

Wu, X., Beecher, G. R., Holden, J. M., Haytowitz, D. B., Gebhardt, S. E., & Prior, R. L. (2006). Concentrations of anthocyanins in common foods in the United States and estimation of normal consumption. Journal of Agricultural and Food Chemistry, 54(11), 4069–4075. https://doi.org/10.1021/jf060300l

Xie, Z., Mi, Y., Kong, L., Gao, M., Chen, S., Chen, W., Meng, X., Sun, W., Chen, S., & Xu, Z. (2023). Cannabis sativa: origin and history, glandular trichome development, and cannabinoid biosynthesis. In Horticulture Research (Vol. 10, Issue 9). Oxford University Press. https://doi.org/10.1093/hr/uhad150

Xue, X., Duan, Y., Wang, J., Ma, F., & Li, P. (2021). Nighttime Temperatures and Sunlight Intensities Interact to Influence Anthocyanin Biosynthesis and Photooxidative Sunburn in "Fuji" Apple. *Frontiers in Plant Science*, *12*. https://doi.org/10.3389/fpls.2021.694954

Zhang, B., Hu, Z., Zhang, Y., Li, Y., Zhou, S., & Chen, G. (2012). A putative functional MYB transcription factor induced by low temperature regulates anthocyanin biosynthesis in purple kale (Brassica Oleracea var. acephala f. tricolor). *Plant Cell Reports*, *31*(2), 281–289. https://doi.org/10.1007/s00299-011-1162-3

Zhang, Q., Zhai, J., Shao, L., Lin, W., & Peng, C. (2019). Accumulation of Anthocyanins: An Adaptation Strategy of Mikania micrantha to Low Temperature in Winter. *Frontiers in Plant Science*, *10*. https://doi.org/10.3389/fpls.2019.01049

Zheljazkov, V. D., Noller, J. S., Maggi, F., & Dale, R. (2022). Terpenes and Cannabinoids Yields and Profile from Direct-Seeded and Transplanted CBD- Cannabis sativa. Journal of Agricultural and Food Chemistry, 70(34), 10417–10428. https://doi.org/10.1021/acs.jafc.1c06912

# CHAPTER 3: GENETIC REGULATION OF ANTHOCYANIN ACCUMULATION IN CANNABIS

## Abstract

Purple pigments in *C. sativa*, attributed to anthocyanin accumulation, enhance aesthetic appeal, differentiate cultivars in the market, cater to consumer preferences, potentially offer therapeutic benefits, and provide plants protection against environmental stressors. Identifying the candidate gene(s) responsible for anthocyanin accumulation in *C. sativa* will create new opportunities for developing cultivars with heightened levels of these compounds and provides valuable insights into the plant's evolutionary history, genetic diversity, and adaptability to stress. To help identify potential candidate genes responsible for anthocyanin biosynthesis in *Cannabis sativa,* a $BC_2F_2$ mapping population and an open-pollinated population (OP) were used to identify quantitative trait loci (QTL) associated with this trait. Across the $BC_2F_2$ and OP populations, the QTL associated with anthocyanin accumulation were found on chromosomes 6 and 8. The $BC_2F_2$ mapping population revealed a QTL associated with flower and leaf coloration on chromosome 6 between 74.54Mb – 75.77Mb, while a QTL associated with stem color was found on chromosome 8 spanning regions 51.90Mb – 54.98Mb. Significant marker associations were found for flower color in the OP population on chromosome 6 at 72.98Mb – 75.86Mb. In both populations, an overlapping QTL for flower pigmentation was found on chromosome 6 in the region 74.54 – 75.77Mb. Within chromosomes 6 and 8 QTL, three candidate genes were found to be associated with anthocyanin biosynthesis. Chromosome 6 contained a transcription factor, MYB113, in the region 75409856 – 75419127 while the QTL on chromosome 8 had one anthocyanin related gene, Coumaroyl-CoA:anthocyanidin 3-O-glucoside-6’’-O-coumaroyltransferase 2, located in region

54001225 – 54002808, and one flavonoid related gene, Ultraviolet-B receptor (UVR8) in region 54728634 – 54732795. Three randomly selected single nucleotide polymorphisms (SNPs) within the QTL on both chromosomes 6 and 8 were selected to elucidate the mode of inheritance of anthocyanin accumulation in the flowers, leaves, and stems. In all cases heterozygous individuals appeared to have intermediate levels of anthocyanins as compared to individuals with homozygous genotypes. Two random SNPs from within the chromosome 6 and 8 QTL were jointly analyzed to observe possible epistatic interactions between the two QTL. No epistasis was identified. Elucidating the mode of inheritance for anthocyanin accumulation contributes to our understanding of cannabis genetics and progresses the development of molecular markers for marker-assisted selection in breeding programs. This research significantly advances our understanding of anthocyanin accumulation in cannabis, with implications spanning cannabis breeding, plant biology, plant medicine, and agriculture.

## Introduction

Many plants owe their purple, blue, red, and pink colors to anthocyanins, water-soluble pigments widely distributed throughout the plant kingdom. Mainly existing in the epidermal layers, these specialized metabolites are synthesized in the cytoplasm and are actively transferred to vacuoles (Kallam et al., 2017; Chaves-Silva et al., 2018). Anthocyanins represent a subgroup of compounds within a large category of plant secondary metabolites called flavonoids. Distributed widely across plant tissues, flavonoids are responsible for the color and aroma of many flowers and fruits and play a significant role in plant defense mechanisms against various biotic and abiotic stressors (Panche et al., 2016). The synthesis of these compounds initiates through the acetate and shikimate pathways (Smeriglio et al., 2016). The shikimate pathway gives rise to phenylalanine, an essential aromatic amino acid, and tyrosine, a nonessential amino acid, which act as precursors for flavonoid synthesis (Chaves-Silva et al., 2018; Maeda & Dudareva, 2012). Through a process of enzymatic reactions, phenylalanine and tyrosine form p-Coumaroyl-CoA using phenylalanine ammonia lyase (PAL) and tyrosine ammonia lyase (TAL) (Chaves-Silva et al., 2018). Once p-Coumaroyl-CoA is produced it is condensed with three molecules of malonyl-CoA to produce chalcone (naringenin chalcone or tetrahydroxy chalcone) via chalcone synthase (CHS). Chalcone scaffolds are the precursor molecules from which all flavonoids are derived. Chalcone isomerase (CHI) is used to convert tetrahydroxy chalcone into flavanone naringenin which acts as the main precursor for various flavonoids (Alappat, B., & Alappat, J., 2020). Thereafter, flavanone-3-hydroxylase (F3H) transforms naringenin into dihydroflavonols which act as the precursor molecules for anthocyanins (Zhang, P., & Zhu, H., 2023). Dihydroflavonol 4-reductase (DFR) then catalyzes dihydroflavonols into colorless leucoanthocyanidins which get converted to anthocyanidins via anthocyanidin synthase (ANS) (Zhang, P., & Zhu, H., 2023). The formation of various anthocyanins is achieved in the last step through the glycosylation and acylation of anthocyanidin aglycones using uridine diphosphate-dependent glucosyltransferase (UGT/UFGT), glucosyltransferase (GT), rhamnosyltransferase (RT), methyltransferase (MT), and acyltransferase (AT) (Khusnutdinov et al., 2021). Modifications by hydroxylation, methylation, glycosylation, and acylation will allow for anthocyanins to vary in color and stability (Alappat, B., & Alappat, J., 2020). Transcriptional genes play a crucial role by encoding transcription factors that govern the expression of structural pathway genes. Transcription factors R2R3 MYB, bHLH, and WD40 collectively form the MYB-bHLH-WD40 (MBW) complex which binds to specific DNA sequences in the promoters of structural genes, activating their transcription (Jaakola, 2013; Albert et al., 2014; Xu, et al., 2015; Chaves-Silva et al., 2018; Zhang & Zhu, 2023). The anthocyanin biosynthetic pathway is regulated by several factors, including light, nutrient availability, temperature, pH, and the developmental stage of the plant (Zhang & Zhu, 2023). It has been demonstrated that high temperatures can significantly reduce anthocyanin accumulation in apple peels due to the reduced expression of the MYB transcription factor MYB10 (Lin-Wang et al., 2011). The pathway for anthocyanin production is relatively conserved in plants but depending on the species, different enzymes can create differences in the anthocyanins produced which can be categorized into different subclasses (Kovinich et al., 2014). Anthocyanin production increases with biotic and abiotic stresses such as harmful UV-Radiation, cold temperatures, salt stress, oxidative stress caused by reactive oxygen species (ROS), pathogens, and herbivory (Falcone Ferreyra et al., 2012; Kim et al., 2017; Naing & Kim 2021). The type of stress the plant endures will play a crucial role in shaping the molecular structure of the anthocyanin it produces (Kovanich et al., 2014). A growing interest in the potential health benefits associated with consuming substantial amounts of anthocyanins has prompted the cultivation of crops with heightened levels of these compounds. In the cannabis industry, purple pigments contribute to market appeal, consumer preferences, potential medicinal effects, and cultivar differentiation. The tissue-specific expression of anthocyanins in cannabis plants results in a diverse array of phenotypic patterns (Figure 3.1). The unique aesthetics associated with anthocyanins can influence branding, marketing strategies, cultivar selections for farmers, and guide breeding directions. Cultivating and preserving purple pigments in cannabis plants can be challenging, requiring the proper genetics with specific growing conditions and expertise. This can set certain cultivators apart, creating a niche for growers and breeders who can consistently produce high-quality, visually appealing cultivars.

Although investigated in various plant species, the genetic mechanisms governing the anthocyanin biosynthetic pathway in *C. sativa* remain poorly understood. A high-quality reference genome for *C. sativa* has been assembled using a high CBD variety, CBDRx (cs10), and is the most complete reference genome for *C. sativa* to date (Grassa et al., 2021). Utilizing the work done by Grassa and colleagues allowed for the first genome-wide analysis of bHLH and MYB families in *C. sativa*, categorizing them into subfamilies through comparative phylogenetic analysis with *Arabidopsis thaliana* (Bassolino et al., 2020). Additionally, 99 R2R3-MYB genes have been identified in the *C. sativa* genome, and the overexpression of *CsMYB33* and *CsMYB78* has been shown to activate the anthocyanin biosynthetic pathway (Kundan et al., 2022). The specific anthocyanins produced by *C. sativa* are not well documented. Recent studies revealed the presence of cyanidin 3-glucoside, cyanidin 3-rutinoside, peonidin 3-glucoside, and peonidin 3-rutinoside in *C. sativa*, with cyanidin 3-rutinoside (keracyanin) being the major anthocyanin responsible for the purple, pink, and red colors in the vegetative and floral tissues (Bassolino et al., 2023). The research done by Bassolino and colleagues indicates that *C. sativa* stands out as a top contender for producing the highest concentrations of cyanidin 3-rutinoside and total anthocyanins among crops listed in the Phenol Explorer database (Neveu et al., 2010). Cyanidin-3-rutinoside (C3R), known for its antioxidant and anti-inflammatory properties, is a compound that can selectively kill leukemic cells (Feng et al., 2007), possesses inherent vasorelaxant actions (Thilavech et al., 2017), alleviates cardiovascular abnormalities in rats (Thilavech et al., 2018), stimulates insulin secretion (Kongthitilerd et al., 2022), increases glucose uptake (Choi et al., 2017), and significantly reduces high glucose-induced apoptosis (Choi et al., 2018).

The aim of our research is to identify quantitative trait loci (QTL) responsible for the biosynthesis of anthocyanins in *Cannabis sativa.* To do this, a backcross mapping population and an open-pollinated population were used to help identify any significant SNPs associated with this trait. Both populations were phenotyped and genotyped, and analyses was facilitated by the Genome Association and Prediction Integrated Tool (GAPIT). Identifying candidate gene(s) responsible for anthocyanin accumulation in *C. sativa* will be advantageous in the development of uniform cultivars with heightened levels of these compounds. Establishing the genetic regulation of this trait will open new possibilities for precision breeding practices, crop improvement, preservation of genetic resources, evolutionary insights, and environment change adaptation in *C. sativa*. In addition to enhancing resilience to environmental stresses, the purple pigments found in *C. sativa* inflorescences can influence market growth by contributing to visual appeal, potential health benefits, and cultivar differentiation. A better understanding of the mechanisms controlling anthocyanin accumulation will allow breeders and farmers to make informed decisions on cultivar selection, breeding strategies, and cultivation practices.

## Materials and Methods

### Plant Material and Phenotyping

#### Backcross Mapping Population

A mapping population was developed by crossing a purple phenotype of 118 Early Harvest, a high cannabidiol (CBD) day-neutral cultivar (7-Mile Farms) to a green phenotype of a high CBD Cherry Wine 307 day-neutral cultivar (HempLogic) (Figure 3.2). The 118 Early Harvest cultivar (118) served as the donor parent while the CBD Cherry Wine 307 cultivar (CW) served as the recurrent parent (Figure 3.2). 118 was first crossed with CW to obtain the $F_1$ generation. $F_1$ hybrids, selected based on pigment expression, were backcrossed to CW to create the $BC_1F_1$ population. This process was repeated with $BC_1F_1$ hybrids to create three related $BC_2F_1$ populations, two of which were segregating for anthocyanin accumulation. From the $BC_2F_1$ populations, eight crosses were made: three in the first population, one in the second population and four in the third population to create eight $BC_2F_2$ families (Figure 3.2). A total of 430 plants from the $BC_2F_2$ populations, along with four to six replicates of the original 118 and CW parents, were grown at Walnut Street Greenhouse (Madison, WI) during the summer of 2023 with an average temperature of 25.5°C and an average humidity of 42.3%. Allowing the plants to reach full maturity was essential for precise phenotypic assessment. A total of 256 plants were phenotyped and genotyped to identify quantitative trait loci associated with anthocyanin pigmentation.

Stem, leaf, and floral tissue from each plant were visually assessed and given a score of 0 (no purple), 1 (pinkish), 2 (purple), or 3 (dark purple), depending on the hue of the tissue. An estimated total percent anthocyanin coverage of the entire plant was also recorded to help improve data interpretation (Supplemental Table 3.1). Scores were used together to calculate a total anthocyanin score for each plant tissue type using the following equations:

Total Leaf Score = leaf score x percent coverage of whole plant

Total Flower Score = flower score x percent coverage of whole plant

Total Stem Score = stem score x percent coverage of whole plant

<u>Open Pollinated Mapping Population</u>

In the summer of 2023, an open pollinated grain cultivar (Indigo) was identified as segregating for purple and green inflorescence color. A binary phenotype (0 = green, 1 = purple) for the inflorescence was assigned to random individual plants, and young leaf tissue was collected evenly between green and purple phenotypes (48 of each type).

<u>Genetic Mapping</u>

Genomic DNA was extracted from 256 $BC_2F_2$ and 96 OP samples using a modified version of the Macherey-Nagel™ NucleoSpin Plant II kit. Approximately 20 mg of fresh leaf tissue was collected in the field or greenhouse and placed into a 96-well plate. Plates were then lyophilized using the Labconco FreeZone, freeze dryer system. After drying, two 3mm glass beads were added to each well and samples were ground to a fine powder using a bead beater. Next 500 µL of buffer PL1 and 10 µL RNase A were added. Samples were lysed for 30 minutes at 65°C and then centrifuged for 20 minutes at full speed (4,500 x g). In a separate MN Square-well Block, 450 µL Binding Buffer PC was added to each well. 400 µL of the cleared lysate was also added to the MN Square-well Block, and properly mixed. The 800 µL of the lysate was put into the NucleoSpin® Plant II Binding Plate, and centrifuged at 4,500 x g for 5 min. After binding the DNA to the silica membrane several washing steps occurred, using 400 µL PW1 and spinning for 4,500 x g for 2 minutes, then using 700 µL PW2 spinning for 4,500 x g for 2 min, repeating this step twice. After washing, DNA was eluted into 100 µL preheated Buffer PE (70 °C) (50 µL at each time) and centrifuged at 4,500 x g for 2 min.

DNA was quantified with a Quant-iT™ PicoGreen® dsDNA kit (Life Technologies, Grand Island, NY) and Genotyping-by-Sequencing (GBS) was performed as in (Elshire et al., 2011), at the University of Wisconsin Biotechnology Center with half-sized reactions. Samples were digested using the *ApeK*I restriction enzyme, barcoded, and pooled for sequencing. Samples were sequenced on an Illumina NovaSeq 6000 machine. SNPs were called using the TASSEL 5.0 Version 2 SNP discovery pipeline (Glaubitz et al. 2014). Identified tags were aligned to *Cannabis sativa* reference genome CS10 (GCA_900626175.2) using the Bowtie2 (v2-2.2.1) aligner with the parameter "-very-sensitive-local" (Langmead and Salzberg, 2012). Samples with more than 20% missing data were removed. Markers with more than 20% missing data, a sequencing depth less than 5X, a minor allele frequency of less than 0.05, and sites with more than two alleles were removed. This led to a total of 45,238 genetic markers and 238 samples in the $BC_2F_2$ population and 54,458 genetic markers and 86 samples in the OP population.

Genome-wide associations were conducted in GAPIT on the $BC_2F_2$ and OP marker datasets to identify significant SNPs associated with quantitative variation in pigmentation. A mixed linear model (MLM) with a kinship matrix and PCA = 3 was selected for analysis to account for genetic relatedness between samples. The mixed linear model was fit using the following model:

$$y = s_i + Q + K + e$$

where $y$ is a vector of observed phenotypes; Si is the testing marker, Q is the population structure as determined through principal component analysis, K is the kinship matrix and **e** is the unobserved vector of residuals according to the GAPIT user manual (Lipka et al. 2012). A Bonferroni correction was used to avoid false positives and identify significant SNPs ($\alpha = 0.05$) for each trait (Haynes et al., 2013). The Bonferroni correction was calculated as $-\log_{10}(0.05/n)$, where $n$ equals the number of SNPs used in the GWAS for each trait.

## Results

Phenotypic distribution across $BC_2F_2$ families

The phenotypic distribution of anthocyanin accumulation varied across the eight $BC_2F_2$ families (Figure 3.3). Total stem color ranged from 0 to 150 and with an average of 8 across all samples. Total flower color ranged from 0 to 105 and averaged 12 across all samples. Total leaf color ranged from 0 to 150 with an average of 20 across all samples. The highest stem pigmentation was found in the parental cultivar 118 Early Harvest, highest leaf pigmentation in family 4.1.3.14, and the highest floral pigmentation was found in families 4.1.3.14 and 4.1.3.3. Family 4.1.19.7 had the lowest level of pigmentation in all tissue types.

Genetic mapping of anthocyanin QTL

Across the $BC_2F_2$ and OP populations, QTL associated with anthocyanin accumulation were found on chromosomes 5, 6, and 8 (Table 3.1). The $BC_2F_2$ mapping population revealed a QTL associated with flower and leaf pigmentation on chromosome 6 between 74.54Mb – 75.77Mb (Figure 3.4A B), while a QTL associated with stem pigmentation was found on chromosome 8 spanning regions 51.90Mb – 54.98Mb (Figure 3.4C). Significant marker association for flower pigmentation was found in the OP population on chromosome 6 spanning regions 72.98Mb – 75.86Mb (Figure 3.4D). In both populations, an overlapping QTL for flower pigmentation was found on chromosome 6 in the region 74.54 – 75.77Mb.

Candidate genes

A total of 130 and 216 genes were annotated within the QTL found on Chromosomes 6 and 8, respectively (Supplemental Tables 3.1 and 3.2). Within the chromosome 6 QTL, one gene was found to share homology to known anthocyanin pathway or regulatory genes. Specifically, a MYB113 transcription factor which is known to regulate anthocyanin biosynthesis was found in the region 75409856 – 75419127. The QTL on chromosome 8 contained one anthocyanin pathway gene, Coumaroyl-CoA:anthocyanidin 3-O-glucoside-6"-O-coumaroyltransferase 2 located at 54001225 – 54002808, and one flavonoid related gene, Ultraviolet-B receptor (UVR8) in region 54728634 – 54732795.

Genotypic influence on anthocyanin accumulation

A random selection of three SNPs within the QTL on chromosomes 6 and 8 were selected to elucidate the mode of inheritance of anthocyanin accumulation in the flowers (Figure 3.5), leaves (Figure 3.6), and stems (Figure 3.7). In all cases heterozygous individuals appeared to have intermediate levels of anthocyanins as compared to individuals with homozygous genotypes. Two random SNPs from within the chromosome 6 and 8 QTL were jointly analyzed to observe possible epistatic interactions between the two QTL (Figure 3.9). No epistasis was identified.

## Discussion

Genetic variability in anthocyanin accumulation

The presence of purple pigmentation in *C. sativa* can be observed in many above-ground plant tissue parts. Cannabis cultivars display notable heterozygosity due to obligate outcrossing, and populations rarely exhibit uniformity. Variety trials carried out by the Ellison lab at UW-Madison displayed an array of cultivars featuring various combinations of purple stems, leaves, and flowers (Figure 3.1). Variability in the levels of anthocyanin accumulation was observed not only across different cultivars but also within cultivars which highlights the pronounced heterozygosity of this species while also suggesting a nuanced response to specific plant stressors imposed on the plant (e.g., plant tissue exposed to higher levels of UV-radiation showed heightened levels of purple pigmentation, provided that the genetic predisposition for synthesizing these compounds was present). Considering marketing dynamics, modifications in these color schemes may augment visual attractiveness, thereby positively influencing product sales. As the cannabis industry progresses, uses for every part of the plant will undoubtedly increase. In light of this, the identification of specific genes governing the biosynthesis of desired compounds will be essential for cultivating uniform varieties showcasing heightened anthocyanin levels.

Candidate genes

Genes associated with anthocyanin biosynthesis within the QTL regions were investigated and three candidate genes, found on chromosomes 6 and 8, were identified. A R2R3 – MYB transcription factor (MYB113) found on chromosome 6, has been shown to regulate flavonoid biosynthesis in Arabidopsis (Koo & Poethig, 2021). MYB113 genes regulate green/red pod color in cacao by the R2R3 MYB transcription factor *TcMYB113* (Motamayor, et al., 2013). Similarly, MYB113 genes regulate anthocyanin biosynthesis in eggplants and potatoes via *SmMYB113* and *StMYB113* respectively (Zhou, et al., 2019, Liu et al., 2016). MYB113 genes have also been identified in carrots and it was proposed that *DcMYB113* may regulate anthocyanin transport in the roots (Xu, et al., 2020). MYB proteins are recognized by their distinctive MYB domain, a highly conserved DNA-binding domain at the N-terminus, comprising one to four imperfect sequence repeats (R) of approximately 52 amino acid residues, with each repeat forming three α–helices (Dubos et al., 2010, Kundan et al., 2020). Characterization through genetic approaches has unveiled numerous R2R3-MYB proteins, showcasing their involvement in the regulation of plant-specific processes such as primary and secondary metabolism, cell fate determination, developmental processes, and responses to biotic and abiotic stresses (Dubos et al., 2010). R2R3-MYB transcription factors usually have an activation or repression domain located at the C terminus (Dubos et al., 2010). These R2R3 MYB transcription factors can be found in rosids, monocots, asterids, byrophytes and chlorophytes (Millard et al., 2019). Bassolino et al. (2020) provided the first genome-wide analysis of bHLH and MYB families in *C. sativa*, categorizing these genes into subfamilies through comparative phylogenetic analysis with Arabidopsis thaliana (Bassolino et al., 2020). In a more recent study, Kundan et al. (2022) identified 99 R2R3-MYB genes in *C. sativa*, highlighting two regulators, CsMYB33 and CsMYB78, which were confirmed through the overexpression of these genes in *Nicotiana benthamiana* leaves (Kundan et al., 2022).

A second candidate gene Coumaroyl-CoA:anthocyanidin 3-O-glucoside-6"-O-coumaroyl transferase 2, was found within the chromosome 8 QTL, and is involved in the acylation of the 6" position of the 3-O-glucose residue of anthocyanin (UniProt Consortium, n.d.). Another interesting candidate gene on chromosome 8, Ultraviolet-B receptor UVR8, is associated with the UV-B signal transduction pathway and can lead to the induction of flavonoid biosynthesis (Kliebenstein et al., 2002). *UVR8* expression increases in response to UV-B, and the incremental expression of *UVR8* is accompanied by the up- regulation of key genes in the anthocyanin biosynthesis pathway involved in the skin coloring of litchi, apple, and eggplant throughout fruit development (Tossi et al., 2019). Conversely, tomato plants with silenced UVR8 (*SlUVR8Ri*) genes demonstrate reduced anthocyanin accumulation which resulted in pale-green fruits when grown under natural sunlight (Li et al., 2018). Given the role of UVR8 in regulating anthocyanin accumulation in various species, including fruits like litchi, apple, eggplant, and tomato, there is potential for similar mechanisms in cannabis as well.

These candidate genes, warrant further investigations to elucidate their involvement in anthocyanin accumulation in *C. sativa*. The identification of two QTL, one shared between unrelated populations, involved in anthocyanin biosynthesis in *C. sativa* contributes significantly to our current understanding of the mechanisms governing accumulation, providing a solid foundation for future research endeavors. These findings not only enhance our comprehension of pigment regulation in this species but also pave the way for targeted breeding efforts and the development of specialized cultivars with enhanced medicinal and agronomic properties.

Evidence of complete or incomplete dominance

Genotypic classes for three SNPs associated with anthocyanin accumulation on both chromosomes 6 and 8 were analyzed for observed phenotypes. Complete and incomplete dominance was observed among the selected markers (Figures 3.6, 3.7, and 3.8), highlighting the genetic complexity of anthocyanin accumulation in *C. sativa.* In cases of complete dominance, heterozygous individuals typically express anthocyanin levels similar to the dominant phenotype, whereas, in cases of incomplete dominance, heterozygotes display an intermediate phenotype distinct from both homozygotes (Figures 3.6, 3.7, and 3.8). Investigations into the mode of inheritance for anthocyanin accumulation in cauliflower and tomato suggest a single dominant gene hypothesis (Singh, et al., 2020, Jones, et al., 2003). To offer further insight into the mode of inheritance governing anthocyanin accumulation in *C. sativa*, additional mapping populations with a large number of individuals should be created.

Jointly analyzing markers from both QTL identified on chromosome 6 and 8 helped provide insight into the allelic interactions and gene action shaping the phenotypic variation within our populations. When analyzing the potential interaction of markers on chromosomes 6 and 8, it appears that purple stem color is not influenced by the allelic composition within the chromosome 6 QTL and appears dominant. Flower and leaf color, which primarily mapped to the chromosome 6 QTL appear to have increased anthocyanin expression when the chromosome 8 QTL is either "AA" or "AG" indicating both QTL are likely contributing to total accumulation. The simultaneous assessment of both markers provides insights into the genetic basis of this trait, shedding light on potential interactions between different loci.

Implications for cannabis breeding and product development

The specific anthocyanins present in *C. sativa* are still being characterized, yet new findings indicate the presence of cyanidin-3-rutinoside, cyanidin-3-glucoside, and peonidin 3-glucoside in *C. sativa*, with cyanidin-3-rutinoside being the most abundant (Bassolino et al., 2023). Based on the reported levels found in Bassolino and colleagues' samples, *C. sativa* emerges as the highest potential producer of cyanidin-3-rutinoside when compared to other crops (Bassolino et al., 2023, Neveu et al., 2010). Cyanidin-3-rutinoside (C3R), recognized for its antioxidant and anti-inflammatory characteristics, can selectively eliminate leukemic cells (Feng et al., 2007). C3R also exhibits inherent vasorelaxant actions when ingested (Thilavech et al., 2017), alleviates cardiovascular abnormalities in rats (Thilavech et al., 2018), promotes insulin secretion (Kongthitilerd et al., 2022), increases glucose uptake (Choi et al., 2017), and significantly reduces high glucose-induced apoptosis (Choi et al., 2018). Identifying the most effective methods to consume these compounds may prove advantageous in the exploration of new health supplements, medications, and superfoods.

With an increasing interest in discovering new food colorants from natural sources, these compounds have the potential to be a valuable resource, providing both health benefits and serving as a natural dye. Cannabis leaves are used for juicing and are considered a superfood. Plants containing higher amounts of anthocyanins in the leaves could lead to cannabis leaf extracts containing high amounts of antioxidants and have potential in creating more nutrient-dense and medicinal products for humans to consume. It is noteworthy that the byproduct of numerous solventless extractions used by cannabis producers contain high amounts of anthocyanins and has potential applications in product development regarding this subject. Acknowledging that particular stressors have the potential to modify the molecular structure of the anthocyanins being synthesized could be of practical significance in when attempting to cultivate specific anthocyanins.

Recent studies have delved into the exploration of the "entourage effect," suggesting that the combined presence of various compounds in *C. sativa*, such as cannabinoids, terpenes, esters, indoles, flavonoids, volatile-sulfur-compounds (VSC), and other phytochemicals, may yield a more pronounced therapeutic impact compared to individual compounds alone (Christensen et al., 2023). The identification of this phenomenon by Ben-Shabat et al. (1998) marked a pivotal moment, showcasing the substantial enhancement of cannabinoid activity through specific esters (Ben-Shabat et al., 1998). To fully grasp the therapeutic possibilities of cannabis, it is vital to look beyond cannabinoids and terpenes and include flavonoids in future investigations.

## Conclusion

Cannabis cultivars containing genes that positively influence anthocyanin synthesis may demonstrate improved resilience to environmental stressors, thereby enhancing the plant's potential for achieving optimal yields. A comprehensive understanding of the genes governing anthocyanin biosynthesis is essential for the advancement of crop breeding strategies targeting this trait. Providing information on the mechanisms controlling anthocyanin accumulation in *C. sativa* contributes to the development of new cultivars with superior adaptability to environmental stressors and increased levels of these compounds which are known to benefit human health. In this study, related $BC_2F_2$ mapping populations and an open-pollinated population were genotyped and phenotyped to identify QTL regions associated with anthocyanin accumulation in *C. sativa.* Analyzing each tissue type (floral, leaf, and stem) separately allowed for the analysis of tissue-specific gene regulation. We observed QTL regions associated with flower and leaf color on chromosome 6, while QTL regions associated with stem color were found on chromosome 8.

Identifying the regions responsible for tissue-specific anthocyanin accumulation in *C. sativa* enables breeders to target genetic markers linked to these desirable traits, which will prove valuable when creating cultivars with unique color patterns in different plant tissues. Evidence of complete and incomplete dominance were observed among the individuals used in our study, highlighting the genetic complexity of anthocyanin accumulation in *C. sativa*. Integrating the combined analysis of SNPs associated with anthocyanin accumulation across chromosomes 6 and 8 provided insights into the combined effects of the alleles influencing anthocyanin variation and adds to the understanding of the genetic basis and inheritance patterns of this trait in *C. sativa*. Anthocyanins not only contribute to color, but they also play a role in stress response. Cultivars with higher anthocyanin content may exhibit enhanced resilience to environmental factors such as UV radiation, temperature fluctuations, and pathogen attacks, thereby increasing overall plant vigor and productivity. Identifying QTL regions associated with anthocyanin accumulation contributes to the knowledge needed to breed cultivars with improved resilience and adaptability to environmental stresses. The presence of climate change underscores the need to cultivate crops that can endure environmental stressors. Understanding the genetic regulation of anthocyanin accumulation in *C. sativa* is a significant contribution to ensuring agricultural sustainability and crop security for this species.

## Future directions

Identifying significant QTL regions associated with anthocyanin accumulation in our populations provides a valuable resource for marker development. Future research targeting genotyping assays for tissue specific anthocyanins can be optimized for cost-effective and efficient genotyping tools, enabling widespread adoption in breeding programs and facilitating marker-assisted selection for anthocyanin traits in *C. sativa*.

Investigating high-throughput phenotyping platforms to screen large populations for individuals with elevated anthocyanin levels will help facilitate rapid selection of superior cultivars with desired pigmentation traits. Establishing phenotyping protocols to accurately quantify anthocyanin content in plant tissues using non-destructive imaging methods (e.g., hyperspectral imaging) will prove useful.

The genetic mechanisms underlying anthocyanin accumulation can be complex, and many combinations of alleles contribute to the observed phenotypic outcomes. Despite this complexity, the joint analysis of markers provides a powerful tool for uncovering the genetic basis of anthocyanin accumulation. By systematically exploring different combinations of alleles and markers, future research can identify key genetic variations associated with the trait and gain insights into the underlying genetic mechanisms.

We have noticed in many of our populations that plant maturity influences when anthocyanins are synthesized, with expression increasing as the plant reaches maturity. To better understand how the developmental stage affects anthocyanin accumulation, temporal transcriptomic analyses, such as time-series RNA sequencing (RNA-seq), to monitor gene expression changes throughout different developmental stages will be needed. Integrating transcriptomic data with anthocyanin content measurements to correlate gene expression patterns with pigment accumulation will help identify key regulatory genes associated with anthocyanin biosynthesis in *C. sativa*.

Future research should explore stress-induced gene expression by subjecting cannabis plants to conditions known to affect anthocyanin accumulation, such as exposure to UV radiation, temperature shifts, or nutrient deprivation, and profiling gene expression changes in response to these stressors. Comparing gene expression between stressed and non-stressed plants will help identify stress-responsive transcription factors and signaling pathways that modulate anthocyanin accumulation under different environmental conditions. Employing time-course RNA-seq experiments to capture stress-induced gene expression changes will help with identifying early and late biosynthetic genes involved in the anthocyanin biosynthesis pathways.

Finally, anthocyanins are synthesized in specific cell types and accumulate in various tissues of cannabis plants, including leaves, flowers, and stems. Identifying tissue-specific regulatory genes by comparing the expression profiles of  genes across different tissue types will help elucidate how anthocyanin biosynthesis is spatially regulated in *C. sativa.*

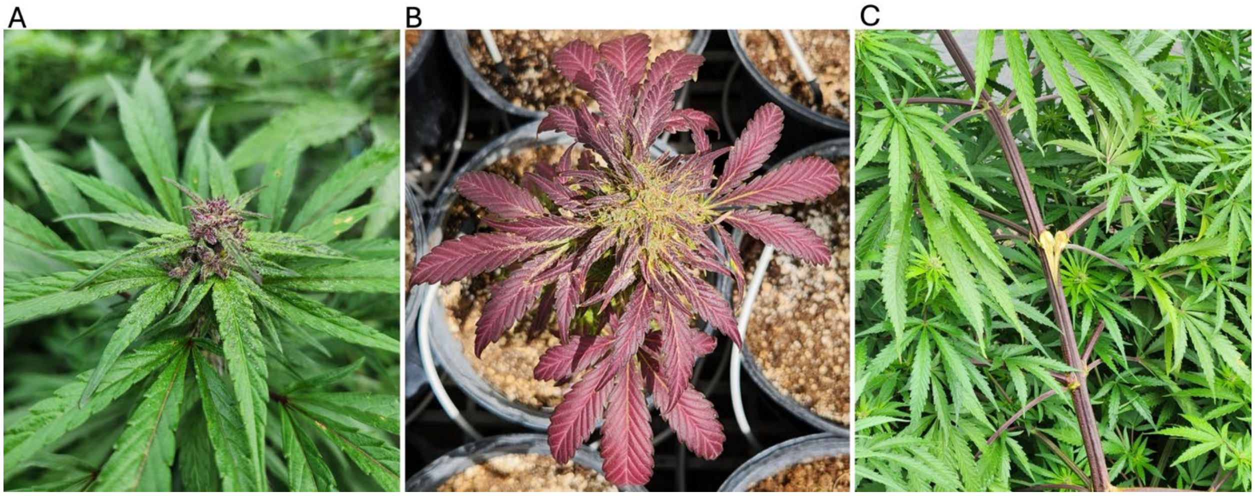


**Figure 3.1**. Tissue-specific expression of anthocyanin accumulation in *C. sativa* showing pigment expression in the (A) inflorescence, (B) leaves, and (C) stems. Each panel highlights the unique spatial distribution of anthocyanin accumulation within different tissue types, contributing to unique phenotypic differences among cannabis cultivars.

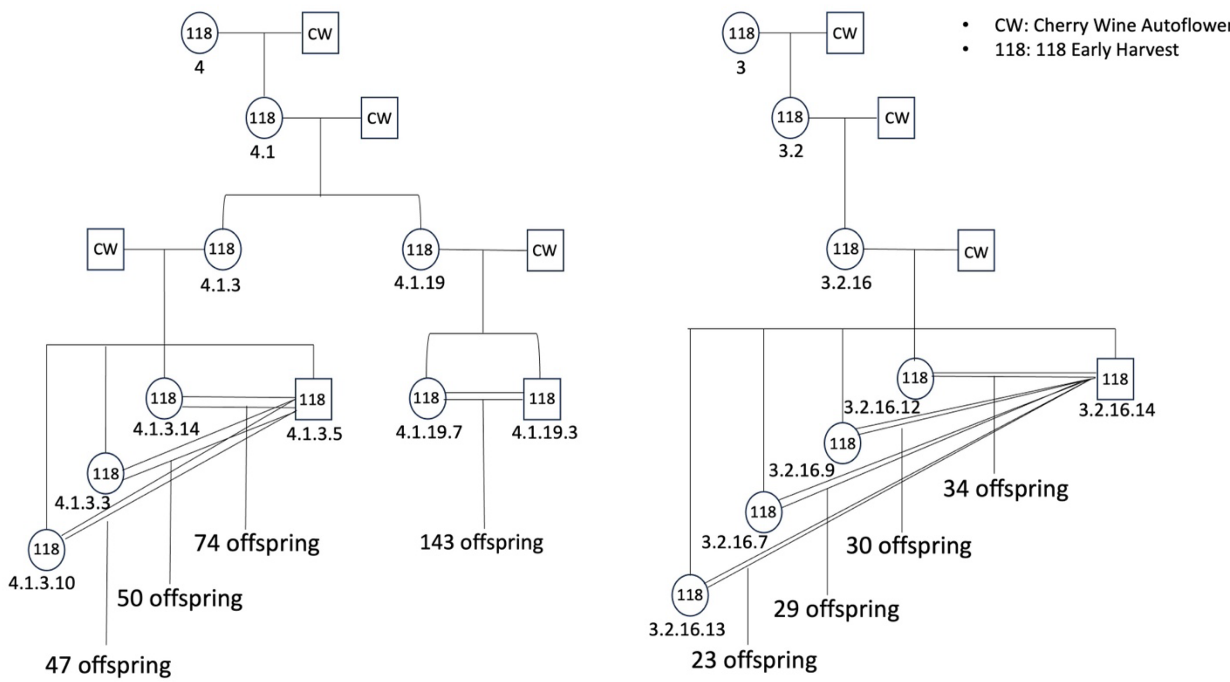


**Figure 3.2**. Pedigree for $BC_2F_2$ mapping populations. The CBD Cherry Wine 307 cultivar (CW) served as the recurrent parent while the 118 Early Harvest cultivar (118) served as the donor parent.

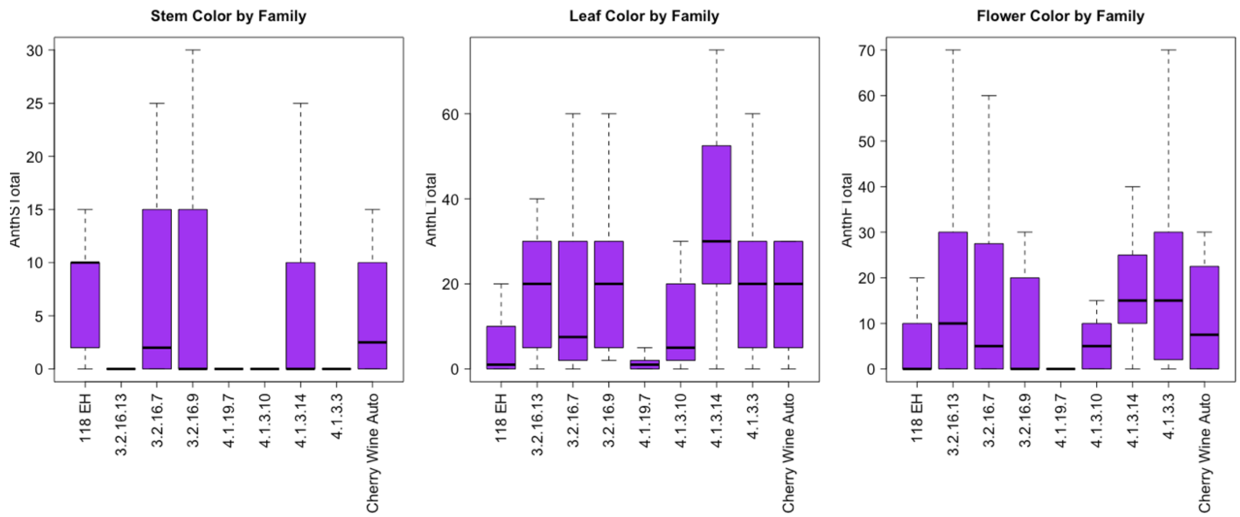


**Figure 3.3**. Box plots illustrating the variation in anthocyanin accumulation in the stem (left panel), leaves (middle panel), and flowers (right panel) across eight $BC_2F_2$ families and the original parents, 118 Early Harvest and Cherry Wine 307. The number of individuals per family are as follows: 118 Early Harvest: **5**, 3.2.16.13: **15**, 3.2.16.7: **29**, 3.2.16.9: **15**, 4.1.19.7: **81**, 4.1.3.10: **29**, 4.1.3.14: **25**, 4.1.3.3: **48**, Cherry Wine Auto: **4.**

**Population 1**

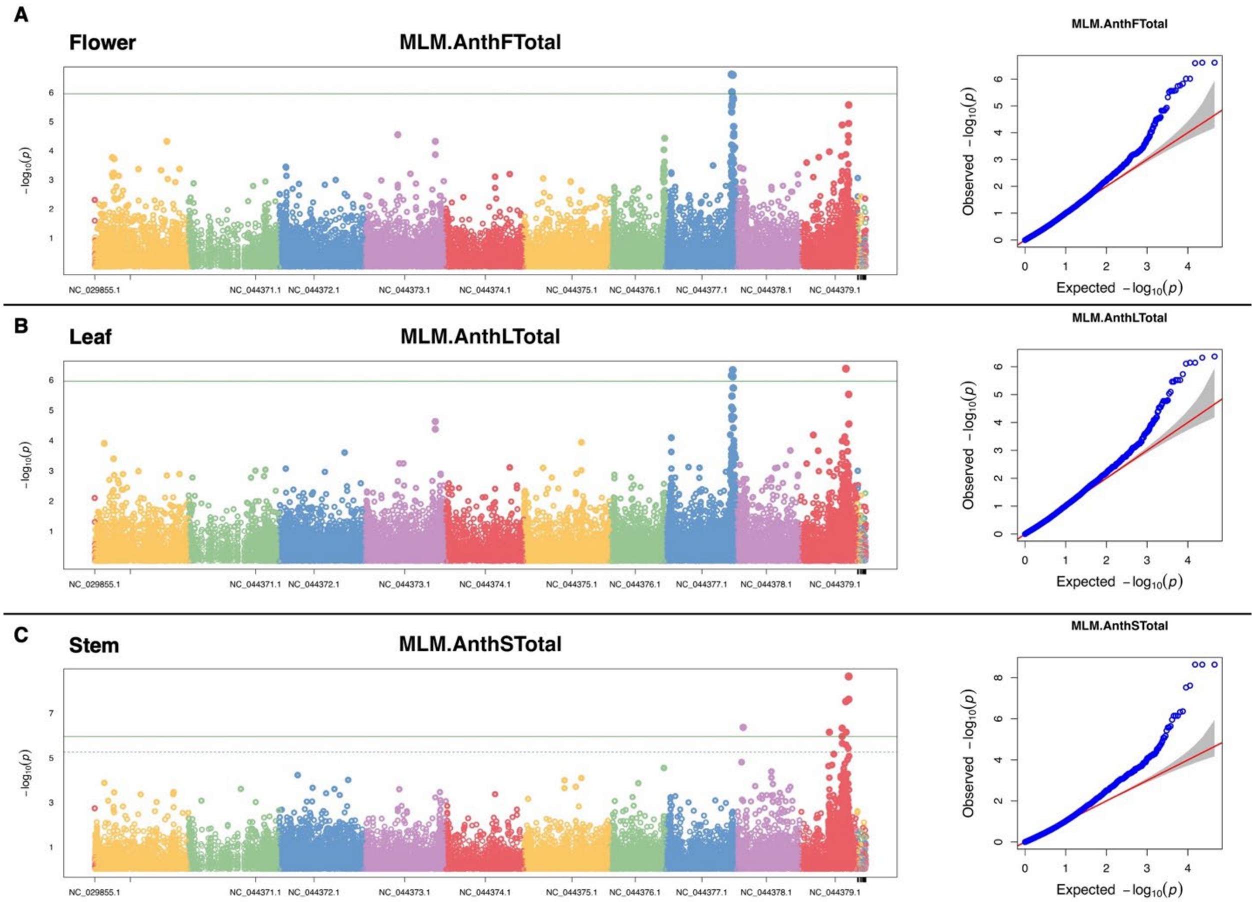


**Population 2**

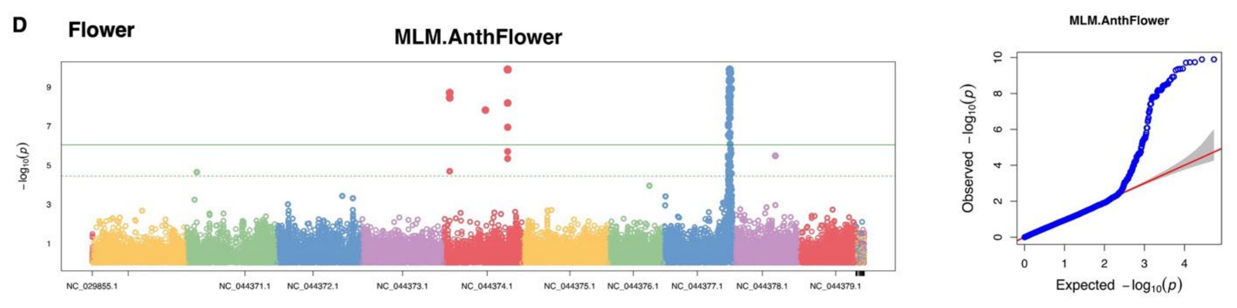


**Figure 3.4.** Manhattan plots and QQ plots illustrating the distribution of significant SNPs and the deviation from expected p-value distributions in two distinct populations. Population 1: $BC_2F_2$ population consisting of eight related families scored for total anthocyanins in the flowers (AnthFTotal), leaves (AnthLTotal), and stems (AnthSTotal) and population 2: open-pollinated

population, where plants were randomly sampled, and data on flower pigment was collected as a binary phenotype (0 = green, 1 = purple). The manhattan plot (left) displays the genomic regions associated with significant SNPs (solid green line represents a p-value = 0.05%), while the QQ plot (right) shows the deviation from the expected distribution of p-values.

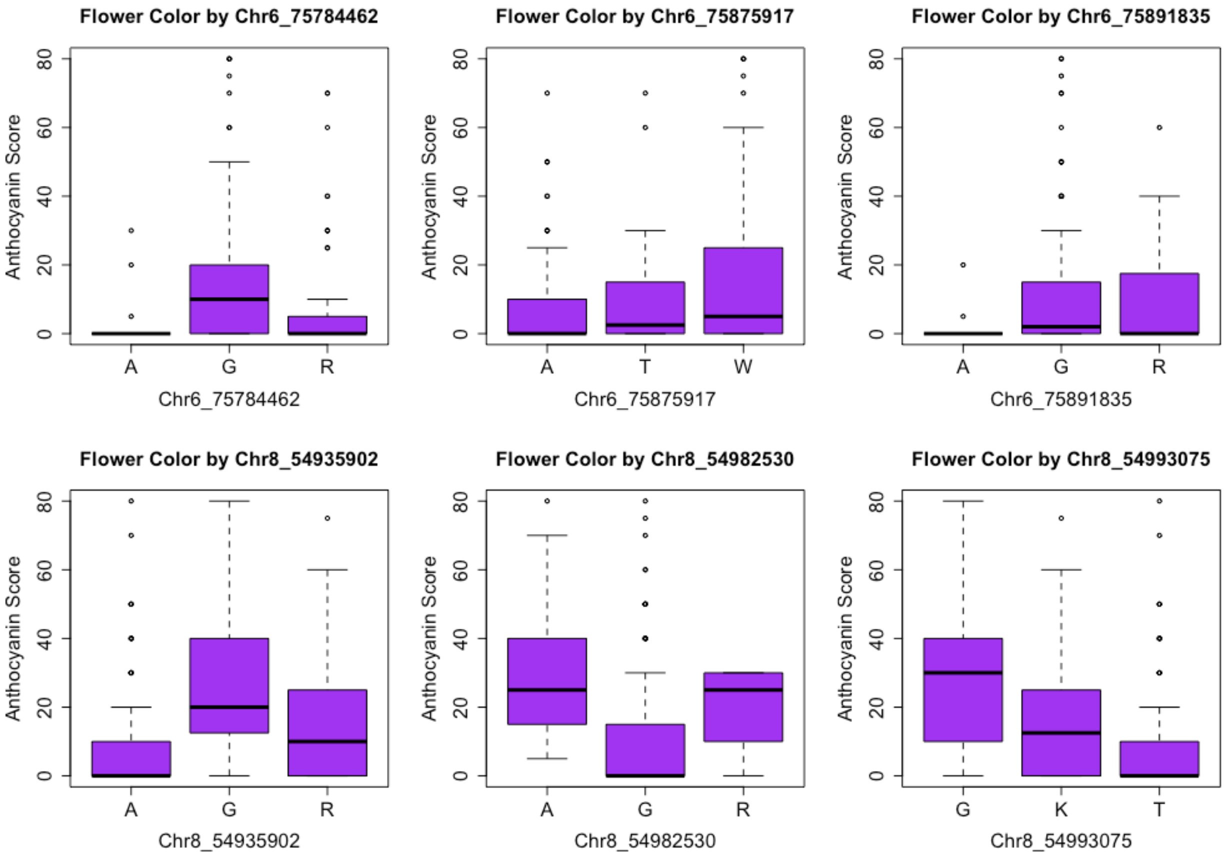


**Figure 3.5.** Phenotypic distribution of anthocyanin accumulation from three randomly selected markers within significant QTL regions on chromosomes 6 (top) and 8 (bottom). Boxplots illustrate total anthocyanin accumulation in the flowers for individuals based on their allelic composition.

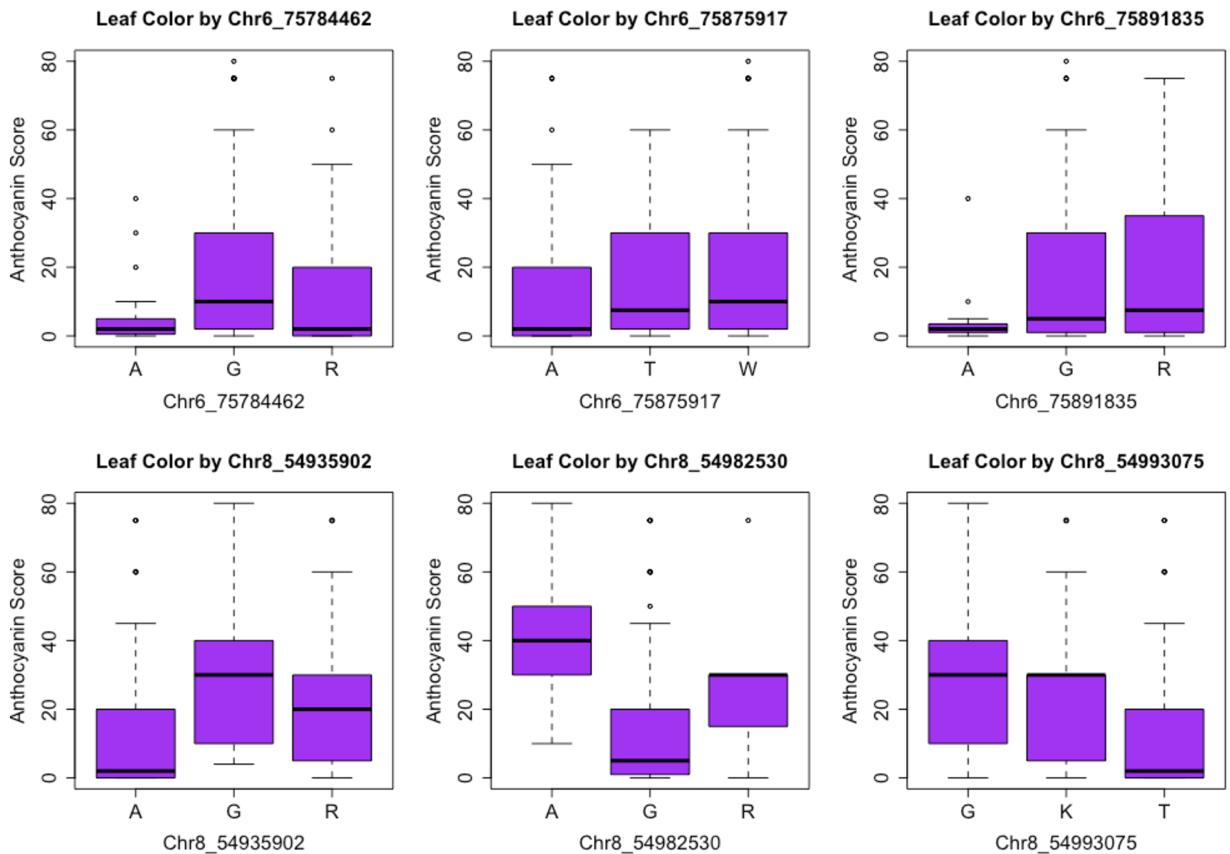


**Figure 3.6**. Phenotypic distribution of anthocyanin accumulation in leaf tissue from three randomly selected markers within significant QTL regions on chromosomes 6 (top) and 8 (bottom). Boxplots illustrate total anthocyanin accumulation in the leaves for individuals based on their allelic composition.

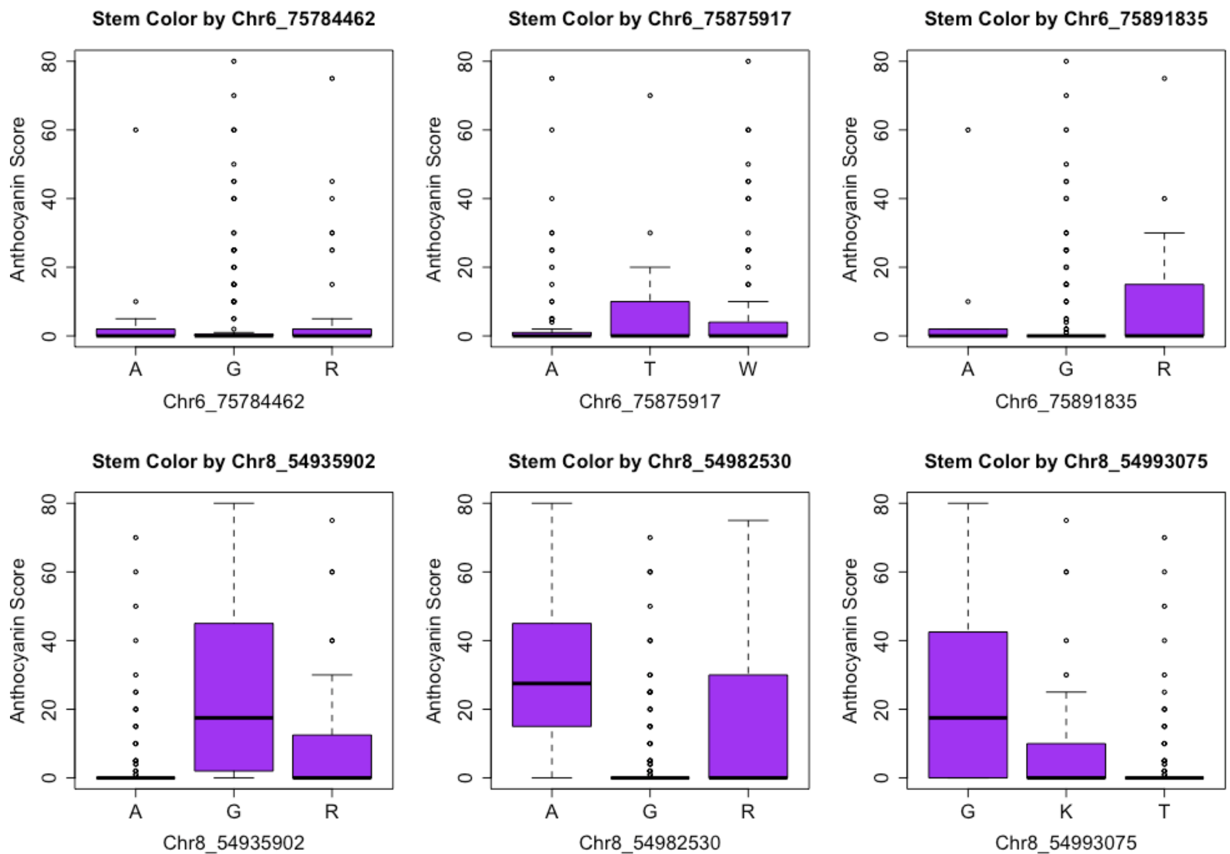


**Figure 3.7**. Phenotypic distribution of anthocyanin accumulation in stem tissue from three randomly selected markers within significant QTL regions on chromosomes 6 (top) and 8 (bottom). Boxplots illustrate total anthocyanin accumulation in the stems for individuals based on their allelic composition.

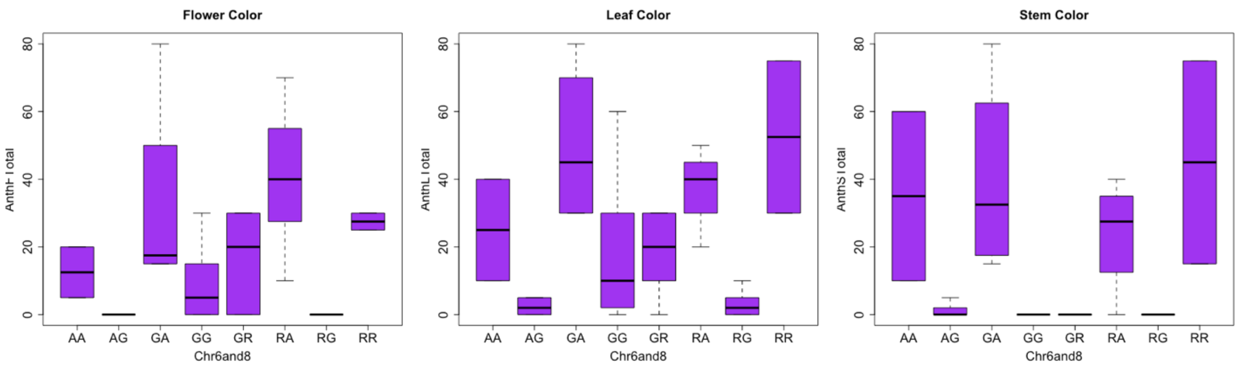


**Figure 3.8.** Combined SNP analysis of anthocyanin accumulation across chromosomes 6 and 8, depicting the phenotypic distribution based on genotype combinations within significant QTL regions. The x-axis represents different allele combinations with the first letter representing the IUPAC genotype on chromosome 6 and the second letter representing the IUPAC genotype on chromosome 8, while the y-axis indicates the corresponding anthocyanin totals for individuals of that genotype combination. Counts for each genetic combo are as follows: AA:**2**, AG:**17**, GA:**5**, GG:**145**, GR:**5**, RA:**7**, RG:**61**, and RR:**2**.

## Tables

**Table 3.1**. Significant Single Nucleotide Polymorphisms (SNPs) identified in regions associated with anthocyanin accumulation from two (BC2F2 and OP) populations.

| Trait | Chr. | Chr. Number | Position | P-value |
|---|---|---|---|---|
| **BC2F2 Flower (MLM.AnthFTotal)** | NC_044377.1 | 6 | 74546221 | 7.18E-07 |
| | NC_044377.1 | 6 | 74546249 | 7.18E-07 |
| | NC_044377.1 | 6 | 74893243 | 9.66E-07 |
| | NC_044377.1 | 6 | 74893275 | 9.66E-07 |
| | NC_044377.1 | 6 | 75779274 | 4.71E-07 |
| **BC2F2 Leaf (MLM.AnthLTotal)** | NC_044377.1 | 6 | 74546221 | 7.18E-07 |
| | NC_044377.1 | 6 | 74546249 | 7.18E-07 |
| | NC_044377.1 | 6 | 75779274 | 4.71E-07 |
| | NC_044377.1 | 6 | 75854965 | 7.80E-07 |
| | NC_044379.1 | 8 | 51902578 | 4.28E-07 |
| **BC2F2 Stem (MLM.AnthSTotal)** | NC_044379.1 | 8 | 33321766 | 7.13E-07 |
| | NC_044379.1 | 8 | 33321770 | 7.13E-07 |
| | NC_044379.1 | 8 | 47633295 | 4.72E-07 |
| | NC_044379.1 | 8 | 51902578 | 3.01E-08 |
| | NC_044379.1 | 8 | 52144012 | 7.10E-07 |
| | NC_044379.1 | 8 | 54982530 | 2.30E-09 |
| | NC_044379.1 | 8 | 54982532 | 2.30E-09 |
| | NC_044379.1 | 8 | 54982553 | 2.30E-09 |
| | NC_044379.1 | 8 | 54982678 | 2.43E-08 |
| **OP Flower (MLM.AnthFlower)** | NC_044374.1 | 5 | 6600131 | 3.56E-09 |
| | NC_044374.1 | 5 | 6600329 | 1.94E-09 |
| | NC_044374.1 | 5 | 6600353 | 3.56E-09 |
| | NC_044374.1 | 5 | 46427360 | 1.53E-08 |
| | NC_044374.1 | 5 | 46427362 | 1.53E-08 |
| | NC_044374.1 | 5 | 46427363 | 1.53E-08 |
| | NC_044374.1 | 5 | 46427371 | 1.53E-08 |
| | NC_044374.1 | 5 | 46427373 | 1.53E-08 |
| | NC_044374.1 | 5 | 46427377 | 1.53E-08 |
| | NC_044374.1 | 5 | 71299408 | 6.55E-09 |
| | NC_044374.1 | 5 | 71299409 | 6.55E-09 |
| | NC_044374.1 | 5 | 71299412 | 6.55E-09 |
| | NC_044374.1 | 5 | 71299413 | 6.55E-09 |
| | NC_044374.1 | 5 | 71299417 | 6.55E-09 |
| | NC_044374.1 | 5 | 71299441 | 1.27E-10 |
| | NC_044374.1 | 5 | 71299466 | 1.14E-07 |
| | NC_044377.1 | 6 | 72985550 | 2.91E-07 |
| | NC_044377.1 | 6 | 73045770 | 7.85E-08 |
| | NC_044377.1 | 6 | 73116553 | 9.87E-08 |
| | NC_044377.1 | 6 | 73328120 | 3.27E-09 |
| | NC_044377.1 | 6 | 74169147 | 1.70E-09 |
| | NC_044377.1 | 6 | 74180064 | 1.44E-08 |
| | NC_044377.1 | 6 | 74180678 | 5.67E-09 |
| | NC_044377.1 | 6 | 74181055 | 1.79E-08 |
| | NC_044377.1 | 6 | 74181199 | 3.90E-09 |

| | | | | |
|---|---|---|---|---|
| | NC_044377.1 | 6 | 74270448 | 1.17E-09 |
| | NC_044377.1 | 6 | 74292078 | 7.76E-09 |
| | NC_044377.1 | 6 | 74292726 | 2.03E-08 |
| | NC_044377.1 | 6 | 74308595 | 3.63E-07 |
| | NC_044377.1 | 6 | 74310904 | 5.09E-10 |
| | NC_044377.1 | 6 | 74322626 | 3.95E-08 |
| | NC_044377.1 | 6 | 74384868 | 1.33E-08 |

## Supplemental Tables

**Supplemental Table 3.1**. Annotated genes within quantitative trait locus (QTL) associated with anthocyanin accumulation on chromosomes 6. The table lists the reference sequence for the chromosome, start and end coordinates, and product information for each annotated gene within the specified regions on Chromosomes 6. Candidate gene in bold.

| Seqname | Start | End | Product |
|---|---|---|---|
| NC_044377.1 | 72984250 | 72988289 | ubiquitin recognition factor in ER-associated degradation protein 1 |
| NC_044377.1 | 72989609 | 72993205 | epimerase family protein SDR39U1 homolog%2C chloroplastic |
| NC_044377.1 | 72996104 | 72998519 | sec-independent protein translocase protein TatB%2C transcript variant X5 |
| NC_044377.1 | 73002419 | 73004761 | BURP domain protein USPL1%2C transcript variant X1 |
| NC_044377.1 | 73006141 | 73008524 | pentatricopeptide repeat-containing protein At4g21065 |
| NC_044377.1 | 73012637 | 73013467 | uncharacterized LOC115695469 |
| NC_044377.1 | 73029451 | 73035487 | kinesin-like protein KIN-7E%2C transcript variant X2 |
| NC_044377.1 | 73044825 | 73048604 | NADH dehydrogenase [ubiquinone] 1 beta subcomplex subunit 9 |
| NC_044377.1 | 73051719 | 73053679 | uncharacterized LOC115695470 |
| NC_044377.1 | 73053737 | 73054390 | 30S ribosomal protein S31%2C mitochondrial |
| NC_044377.1 | 73084475 | 73087604 | B-box zinc finger protein 19 |
| NC_044377.1 | 73089053 | 73091247 | fructose-bisphosphate aldolase 1%2C chloroplastic |
| NC_044377.1 | 73092500 | 73094859 | uncharacterized LOC115724514 |
| NC_044377.1 | 73111843 | 73116908 | endoglucanase 24 |
| NC_044377.1 | 73136890 | 73140901 | zinc finger protein GIS2%2C transcript variant X1 |
| NC_044377.1 | 73151308 | 73159701 | zinc finger CCCH domain-containing protein 19 |
| NC_044377.1 | 73169371 | 73171231 | uncharacterized LOC115695472 |
| NC_044377.1 | 73245797 | 73253515 | uncharacterized LOC115695473 |
| NC_044377.1 | 73265447 | 73267869 | uncharacterized LOC115695942%2C transcript variant X2 |
| NC_044377.1 | 73277136 | 73280314 | uncharacterized LOC115695236 |
| NC_044377.1 | 73290838 | 73292543 | GATA transcription factor 5 |
| NC_044377.1 | 73351466 | 73354764 | SH3 domain-containing protein 2 |
| NC_044377.1 | 73368271 | 73377142 | uncharacterized LOC115695474 |
| NC_044377.1 | 73381692 | 73389082 | squalene synthase 2%2C transcript variant X1 |
| NC_044377.1 | 73551707 | 73554626 | myosin-15%2C transcript variant X2 |
| NC_044377.1 | 73758129 | 73762139 | uncharacterized LOC115694792 |
| NC_044377.1 | 73773209 | 73776244 | stellacyanin-like |
| NC_044377.1 | 73821872 | 73822630 | uncharacterized LOC115695475 |
| NC_044377.1 | 73826394 | 73827550 | cucumber peeling cupredoxin |
| NC_044377.1 | 73842267 | 73843742 | putative pectinesterase 63 |
| NC_044377.1 | 73885664 | 73890779 | uncharacterized LOC115695477 |
| NC_044377.1 | 73891679 | 73893614 | uncharacterized LOC115695478 |
| NC_044377.1 | 73904317 | 73908121 | uncharacterized LOC115695479 |
| NC_044377.1 | 73908224 | 73911506 | uncharacterized LOC115695480 |
| NC_044377.1 | 73954484 | 73956077 | putative pectinesterase 63 |
| NC_044377.1 | 73977700 | 73979619 | cucumber peeling cupredoxin |
| NC_044377.1 | 74011708 | 74020632 | uncharacterized LOC115725502 |
| NC_044377.1 | 74038489 | 74050187 | WD repeat-containing protein 11 |
| NC_044377.1 | 74050049 | 74052667 | actin-related protein 6 |
| NC_044377.1 | 74122963 | 74124133 | uncharacterized LOC115725643 |

| | | | |
|---|---|---|---|
| NC_044377.1 | 74124217 | 74129644 | coiled-coil domain-containing protein 93%2C transcript variant X1 |
| NC_044377.1 | 74154579 | 74155972 | protein terminal ear1 homolog |
| NC_044377.1 | 74162590 | 74164680 | protein MEI2-like 6 |
| NC_044377.1 | 74179782 | 74182540 | THO complex subunit 5B%2C transcript variant X4 |
| NC_044377.1 | 74183062 | 74187019 | THO complex subunit 5A%2C transcript variant X1 |
| NC_044377.1 | 74203142 | 74206397 | uncharacterized LOC115724609%2C transcript variant X4 |
| NC_044377.1 | 74210461 | 74212531 | uncharacterized LOC115725317 |
| NC_044377.1 | 74214327 | 74219901 | uncharacterized LOC115725316%2C transcript variant X2 |
| NC_044377.1 | 74226991 | 74227942 | translation initiation factor IF-2-like |
| NC_044377.1 | 74243428 | 74245270 | B-box zinc finger protein 20 |
| NC_044377.1 | 74269267 | 74279067 | kinesin-like protein KIN-7D%2C mitochondrial |
| NC_044377.1 | 74290929 | 74294021 | D-ribulose kinase%2C transcript variant X1 |
| NC_044377.1 | 74295905 | 74300957 | probable inactive receptor kinase At3g08680%2C transcript variant X2 |
| NC_044377.1 | 74305083 | 74309618 | gem-associated protein 2 |
| NC_044377.1 | 74310641 | 74316062 | protein CHROMATIN REMODELING 35 |
| NC_044377.1 | 74317874 | 74323439 | coatomer subunit alpha-1%2C transcript variant X1 |
| NC_044377.1 | 74327376 | 74328293 | acidic leucine-rich nuclear phosphoprotein 32 family member B |
| NC_044377.1 | 74382077 | 74387262 | DNA replication licensing factor MCM4 |
| NC_044377.1 | 74394285 | 74402671 | V-type proton ATPase subunit a3 |
| NC_044377.1 | 74405882 | 74407838 | cysteine protease RD19A |
| NC_044377.1 | 74444592 | 74447803 | purple acid phosphatase 2 |
| NC_044377.1 | 74451694 | 74456755 | WD repeat-containing protein 13 |
| NC_044377.1 | 74465403 | 74467832 | chromatin remodeling protein SHL |
| NC_044377.1 | 74473368 | 74479122 | beta-galactosidase 5 |
| NC_044377.1 | 74485701 | 74494683 | RNA-binding protein 28%2C transcript variant X2 |
| NC_044377.1 | 74533765 | 74539727 | BEL1-like homeodomain protein 7%2C transcript variant X1 |
| NC_044377.1 | 74542227 | 74547473 | protein CHROMATIN REMODELING 35 |
| NC_044377.1 | 74554261 | 74564751 | putative B3 domain-containing protein At5g35780 |
| NC_044377.1 | 74561972 | 74564120 | probable rRNA-processing protein EBP2 homolog |
| NC_044377.1 | 74568690 | 74573951 | SUMO-activating enzyme subunit 2 |
| NC_044377.1 | 74574030 | 74575263 | uncharacterized LOC115725109 |
| NC_044377.1 | 74593941 | 74597045 | probable receptor-like protein kinase At4g39110 |
| NC_044377.1 | 74602074 | 74605498 | 26S proteasome regulatory subunit S10B homolog B |
| NC_044377.1 | 74607242 | 74611239 | bifunctional phosphatase IMPL2%2C chloroplastic%2C transcript variant X3 |
| NC_044377.1 | 74617419 | 74618210 | F-box protein At3g07870-like |
| NC_044377.1 | 74631494 | 74633064 | uncharacterized LOC115725633 |
| NC_044377.1 | 74637014 | 74638496 | embryogenic cell protein 40-like |
| NC_044377.1 | 74644788 | 74648437 | uncharacterized LOC115724948%2C transcript variant X1 |
| NC_044377.1 | 74662399 | 74663843 | protein CASPARIAN STRIP INTEGRITY FACTOR 2-like |
| NC_044377.1 | 74681563 | 74686496 | chaperone protein dnaJ 10 |
| NC_044377.1 | 74688289 | 74689967 | glutathione transferase GST 23 |
| NC_044377.1 | 74718980 | 74720457 | bZIP transcription factor 11 |
| NC_044377.1 | 74761481 | 74772156 | transcription factor TFIIIB component B'' homolog%2C transcript variant X1 |
| NC_044377.1 | 74779574 | 74779948 | circumsporozoite protein-like |
| NC_044377.1 | 74795530 | 74801355 | phosphatidylinositol/phosphatidylcholine transfer protein SFH8%2C transcript variant X2 |
| NC_044377.1 | 74801453 | 74806868 | phosphatidylinositol/phosphatidylcholine transfer protein SFH3%2C transcript variant X2 |

| | | | |
|---|---|---|---|
| NC_044377.1 | 74855965 | 74857131 | uncharacterized LOC115695487 |
| NC_044377.1 | 74874478 | 74876916 | |
| NC_044377.1 | 74887182 | 74889666 | AAA-ATPase At3g50940 |
| NC_044377.1 | 74891674 | 74893618 | H/ACA ribonucleoprotein complex subunit 4-like |
| NC_044377.1 | 74896177 | 74901364 | benzoate carboxyl methyltransferase |
| NC_044377.1 | 74942897 | 74964633 | 7-methylxanthosine synthase 1%2C transcript variant X2 |
| NC_044377.1 | 74990807 | 74992141 | benzoate carboxyl methyltransferase-like |
| NC_044377.1 | 75011830 | 75027198 | 7-methylxanthosine synthase 1-like |
| NC_044377.1 | 75051169 | 75054374 | theobromine synthase 2-like |
| NC_044377.1 | 75059036 | 75073167 | 7-methylxanthosine synthase 1-like |
| NC_044377.1 | 75105266 | 75138300 | 7-methylxanthosine synthase 1 |
| NC_044377.1 | 75158134 | 75159705 | uncharacterized LOC115695489 |
| NC_044377.1 | 75187922 | 75189943 | uncharacterized LOC115695490 |
| NC_044377.1 | 75218088 | 75226356 | uncharacterized LOC115695491 |
| NC_044377.1 | 75234852 | 75235770 | uncharacterized LOC115695492 |
| NC_044377.1 | 75254957 | 75256849 | uncharacterized LOC115695493 |
| NC_044377.1 | 75261048 | 75261728 | mediator of RNA polymerase II transcription subunit 9-like |
| NC_044377.1 | 75324740 | 75325237 | uncharacterized LOC115695495 |
| NC_044377.1 | 75366562 | 75368457 | uncharacterized LOC115695497 |
| NC_044377.1 | 75384323 | 75387404 | uncharacterized LOC115695498 |
| NC_044377.1 | 75387693 | 75388389 | uncharacterized LOC115695499 |
| **NC_044377.1** | **75409856** | **75419127** | **transcription factor MYB113** |
| NC_044377.1 | 75482934 | 75486178 | 7-methylxanthosine synthase 1-like%2C transcript variant X2 |
| NC_044377.1 | 75496650 | 75499393 | 7-methylxanthosine synthase 1 |
| NC_044377.1 | 75531975 | 75541238 | uncharacterized LOC115695757 |
| NC_044377.1 | 75592811 | 75593467 | uncharacterized LOC115695500 |
| NC_044377.1 | 75616748 | 75618861 | uncharacterized LOC115695501 |
| NC_044377.1 | 75619366 | 75623069 | uncharacterized LOC115695760%2C transcript variant X1 |
| NC_044377.1 | 75661305 | 75665353 | uncharacterized LOC115695504 |
| NC_044377.1 | 75668949 | 75670955 | G2/mitotic-specific cyclin C13-1%2C transcript variant X2 |
| NC_044377.1 | 75672199 | 75674316 | putative cyclin-A3-1 |
| NC_044377.1 | 75674424 | 75677170 | 7-methylxanthosine synthase 1 |
| NC_044377.1 | 75682148 | 75683814 | uncharacterized LOC115695506 |
| NC_044377.1 | 75706808 | 75708110 | hybrid signal transduction histidine kinase M |
| NC_044377.1 | 75738803 | 75766534 | peroxidase 15%2C transcript variant X1 |
| NC_044377.1 | 75772819 | 75776213 | peroxidase 15 |
| NC_044377.1 | 75777238 | 75781844 | histone-lysine N-methyltransferase ASHR1%2C transcript variant X3 |
| NC_044377.1 | 75782014 | 75785694 | formate--tetrahydrofolate ligase |
| NC_044377.1 | 75794647 | 75796002 | uncharacterized LOC115724731 |
| NC_044377.1 | 75795943 | 75803913 | uncharacterized LOC115695507 |
| NC_044377.1 | 75810828 | 75813380 | uncharacterized LOC115695671%2C transcript variant X1 |
| NC_044377.1 | 75819033 | 75821603 | E3 ubiquitin-protein ligase SINAT2%2C transcript variant X1 |
| NC_044377.1 | 75823818 | 75824307 | E3 ubiquitin-protein ligase SINAT2-like |
| NC_044377.1 | 75858127 | 75861372 | metal tolerance protein 4 |

**Supplemental Table 3.2**. Annotated genes within quantitative trait locus (QTL) associated with anthocyanin accumulation on chromosomes 8. The table lists the reference sequence for the chromosome, start and end coordinates, and product information for each annotated gene within the specified regions on Chromosomes 8. Candidate genes in bold.

| Seqname | Start | End | Product |
|---|---|---|---|
| NC_044379.1 | 51901047 | 51904135 | uncharacterized LOC115699498 |
| NC_044379.1 | 51920737 | 51925679 | calcium permeable stress-gated cation channel 1 |
| NC_044379.1 | 51926196 | 51930032 | uncharacterized membrane protein YuiD%2C transcript variant X2 |
| NC_044379.1 | 51938287 | 51942714 | condensin complex subunit 2 |
| NC_044379.1 | 51951025 | 51958560 | fatty acid hydroperoxide lyase%2C chloroplastic |
| NC_044379.1 | 51961679 | 51965018 | uncharacterized LOC115699570 |
| NC_044379.1 | 51967927 | 51970930 | uncharacterized LOC115700586 |
| NC_044379.1 | 51970922 | 51973907 | CCR4-NOT transcription complex subunit 9 |
| NC_044379.1 | 51987468 | 51995152 | cellulose synthase-like protein H1%2C transcript variant X2 |
| NC_044379.1 | 52024027 | 52025694 | uncharacterized LOC115700247 |
| NC_044379.1 | 52036176 | 52036940 | uncharacterized LOC115700248 |
| NC_044379.1 | 52037051 | 52043366 | cellulose synthase-like protein H1 |
| NC_044379.1 | 52046577 | 52059622 | DNA (cytosine-5)-methyltransferase 2-like%2C transcript variant X1 |
| NC_044379.1 | 52048900 | 52053718 | uncharacterized LOC115699180%2C transcript variant X1 |
| NC_044379.1 | 52064520 | 52069770 | uncharacterized LOC115699183%2C transcript variant X1 |
| NC_044379.1 | 52073886 | 52078575 | uncharacterized LOC115699184%2C transcript variant X2 |
| NC_044379.1 | 52082901 | 52085898 | protein usf |
| NC_044379.1 | 52129963 | 52132929 | probable WRKY transcription factor 31%2C transcript variant X1 |
| NC_044379.1 | 52140639 | 52144657 | aspartic proteinase A1 |
| NC_044379.1 | 52166710 | 52168151 | mitogen-activated protein kinase kinase kinase 18 |
| NC_044379.1 | 52181136 | 52183306 | S-type anion channel SLAH1 |
| NC_044379.1 | 52198621 | 52199205 | dirigent protein 2-like |
| NC_044379.1 | 52206237 | 52206822 | EG45-like domain containing protein |
| NC_044379.1 | 52209505 | 52213666 | chorismate mutase 2 |
| NC_044379.1 | 52227826 | 52229170 | S-type anion channel SLAH1-like |
| NC_044379.1 | 52245866 | 52248028 | B-cell receptor-associated protein 31 |
| NC_044379.1 | 52257375 | 52263302 | DNA repair protein RAD16%2C transcript variant X2 |
| NC_044379.1 | 52280049 | 52283270 | L-ascorbate oxidase homolog |
| NC_044379.1 | 52285053 | 52286438 | vacuolar-sorting receptor 3-like |
| NC_044379.1 | 52305740 | 52306777 | aquaporin SIP1-1-like |
| NC_044379.1 | 52323973 | 52329126 | arogenate dehydratase/prephenate dehydratase 1%2C chloroplastic%2C transcript variant X1 |
| NC_044379.1 | 52364432 | 52366378 | probable membrane metalloprotease ARASP2%2C chloroplastic |
| NC_044379.1 | 52373392 | 52374534 | uncharacterized LOC115700253 |
| NC_044379.1 | 52383700 | 52386654 | transcription factor MYB101 |
| NC_044379.1 | 52417350 | 52419706 | probable inactive serine/threonine-protein kinase scy2 |
| NC_044379.1 | 52440455 | 52441857 | 60S ribosomal protein L31 |
| NC_044379.1 | 52449313 | 52451518 | uncharacterized LOC115701575 |
| NC_044379.1 | 52451940 | 52455052 | histone acetyltransferase type B catalytic subunit |
| NC_044379.1 | 52475210 | 52477103 | autophagy-related protein 8C-like |

| | | | |
|---|---|---|---|
| NC_044379.1 | 52489668 | 52493790 | probable beta-1%2C3-galactosyltransferase 2%2C transcript variant X4 |
| NC_044379.1 | 52510440 | 52512202 | probable protein S-acyltransferase 7 |
| NC_044379.1 | 52530154 | 52535401 | protein RRP6-like 3%2C transcript variant X2 |
| NC_044379.1 | 52536324 | 52542385 | NEDD8-activating enzyme E1 regulatory subunit AXR1 |
| NC_044379.1 | 52545406 | 52546036 | uncharacterized LOC115698726 |
| NC_044379.1 | 52575513 | 52582389 | aconitate hydratase%2C cytoplasmic |
| NC_044379.1 | 52588930 | 52589880 | uncharacterized LOC115700256 |
| NC_044379.1 | 52590599 | 52591200 | uncharacterized LOC115701531 |
| NC_044379.1 | 52602607 | 52606175 | uncharacterized GPI-anchored protein At1g61900%2C transcript variant X1 |
| NC_044379.1 | 52617979 | 52618487 | uncharacterized LOC115700257 |
| NC_044379.1 | 52627830 | 52635773 | protein DETOXIFICATION 40 |
| NC_044379.1 | 52641229 | 52643021 | high mobility group B protein 3 |
| NC_044379.1 | 52643228 | 52646257 | 50S ribosomal protein L6%2C chloroplastic |
| NC_044379.1 | 52652581 | 52653078 | uncharacterized LOC115700258 |
| NC_044379.1 | 52661462 | 52665470 | glutamate receptor 3.7%2C transcript variant X1 |
| NC_044379.1 | 52687968 | 52693730 | glutamate receptor 3.5%2C transcript variant X1 |
| NC_044379.1 | 52698920 | 52700454 | uncharacterized LOC115700259 |
| NC_044379.1 | 52711806 | 52714393 | septum-promoting GTP-binding protein 1 |
| NC_044379.1 | 52714494 | 52716657 | uncharacterized LOC115700886 |
| NC_044379.1 | 52716782 | 52718968 | uncharacterized LOC115700885 |
| NC_044379.1 | 52719744 | 52721381 | sigma intracellular receptor 2 |
| NC_044379.1 | 52728392 | 52735653 | homeobox-leucine zipper protein HDG2%2C transcript variant X7 |
| NC_044379.1 | 52808464 | 52809677 | vascular-related unknown protein 1 |
| NC_044379.1 | 52819039 | 52819879 | uncharacterized LOC115700970 |
| NC_044379.1 | 52819911 | 52825301 | uncharacterized LOC115700260 |
| NC_044379.1 | 52832769 | 52833359 | uncharacterized LOC115700261 |
| NC_044379.1 | 52858501 | 52863867 | syntaxin-132 |
| NC_044379.1 | 52866286 | 52868825 | UDP-N-acetylglucosamine diphosphorylase 2 |
| NC_044379.1 | 52876064 | 52877430 | peroxidase 27 |
| NC_044379.1 | 52883536 | 52884324 | uncharacterized LOC115700264 |
| NC_044379.1 | 52892730 | 52894945 | protein translation factor SUI1 homolog 1 |
| NC_044379.1 | 52916880 | 52917807 | replication factor A protein 1-like |
| NC_044379.1 | 52918609 | 52919516 | MYB-like transcription factor ETC1 |
| NC_044379.1 | 52934560 | 52937334 | isocitrate lyase |
| NC_044379.1 | 52959833 | 52961435 | peroxidase 27 |
| NC_044379.1 | 52991183 | 52993125 | peroxidase 3 |
| NC_044379.1 | 53021220 | 53024835 | traB domain-containing protein |
| NC_044379.1 | 53029356 | 53034327 | zinc finger CCCH domain-containing protein 13%2C transcript variant X5 |
| NC_044379.1 | 53034403 | 53041320 | histone-lysine N-methyltransferase ATXR2%2C transcript variant X2 |
| NC_044379.1 | 53047674 | 53051085 | peroxisome biogenesis protein 22 |
| NC_044379.1 | 53064720 | 53065907 | cyclin-U1-1 |
| NC_044379.1 | 53066183 | 53072846 | SPX and EXS domain-containing protein 1%2C transcript variant X3 |
| NC_044379.1 | 53091445 | 53093685 | zinc finger protein CONSTANS-LIKE 12 |
| NC_044379.1 | 53100972 | 53104702 | uncharacterized LOC115700899 |
| NC_044379.1 | 53110357 | 53114364 | uncharacterized LOC115698969 |

| | | | |
|---|---|---|---|
| NC_044379.1 | 53124872 | 53127609 | uncharacterized LOC115698617%2C transcript variant X2 |
| NC_044379.1 | 53143643 | 53144568 | cysteine-rich repeat secretory protein 38 |
| NC_044379.1 | 53150731 | 53151714 | uclacyanin 1 |
| NC_044379.1 | 53171207 | 53173916 | transcription factor ILR3 |
| NC_044379.1 | 53193487 | 53193963 | extensin |
| NC_044379.1 | 53201560 | 53205083 | beta-amylase |
| NC_044379.1 | 53212943 | 53214532 | STOREKEEPER protein-like |
| NC_044379.1 | 53222604 | 53223488 | uncharacterized LOC115700269 |
| NC_044379.1 | 53223499 | 53224374 | uncharacterized LOC115700270 |
| NC_044379.1 | 53239640 | 53243040 | probable terpene synthase 9 |
| NC_044379.1 | 53249837 | 53254191 | serine/threonine-protein kinase MPS1%2C transcript variant X1 |
| NC_044379.1 | 53254596 | 53255968 | uncharacterized LOC115700634 |
| NC_044379.1 | 53257437 | 53258662 | transcription factor bHLH117 |
| NC_044379.1 | 53269417 | 53281409 | histone-lysine N-methyltransferase ATXR3%2C transcript variant X3 |
| NC_044379.1 | 53293303 | 53294662 | uncharacterized LOC115700271 |
| NC_044379.1 | 53302491 | 53303295 | uncharacterized LOC115698880 |
| NC_044379.1 | 53318161 | 53320562 | uncharacterized LOC115700272 |
| NC_044379.1 | 53323863 | 53325960 | scarecrow-like protein 32 |
| NC_044379.1 | 53334794 | 53338531 | BTB/POZ domain-containing protein At3g22104%2C transcript variant X1 |
| NC_044379.1 | 53346486 | 53348063 | 60S ribosomal protein L8-1-like |
| NC_044379.1 | 53352487 | 53354780 | probable mediator of RNA polymerase II transcription subunit 36b |
| NC_044379.1 | 53356338 | 53357819 | 60S ribosomal protein L8-1-like |
| NC_044379.1 | 53364266 | 53368502 | probable terpene synthase 11 |
| NC_044379.1 | 53385514 | 53387861 | xyloglucan endotransglucosylase/hydrolase protein 9 |
| NC_044379.1 | 53464082 | 53466095 | putative dehydration-responsive element-binding protein 2H |
| NC_044379.1 | 53490188 | 53491384 | fasciclin-like arabinogalactan protein 21 |
| NC_044379.1 | 53491802 | 53492854 | uncharacterized LOC115701517 |
| NC_044379.1 | 53497212 | 53499896 | putative F-box/FBD/LRR-repeat protein At4g03220 |
| NC_044379.1 | 53504586 | 53508116 | indole-3-acetic acid-amido synthetase GH3.6 |
| NC_044379.1 | 53540070 | 53540742 | calcium-binding protein KRP1 |
| NC_044379.1 | 53548258 | 53552386 | G-type lectin S-receptor-like serine/threonine-protein kinase At4g03230 |
| NC_044379.1 | 53568614 | 53579721 | G-type lectin S-receptor-like serine/threonine-protein kinase At4g03230 |
| NC_044379.1 | 53589129 | 53591296 | G-type lectin S-receptor-like serine/threonine-protein kinase At4g03230 |
| NC_044379.1 | 53597182 | 53598513 | G-type lectin S-receptor-like serine/threonine-protein kinase At4g03230 |
| NC_044379.1 | 53618570 | 53624597 | G-type lectin S-receptor-like serine/threonine-protein kinase At4g03230 |
| NC_044379.1 | 53640448 | 53652638 | G-type lectin S-receptor-like serine/threonine-protein kinase At4g03230 |
| NC_044379.1 | 53652401 | 53659929 | G-type lectin S-receptor-like serine/threonine-protein kinase At4g03230%2C transcript variant X3 |
| NC_044379.1 | 53653821 | 53654862 | uncharacterized LOC115700276 |
| NC_044379.1 | 53661148 | 53665254 | G-type lectin S-receptor-like serine/threonine-protein kinase At4g03230%2C transcript variant X2 |

| | | | |
|---|---|---|---|
| NC_044379.1 | 53672523 | 53675765 | G-type lectin S-receptor-like serine/threonine-protein kinase At4g03230 |
| NC_044379.1 | 53716327 | 53717628 | zinc finger protein CONSTANS-LIKE 1 |
| NC_044379.1 | 53729662 | 53733920 | uncharacterized LOC115699760%2C transcript variant X2 |
| NC_044379.1 | 53734432 | 53736331 | universal stress protein PHOS34%2C transcript variant X2 |
| NC_044379.1 | 53761117 | 53763515 | 5' exonuclease Apollo |
| NC_044379.1 | 53770344 | 53773483 | G-type lectin S-receptor-like serine/threonine-protein kinase At2g19130 |
| NC_044379.1 | 53779865 | 53782529 | G-type lectin S-receptor-like serine/threonine-protein kinase At2g19130 |
| NC_044379.1 | 53784064 | 53786902 | gene=LOC115701574 |
| NC_044379.1 | 53795315 | 53798075 | G-type lectin S-receptor-like serine/threonine-protein kinase At2g19130 |
| NC_044379.1 | 53826657 | 53828299 | transcription factor MYB14 |
| NC_044379.1 | 53867101 | 53869142 | transcription factor MYB14 |
| NC_044379.1 | 53890928 | 53893339 | putative cyclin-D6-1 |
| NC_044379.1 | 53915479 | 53917249 | tryptophan decarboxylase TDC2 |
| NC_044379.1 | 53933431 | 53936510 | equilibrative nucleotide transporter 3 |
| NC_044379.1 | 53937344 | 53939620 | uncharacterized GPI-anchored protein At4g28100 |
| NC_044379.1 | 53964223 | 53965881 | transcription factor MYB102 |
| **NC_044379.1** | **54001225** | **54002808** | **coumaroyl-CoA:anthocyanidin 3-O-glucoside-6''-O-coumaroyltransferase 2** |
| NC_044379.1 | 54018433 | 54023298 | diacylglycerol kinase 5%2C transcript variant X1 |
| NC_044379.1 | 54023533 | 54027100 | protein THYLAKOID FORMATION1%2C chloroplastic |
| NC_044379.1 | 54047250 | 54051184 | vesicle-associated protein 4-2%2C transcript variant X1 |
| NC_044379.1 | 54079378 | 54088322 | vacuolar sorting protein 18 |
| NC_044379.1 | 54088820 | 54092181 | pentatricopeptide repeat-containing protein At1g11900%2C transcript variant X1 |
| NC_044379.1 | 54095379 | 54099610 | external alternative NAD(P)H-ubiquinone oxidoreductase B1%2C mitochondrial |
| NC_044379.1 | 54101346 | 54103804 | uncharacterized LOC115701212 |
| NC_044379.1 | 54109185 | 54112955 | protein TIC 20-IV%2C chloroplastic |
| NC_044379.1 | 54113641 | 54116575 | probable galacturonosyltransferase 10 |
| NC_044379.1 | 54117806 | 54120467 | QWRF motif-containing protein 3 |
| NC_044379.1 | 54125667 | 54128280 | uncharacterized LOC115700746 |
| NC_044379.1 | 54128448 | 54129707 | uncharacterized LOC115700280 |
| NC_044379.1 | 54139003 | 54141483 | formimidoyltransferase-cyclodeaminase |
| NC_044379.1 | 54152168 | 54155971 | protein ULTRAPETALA 1 |
| NC_044379.1 | 54158846 | 54159333 | uncharacterized LOC115698660 |
| NC_044379.1 | 54161382 | 54163053 | uncharacterized LOC115700281 |
| NC_044379.1 | 54166349 | 54168433 | pentatricopeptide repeat-containing protein At1g03540 |
| NC_044379.1 | 54170925 | 54174617 | pentatricopeptide repeat-containing protein At1g73710 |
| NC_044379.1 | 54174734 | 54180244 | secretory carrier-associated membrane protein 1%2C transcript variant X3 |
| NC_044379.1 | 54180758 | 54188293 | protein STRUBBELIG-RECEPTOR FAMILY 3%2C transcript variant X2 |
| NC_044379.1 | 54204500 | 54205827 | uncharacterized LOC115701201 |
| NC_044379.1 | 54225838 | 54228982 | lipoyl synthase%2C mitochondrial |
| NC_044379.1 | 54240718 | 54244740 | uncharacterized LOC115698857 |
| NC_044379.1 | 54276191 | 54278991 | indole-3-acetic acid-amido synthetase GH3.10%2C transcript variant X2 |

| | | | |
|---|---|---|---|
| NC_044379.1 | 54313389 | 54316894 | mpv17-like protein |
| NC_044379.1 | 54322009 | 54322458 | putative cell wall protein |
| NC_044379.1 | 54325137 | 54330641 | probable protein phosphatase 2C 52 |
| NC_044379.1 | 54345012 | 54345881 | photosystem II repair protein PSB27-H1%2C chloroplastic |
| NC_044379.1 | 54371138 | 54374847 | uncharacterized LOC115699650 |
| NC_044379.1 | 54400687 | 54404400 | desmethylxanthohumol 6'-O-methyltransferase |
| NC_044379.1 | 54406494 | 54410379 | xanthohumol 4-O-methyltransferase |
| NC_044379.1 | 54418419 | 54422941 | ELMO domain-containing protein A%2C transcript variant X5 |
| NC_044379.1 | 54427662 | 54428965 | protein EPIDERMAL PATTERNING FACTOR 1 |
| NC_044379.1 | 54432470 | 54433174 | NDR1/HIN1-like protein 13 |
| NC_044379.1 | 54437775 | 54441954 | uncharacterized protein At4g04980 |
| NC_044379.1 | 54466656 | 54469766 | uncharacterized LOC115699009 |
| NC_044379.1 | 54483264 | 54485035 | LOB domain-containing protein 40 |
| NC_044379.1 | 54496322 | 54499084 | uncharacterized LOC115700284 |
| NC_044379.1 | 54499313 | 54500276 | L10-interacting MYB domain-containing protein-like |
| NC_044379.1 | 54520358 | 54526817 | NADPH-dependent diflavin oxidoreductase 1%2C transcript variant X1 |
| NC_044379.1 | 54530509 | 54531707 | 30S ribosomal protein 3%2C chloroplastic |
| NC_044379.1 | 54531936 | 54534316 | pinin%2C transcript variant X2 |
| NC_044379.1 | 54535064 | 54537634 | uncharacterized LOC115701520 |
| NC_044379.1 | 54539631 | 54544216 | ubiquitin receptor RAD23d |
| NC_044379.1 | 54592752 | 54595989 | cytokinin hydroxylase |
| NC_044379.1 | 54634395 | 54636343 | glutathione S-transferase DHAR2%2C transcript variant X1 |
| NC_044379.1 | 54656401 | 54678789 | protein SWEETIE%2C transcript variant X2 |
| NC_044379.1 | 54685210 | 54686382 | probable carboxylesterase 17 |
| NC_044379.1 | 54691977 | 54696892 | T-complex protein 1 subunit zeta 1 |
| NC_044379.1 | 54699842 | 54704732 | zinc finger CCCH domain-containing protein 17%2C transcript variant X1 |
| NC_044379.1 | 54707904 | 54710089 | uncharacterized protein DDB_G0275933 |
| NC_044379.1 | 54725426 | 54727989 | 14-3-3-like protein A%2C transcript variant X1 |
| **NC_044379.1** | **54728634** | **54732795** | **ultraviolet-B receptor UVR8** |
| NC_044379.1 | 54732756 | 54733888 | membrane protein PM19L |
| NC_044379.1 | 54734343 | 54736904 | RHOMBOID-like protein 9%2C chloroplastic%2C transcript variant X2 |
| NC_044379.1 | 54740785 | 54745544 | uncharacterized LOC115700494 |
| NC_044379.1 | 54748482 | 54758142 | thylakoid membrane protein slr0575 |
| NC_044379.1 | 54751165 | 54754503 | histone-lysine N-methyltransferase ASHH2-like |
| NC_044379.1 | 54759118 | 54762281 | transcription initiation factor TFIID subunit 3 |
| NC_044379.1 | 54764555 | 54769811 | uncharacterized LOC115700500 |
| NC_044379.1 | 54774852 | 54776132 | allene oxide cyclase%2C chloroplastic |
| NC_044379.1 | 54784220 | 54785234 | allene oxide cyclase%2C chloroplastic |
| NC_044379.1 | 54790508 | 54791820 | protein rough sheath 2 homolog |
| NC_044379.1 | 54802027 | 54803721 | protein rough sheath 2 homolog |
| NC_044379.1 | 54825267 | 54825835 | uncharacterized LOC115700966 |
| NC_044379.1 | 54876799 | 54878875 | transcription factor DICHOTOMA |
| NC_044379.1 | 54895175 | 54897532 | cyclin-B1-2 |
| NC_044379.1 | 54898959 | 54903190 | translation initiation factor eIF-2B subunit delta |
| NC_044379.1 | 54909712 | 54911764 | uncharacterized LOC115700287 |
| NC_044379.1 | 54922162 | 54924522 | probable transmembrane ascorbate ferrireductase 2 |
| NC_044379.1 | 54932829 | 54938655 | protein CROWDED NUCLEI 1 |
| NC_044379.1 | 54940010 | 54945827 | uncharacterized LOC115699494 |

| | | | |
|---|---|---|---|
| NC_044379.1 | 54952037 | 54952885 | uncharacterized LOC115700288 |
| NC_044379.1 | 54962743 | 54963625 | uncharacterized LOC115700867 |
| NC_044379.1 | 54971704 | 54974873 | tetraketide alpha-pyrone reductase 1%2C transcript variant X1 |

**Supplemental Table 3.3.** Raw data for anthocyanin accumulation in our $BC_2F2_2$ population. Data was collected across various tissue parts (Stems, Leaves, and Flowers), with ratings ranging from 0 to 3 based on tissue hue (0: green/no pigmentation, 1: lilac/pink, 2: magenta/reddish, and 3: purple/dark purple). Additionally, total percent anthocyanin coverage of the whole plant (AnthCoverage) was recorded. Total anthocyanin scores for flowers (AnthFTotal), leaves (AnthLTotal), and stems (AnthSTotal) were calculated by multiplying each tissue rating by AnthCoverage.

| Taxa | Anth Stem | Anth Leaf | Anth Flow | AnthCoverage | AnthFTotal | AnthLTotal | AnthSTotal |
|---|---|---|---|---|---|---|---|
| SK-1 | 2 | 0 | 0 | 2 | 0 | 0 | 4 |
| SK-2 | 0 | 0 | 0 | 0 | 0 | 0 | 0 |
| SK-3 | 0 | 0 | 0 | 0 | 0 | 0 | 0 |
| SK-4 | 0 | 0 | 0 | 0 | 0 | 0 | 0 |
| SK-6 | 0 | 3 | 2 | 25 | 50 | 75 | 0 |
| SK-7 | 2 | 3 | 0 | 30 | 0 | 90 | 60 |
| SK-8 | 0 | 2 | 2 | 15 | 30 | 30 | 0 |
| SK-9 | 0 | 1 | 1 | 10 | 10 | 10 | 0 |
| SK-10 | 2 | 2 | 1 | 20 | 20 | 40 | 40 |
| SK-11 | 3 | 3 | 1 | 25 | 25 | 75 | 75 |
| SK-13 | 0 | 2 | 0 | 2 | 0 | 4 | 0 |
| SK-14 | 0 | 1 | 0 | 1 | 0 | 1 | 0 |
| SK-16 | 2 | 3 | 2 | 25 | 50 | 75 | 50 |
| SK-17 | 0 | 2 | 0 | 15 | 0 | 30 | 0 |
| SK-18 | 0 | 2 | 1 | 20 | 20 | 40 | 0 |
| SK-19 | 1 | 3 | 2 | 25 | 50 | 75 | 25 |
| SK-20 | 0 | 1 | 1 | 10 | 10 | 10 | 0 |
| SK-21 | 1 | 1 | 1 | 10 | 10 | 10 | 10 |
| SK-22 | 0 | 0 | 0 | 0 | 0 | 0 | 0 |
| SK-23 | 0 | 0 | 0 | 0 | 0 | 0 | 0 |
| SK-24 | 0 | 1 | 0 | 2 | 0 | 2 | 0 |
| SK-25 | 0 | 1 | 0 | 2 | 0 | 2 | 0 |
| SK-26 | 0 | 0 | 0 | 0 | 0 | 0 | 0 |
| SK-27 | 2 | 3 | 3 | 35 | 105 | 105 | 70 |
| SK-28 | 0 | 1 | 1 | 2 | 2 | 2 | 0 |
| SK-29 | 0 | 2 | 2 | 10 | 20 | 20 | 0 |
| SK-30 | 0 | 0 | 1 | 2 | 2 | 0 | 0 |
| SK-31 | 0 | 2 | 1 | 10 | 10 | 20 | 0 |
| SK-32 | 3 | 3 | 1 | 40 | 40 | 120 | 120 |
| SK-35 | 1 | 2 | 0 | 2 | 0 | 4 | 2 |
| SK-36 | 1 | 0 | 0 | 2 | 0 | 0 | 2 |

| | | | | | | | |
|---|---|---|---|---|---|---|---|
| SK-37 | 0 | 2 | 2 | 5 | 10 | 10 | 0 |
| SK-38 | 3 | 3 | 2 | 50 | 100 | 150 | 150 |
| SK-39 | 2 | 1 | 0 | 2 | 0 | 2 | 4 |
| SK-40 | 2 | 2 | 2 | 40 | 80 | 80 | 80 |
| SK-41 | 0 | 3 | 2 | 35 | 70 | 105 | 0 |
| SK-42 | 0 | 2 | 1 | 15 | 15 | 30 | 0 |
| SK-43 | 0 | 1 | 1 | 5 | 5 | 5 | 0 |
| SK-44 | 0 | 1 | 1 | 5 | 5 | 5 | 0 |
| SK-45 | 0 | 1 | 0 | 10 | 0 | 10 | 0 |
| SK-46 | 0 | 0 | 0 | 0 | 0 | 0 | 0 |
| SK-47 | 1 | 1 | 0 | 2 | 0 | 2 | 2 |
| SK-48 | 0 | 0 | 0 | 0 | 0 | 0 | 0 |
| SK-49 | 0 | 2 | 1 | 10 | 10 | 20 | 0 |
| SK-50 | 0 | 1 | 0 | 5 | 0 | 5 | 0 |
| SK-51 | 1 | 2 | 1 | 10 | 10 | 20 | 10 |
| SK-52 | 0 | 2 | 1 | 15 | 15 | 30 | 0 |
| SK-53 | 0 | 2 | 0 | 2 | 0 | 4 | 0 |
| SK-54 | 1 | 3 | 2 | 40 | 80 | 120 | 40 |
| SK-57 | 1 | 1 | 0 | 1 | 0 | 1 | 1 |
| SK-58 | 1 | 1 | 0 | 5 | 0 | 5 | 5 |
| SK-59 | 1 | 1 | 0 | 2 | 0 | 2 | 2 |
| SK-60 | 1 | 2 | 0 | 5 | 0 | 10 | 5 |
| SK-61 | 0 | 1 | 1 | 5 | 5 | 5 | 0 |
| SK-62 | 0 | 1 | 0 | 2 | 0 | 2 | 0 |
| SK-63 | 0 | 1 | 0 | 2 | 0 | 2 | 0 |
| SK-64 | 0 | 1 | 0 | 2 | 0 | 2 | 0 |
| SK-65 | 0 | 0 | 0 | 0 | 0 | 0 | 0 |
| SK-67 | 0 | 2 | 2 | 15 | 30 | 30 | 0 |
| SK-68 | 1 | 1 | 0 | 2 | 0 | 2 | 2 |
| SK-69 | 0 | 1 | 0 | 5 | 0 | 5 | 0 |
| SK-70 | 3 | 2 | 2 | 30 | 60 | 60 | 90 |
| SK-71 | 3 | 3 | 2 | 40 | 80 | 120 | 120 |
| SK-72 | 0 | 2 | 0 | 10 | 0 | 20 | 0 |
| SK-73 | 0 | 0 | 0 | 0 | 0 | 0 | 0 |
| SK-74 | 0 | 1 | 1 | 5 | 5 | 5 | 0 |
| SK-75 | 0 | 2 | 0 | 5 | 0 | 10 | 0 |
| SK-76 | 0 | 2 | 2 | 15 | 30 | 30 | 0 |
| SK-77 | 0 | 1 | 0 | 2 | 0 | 2 | 0 |
| SK-78 | 0 | 1 | 0 | 2 | 0 | 2 | 0 |

| | | | | | | | |
|---|---|---|---|---|---|---|---|
| SK-79 | 0 | 1 | 0 | 1 | 0 | 1 | 0 |
| SK-80 | 0 | 0 | 0 | 0 | 0 | 0 | 0 |
| SK-81 | 0 | 1 | 0 | 5 | 0 | 5 | 0 |
| SK-82 | 0 | 2 | 1 | 15 | 15 | 30 | 0 |
| SK-83 | 1 | 3 | 2 | 25 | 50 | 75 | 25 |
| SK-84 | 0 | 2 | 2 | 15 | 30 | 30 | 0 |
| SK-85 | 1 | 3 | 2 | 30 | 60 | 90 | 30 |
| SK-86 | 0 | 1 | 0 | 5 | 0 | 5 | 0 |
| SK-87 | 0 | 1 | 0 | 1 | 0 | 1 | 0 |
| SK-91 | 1 | 2 | 0 | 5 | 0 | 10 | 5 |
| SK-92 | 0 | 0 | 0 | 0 | 0 | 0 | 0 |
| SK-93 | 0 | 2 | 0 | 10 | 0 | 20 | 0 |
| SK-94 | 0 | 2 | 0 | 5 | 0 | 10 | 0 |
| SK-96 | 0 | 2 | 2 | 20 | 40 | 40 | 0 |
| SK-97 | 0 | 2 | 1 | 15 | 15 | 30 | 0 |
| SK-98 | 0 | 1 | 0 | 5 | 0 | 5 | 0 |
| SK-99 | 0 | 2 | 2 | 10 | 20 | 20 | 0 |
| SK-100 | 0 | 2 | 1 | 2 | 2 | 4 | 0 |
| SK-101 | 1 | 2 | 2 | 10 | 20 | 20 | 10 |
| SK-102 | 1 | 1 | 0 | 2 | 0 | 2 | 2 |
| SK-103 | 2 | 2 | 1 | 5 | 5 | 10 | 10 |
| SK-108 | 0 | 2 | 1 | 5 | 5 | 10 | 0 |
| SK-111 | 0 | 2 | 2 | 10 | 20 | 20 | 0 |
| SK-112 | 1 | 3 | 2 | 25 | 50 | 75 | 25 |
| SK-113 | 0 | 3 | 1 | 20 | 20 | 60 | 0 |
| SK-114 | 0 | 0 | 0 | 0 | 0 | 0 | 0 |
| SK-115 | 0 | 1 | 0 | 5 | 0 | 5 | 0 |
| SK-116 | 2 | 0 | 0 | 2 | 0 | 0 | 4 |
| SK-117 | 0 | 0 | 0 | 0 | 0 | 0 | 0 |
| SK-118 | 0 | 0 | 0 | 0 | 0 | 0 | 0 |
| SK-119 | 0 | 1 | 0 | 1 | 0 | 1 | 0 |
| SK-120 | 0 | 0 | 0 | 0 | 0 | 0 | 0 |
| SK-121 | 1 | 3 | 3 | 25 | 75 | 75 | 25 |
| SK-122 | 0 | 2 | 1 | 15 | 15 | 30 | 0 |
| SK-123 | 0 | 0 | 1 | 2 | 2 | 0 | 0 |
| SK-124 | 0 | 2 | 2 | 10 | 20 | 20 | 0 |
| SK-125 | 0 | 1 | 1 | 5 | 5 | 5 | 0 |
| SK-126 | 0 | 2 | 2 | 15 | 30 | 30 | 0 |
| SK-127 | 3 | 2 | 1 | 20 | 20 | 40 | 60 |

| | | | | | | | |
|---|---|---|---|---|---|---|---|
| SK-129 | 1 | 2 | 1 | 15 | 15 | 30 | 15 |
| SK-131 | 0 | 0 | 0 | 0 | 0 | 0 | 0 |
| SK-132 | 0 | 1 | 0 | 1 | 0 | 1 | 0 |
| SK-133 | 0 | 1 | 0 | 2 | 0 | 2 | 0 |
| SK-134 | 0 | 2 | 0 | 20 | 0 | 40 | 0 |
| SK-135 | 0 | 0 | 0 | 0 | 0 | 0 | 0 |
| SK-136 | 0 | 1 | 1 | 10 | 10 | 10 | 0 |
| SK-137 | 1 | 3 | 2 | 20 | 40 | 60 | 20 |
| SK-138 | 0 | 1 | 1 | 10 | 10 | 10 | 0 |
| SK-139 | 0 | 2 | 1 | 10 | 10 | 20 | 0 |
| SK-140 | 0 | 2 | 2 | 15 | 30 | 30 | 0 |
| SK-141 | 0 | 0 | 0 | 0 | 0 | 0 | 0 |
| SK-142 | 1 | 1 | 0 | 5 | 0 | 5 | 5 |
| SK-143 | 0 | 2 | 1 | 10 | 10 | 20 | 0 |
| SK-144 | 0 | 2 | 1 | 5 | 5 | 10 | 0 |
| SK-145 | 0 | 1 | 0 | 2 | 0 | 2 | 0 |
| SK-146 | 0 | 2 | 2 | 15 | 30 | 30 | 0 |
| SK-147 | 2 | 2 | 2 | 15 | 30 | 30 | 30 |
| SK-148 | 0 | 2 | 1 | 10 | 10 | 20 | 0 |
| SK-149 | 0 | 2 | 1 | 10 | 10 | 20 | 0 |
| SK-150 | 0 | 1 | 0 | 1 | 0 | 1 | 0 |
| SK-151 | 1 | 2 | 1 | 25 | 25 | 50 | 25 |
| SK-152 | 3 | 2 | 2 | 15 | 30 | 30 | 45 |
| SK-156 | 3 | 2 | 1 | 15 | 15 | 30 | 45 |
| SK-157 | 1 | 1 | 0 | 5 | 0 | 5 | 5 |
| SK-158 | 0 | 1 | 0 | 2 | 0 | 2 | 0 |
| SK-159 | 0 | 2 | 2 | 20 | 40 | 40 | 0 |
| SK-160 | 1 | 1 | 0 | 5 | 0 | 5 | 5 |
| SK-161 | 1 | 3 | 1 | 30 | 30 | 90 | 30 |
| SK-162 | 0 | 1 | 1 | 5 | 5 | 5 | 0 |
| SK-163 | 1 | 2 | 2 | 15 | 30 | 30 | 15 |
| SK-164 | 0 | 1 | 0 | 5 | 0 | 5 | 0 |
| SK-165 | 0 | 2 | 0 | 15 | 0 | 30 | 0 |
| SK-166 | 0 | 0 | 0 | 0 | 0 | 0 | 0 |
| SK-169 | 0 | 1 | 0 | 5 | 0 | 5 | 0 |
| SK-170 | 0 | 1 | 0 | 2 | 0 | 2 | 0 |
| SK-171 | 0 | 2 | 1 | 15 | 15 | 30 | 0 |
| SK-172 | 0 | 0 | 1 | 2 | 2 | 0 | 0 |
| SK-173 | 2 | 1 | 0 | 10 | 0 | 10 | 20 |

| | | | | | | | |
|---|---|---|---|---|---|---|---|
| SK-174 | 0 | 1 | 1 | 5 | 5 | 5 | 0 |
| SK-175 | 0 | 1 | 1 | 5 | 5 | 5 | 0 |
| SK-176 | 0 | 0 | 0 | 0 | 0 | 0 | 0 |
| SK-177 | 0 | 0 | 0 | 0 | 0 | 0 | 0 |
| SK-178 | 0 | 1 | 0 | 2 | 0 | 2 | 0 |
| SK-179 | 1 | 0 | 0 | 1 | 0 | 0 | 1 |
| SK-180 | 0 | 0 | 0 | 0 | 0 | 0 | 0 |
| SK-181 | 0 | 0 | 0 | 0 | 0 | 0 | 0 |
| SK-182 | 1 | 0 | 0 | 2 | 0 | 0 | 2 |
| SK-183 | 0 | 1 | 0 | 2 | 0 | 2 | 0 |
| SK-184 | 0 | 2 | 1 | 10 | 10 | 20 | 0 |
| SK-185 | 1 | 2 | 1 | 15 | 15 | 30 | 15 |
| SK-186 | 0 | 0 | 0 | 0 | 0 | 0 | 0 |
| SK-187 | 2 | 2 | 1 | 10 | 10 | 20 | 20 |
| SK-188 | 0 | 2 | 0 | 10 | 0 | 20 | 0 |
| SK-189 | 1 | 3 | 1 | 20 | 20 | 60 | 20 |
| SK-190 | 0 | 1 | 0 | 2 | 0 | 2 | 0 |
| SK-191 | 0 | 1 | 0 | 2 | 0 | 2 | 0 |
| SK-192 | 1 | 2 | 1 | 15 | 15 | 30 | 15 |
| SK-193 | 0 | 0 | 0 | 0 | 0 | 0 | 0 |
| SK-194 | 0 | 1 | 0 | 2 | 0 | 2 | 0 |
| SK-195 | 0 | 0 | 0 | 0 | 0 | 0 | 0 |
| SK-196 | NA | NA | NA | NA | NA | NA | NA |
| SK-197 | 0 | 0 | 0 | 0 | 0 | 0 | 0 |
| SK-198 | 1 | 2 | 0 | 10 | 0 | 20 | 10 |
| SK-199 | 3 | 3 | 2 | 20 | 40 | 60 | 60 |
| SK-200 | 0 | 0 | 0 | 0 | 0 | 0 | 0 |
| SK-201 | 0 | 1 | 0 | 1 | 0 | 1 | 0 |
| SK-202 | 0 | 1 | 0 | 2 | 0 | 2 | 0 |
| SK-203 | 0 | 1 | 0 | 10 | 0 | 10 | 0 |
| SK-204 | 0 | 1 | 0 | 5 | 0 | 5 | 0 |
| SK-205 | 0 | 2 | 0 | 10 | 0 | 20 | 0 |
| SK-206 | 0 | 2 | 1 | 20 | 20 | 40 | 0 |
| SK-207 | 1 | 2 | 1 | 25 | 25 | 50 | 25 |
| SK-208 | 0 | 1 | 0 | 5 | 0 | 5 | 0 |
| SK-210 | 0 | 1 | 1 | 5 | 5 | 5 | 0 |
| SK-211 | 0 | 1 | 0 | 5 | 0 | 5 | 0 |
| SK-212 | 0 | 0 | 0 | 0 | 0 | 0 | 0 |
| SK-213 | 0 | 1 | 0 | 2 | 0 | 2 | 0 |

| | | | | | | | |
|---|---|---|---|---|---|---|---|
| SK-214 | 0 | 0 | 0 | 0 | 0 | 0 | 0 |
| SK-215 | 0 | 1 | 0 | 2 | 0 | 2 | 0 |
| SK-216 | 0 | 1 | 0 | 1 | 0 | 1 | 0 |
| SK-423 | 0 | 0 | 0 | 0 | 0 | 0 | 0 |
| SK-424 | 1 | 1 | 0 | 2 | 0 | 2 | 2 |
| SK-425 | 2 | 2 | 2 | 20 | 40 | 40 | 40 |
| SK-426 | 1 | 2 | 1 | 10 | 10 | 20 | 10 |
| SK-427 | 2 | 3 | 2 | 30 | 60 | 90 | 60 |
| SK-428 | 1 | 3 | 2 | 25 | 50 | 75 | 25 |
| SK-429 | 0 | 3 | 1 | 20 | 20 | 60 | 0 |
| SK-430 | 0 | 1 | 0 | 1 | 0 | 1 | 0 |
| SK-431 | 0 | 2 | 2 | 15 | 30 | 30 | 0 |
| SK-432 | 0 | 2 | 1 | 15 | 15 | 30 | 0 |
| SK-433 | 0 | 1 | 0 | 1 | 0 | 1 | 0 |
| SK-435 | 3 | 2 | 2 | 15 | 30 | 30 | 45 |
| SK-436 | 0 | 2 | 1 | 10 | 10 | 20 | 0 |
| SK-437 | 0 | 0 | 0 | 0 | 0 | 0 | 0 |
| SK-439 | 2 | 2 | 0 | 15 | 0 | 30 | 30 |
| SK-440 | 0 | 2 | 2 | 15 | 30 | 30 | 0 |
| SK-441 | 0 | 1 | 0 | 1 | 0 | 1 | 0 |
| SK-442 | 0 | 1 | 0 | 2 | 0 | 2 | 0 |
| SK-443 | 0 | 0 | 0 | 0 | 0 | 0 | 0 |
| SK-444 | 0 | 0 | 0 | 0 | 0 | 0 | 0 |
| SK-445 | 0 | 1 | 0 | 1 | 0 | 1 | 0 |
| SK-446 | 0 | 2 | 1 | 10 | 10 | 20 | 0 |
| SK-447 | 1 | 3 | 1 | 15 | 15 | 45 | 15 |
| SK-448 | 0 | 1 | 0 | 10 | 0 | 10 | 0 |
| SK-449 | 1 | 1 | 1 | 10 | 10 | 10 | 10 |
| SK-450 | 0 | 3 | 1 | 25 | 25 | 75 | 0 |
| SK-451 | 0 | 0 | 0 | 0 | 0 | 0 | 0 |
| SK-453 | 0 | 0 | 0 | 0 | 0 | 0 | 0 |
| SK-454 | 0 | 1 | 0 | 1 | 0 | 1 | 0 |
| SK-455 | 0 | 1 | 0 | 2 | 0 | 2 | 0 |
| SK-456 | 0 | 2 | 1 | 10 | 10 | 20 | 0 |
| SK-457 | 0 | 0 | 0 | 0 | 0 | 0 | 0 |
| SK-458 | 2 | 2 | 2 | 20 | 40 | 40 | 40 |
| SK-459 | 0 | 2 | 1 | 10 | 10 | 20 | 0 |
| SK-460 | 0 | 1 | 0 | 5 | 0 | 5 | 0 |
| SK-461 | 0 | 2 | 1 | 15 | 15 | 30 | 0 |

| | | | | | | | |
|---|---|---|---|---|---|---|---|
| SK-462 | 0 | 2 | 1 | 15 | 15 | 30 | 0 |
| SK-463 | 1 | 3 | 2 | 25 | 50 | 75 | 25 |
| SK-464 | 0 | 0 | 0 | 0 | 0 | 0 | 0 |
| SK-465 | 0 | 3 | 1 | 15 | 15 | 45 | 0 |
| SK-466 | 0 | 1 | 0 | 1 | 0 | 1 | 0 |
| SK-467 | 0 | 1 | 0 | 1 | 0 | 1 | 0 |
| SK-468 | 0 | 0 | 0 | 0 | 0 | 0 | 0 |
| SK-469 | 0 | 0 | 0 | 0 | 0 | 0 | 0 |
| SK-470 | 1 | 1 | 0 | 5 | 0 | 5 | 5 |
| SK-471 | 1 | 2 | 1 | 15 | 15 | 30 | 15 |
| SK-472 | 0 | 2 | 1 | 15 | 15 | 30 | 0 |
| SK-473 | 0 | 2 | 1 | 15 | 15 | 30 | 0 |
| SK-474 | 0 | 3 | 2 | 20 | 40 | 60 | 0 |
| SK-475 | 0 | 1 | 0 | 1 | 0 | 1 | 0 |
| SK-476 | 0 | 3 | 1 | 20 | 20 | 60 | 0 |
| SK-477 | 3 | 3 | 2 | 35 | 70 | 105 | 105 |
| SK-478 | 3 | 3 | 2 | 35 | 70 | 105 | 105 |
| SK-479 | NA | NA | NA | NA | NA | NA | NA |
| SK-481 | 0 | 1 | 0 | 1 | 0 | 1 | 0 |
| SK-482 | 0 | 1 | 1 | 2 | 2 | 2 | 0 |
| SK-483 | 0 | 0 | 1 | 2 | 2 | 0 | 0 |
| SK-484 | 0 | 0 | 0 | 0 | 0 | 0 | 0 |
| SK-485 | 0 | 0 | 0 | 0 | 0 | 0 | 0 |
| SK-486 | 0 | 2 | 1 | 15 | 15 | 30 | 0 |
| SK-487 | 0 | 2 | 1 | 15 | 15 | 30 | 0 |
| SK-488 | 0 | 2 | 0 | 10 | 0 | 20 | 0 |
| SK-489 | 0 | 2 | 1 | 10 | 10 | 20 | 0 |
| SK-490 | 0 | 2 | 2 | 15 | 30 | 30 | 0 |
| SK-491 | 3 | 0 | 0 | 5 | 0 | 0 | 15 |
| SK-492 | 0 | 0 | 0 | 0 | 0 | 0 | 0 |

**Supplemental Figure 3.4.** Data from our open-pollinated population used for QTL analysis. Inflorescence from each individual was phenotyped as a binary trait (0 = green, 1 = purple).

| Taxa | AnthFlower |
|---|---:|
| ID1-SK-BoxF-A1 | 0 |
| ID10-SK-BoxF-G2 | 0 |
| ID11-SK-BoxF-F2 | 0 |
| ID12-SK-BoxF-E2 | 0 |
| ID13-SK-BoxF-D2 | 0 |
| ID14-SK-BoxF-C2 | 0 |
| ID15-SK-BoxF-B2 | 0 |
| ID16-SK-BoxF-A2 | 0 |
| ID17-SK-BoxF-A3 | 0 |
| ID18-SK-BoxF-B3 | 0 |
| ID19-SK-BoxF-C3 | 0 |
| ID2-SK-BoxF-B1 | 0 |
| ID20-SK-BoxF-D3 | 0 |
| ID21-SK-BoxF-E3 | 0 |
| ID22-SK-BoxF-F3 | 0 |
| ID23-SK-BoxF-G3 | 0 |
| ID24-SK-BoxF-H3 | 0 |
| ID25-SK-BoxF-H4 | 0 |
| ID26-SK-BoxF-G4 | 0 |
| ID27-SK-BoxF-F4 | 0 |
| ID28-SK-BoxF-E4 | 0 |
| ID29-SK-BoxF-D4 | 0 |
| ID3-SK-BoxF-C1 | 0 |
| ID30-SK-BoxF-C4 | 0 |
| ID31-SK-BoxF-B4 | 0 |
| ID32-SK-BoxF-A4 | 0 |
| ID33-SK-BoxF-A5 | 0 |
| ID34-SK-BoxF-B5 | 0 |
| ID35-SK-BoxF-C5 | 0 |
| ID36-SK-BoxF-D5 | 0 |
| ID37-SK-BoxF-E5 | 0 |
| ID38-SK-BoxF-F5 | 0 |
| ID39-SK-BoxF-G5 | 0 |
| ID4-SK-BoxF-D1 | 0 |
| ID40-SK-BoxF-H5 | 0 |
| ID41-SK-BoxF-H6 | 0 |

| | |
|---|---|
| ID42-SK-BoxF-G6 | 0 |
| ID43-SK-BoxF-F6 | 0 |
| ID44-SK-BoxF-E6 | 0 |
| ID45-SK-BoxF-D6 | 0 |
| ID46-SK-BoxF-C6 | 0 |
| ID47-SK-BoxF-B6 | 0 |
| ID48-SK-BoxF-A6 | 0 |
| ID49-SK-BoxF-A7 | 1 |
| ID5-SK-BoxF-E1 | 0 |
| ID50-SK-BoxF-B7 | 1 |
| ID51-SK-BoxF-C7 | 1 |
| ID52-SK-BoxF-D7 | 1 |
| ID53-SK-BoxF-E7 | 1 |
| ID54-SK-BoxF-F7 | 1 |
| ID55-SK-BoxF-G7 | 1 |
| ID56-SK-BoxF-H7 | 1 |
| ID57-SK-BoxF-H8 | 1 |
| ID58-SK-BoxF-G8 | 1 |
| ID59-SK-BoxF-F8 | 1 |
| ID6-SK-BoxF-F1 | 0 |
| ID60-SK-BoxF-E8 | 1 |
| ID61-SK-BoxF-D8 | 1 |
| ID62-SK-BoxF-C8 | 1 |
| ID63-SK-BoxF-B8 | 1 |
| ID64-SK-BoxF-A8 | 1 |
| ID65-SK-BoxF-A9 | 1 |
| ID66-SK-BoxF-B9 | 1 |
| ID67-SK-BoxF-C9 | 1 |
| ID68-SK-BoxF-D9 | 1 |
| ID69-SK-BoxF-E9 | 1 |
| ID7-SK-BoxF-G1 | 0 |
| ID70-SK-BoxF-F9 | 1 |
| ID71-SK-BoxF-G9 | 1 |
| ID72-SK-BoxF-H9 | 1 |
| ID73-SK-BoxF-H10 | 1 |
| ID74-SK-BoxF-G10 | 1 |
| ID75-SK-BoxF-F10 | 1 |
| ID76-SK-BoxF-E10 | 1 |
| ID77-SK-BoxF-D10 | 1 |

| | |
|---|---|
| ID78-SK-BoxF-C10 | 1 |
| ID79-SK-BoxF-B10 | 1 |
| ID8-SK-BoxF-H1 | 0 |
| ID80-SK-BoxF-A10 | 1 |
| ID81-SK-BoxF-A11 | 1 |
| ID82-SK-BoxF-B11 | 1 |
| ID83-SK-BoxF-C11 | 1 |
| ID84-SK-BoxF-D11 | 1 |
| ID85-SK-BoxF-E11 | 1 |
| ID86-SK-BoxF-F11 | 1 |
| ID87-SK-BoxF-G11 | 1 |
| ID88-SK-BoxF-H11 | 1 |
| ID89-SK-BoxE-E9 | 1 |
| ID9-SK-BoxF-H2 | 0 |
| ID90-SK-BoxF-G12 | 1 |
| ID91-SK-BoxF-F12 | 1 |
| ID92-SK-BoxF-E12 | 1 |
| ID93-SK-BoxF-D12 | 1 |
| ID94-SK-BoxF-C12 | 1 |
| ID95-SK-BoxF-B12 | 1 |
| ID96-SK-BoxF-A12 | 1 |

## Chapter 3 References

Albert, N. W., Davies, K. M., Lewis, D. H., Zhang, H., Montefiori, M., Brendolise, C., Boase, M. R., Ngo, H., Jameson, P. E., & Schwinn, K. E. (2014). A conserved network of transcriptional activators and repressors regulates anthocyanin pigmentation in Eudicots. *Plant Cell*, *26*(3), 962–980. https://doi.org/10.1105/tpc.113.122069

Alappat, B., & Alappat, J. (2020). Anthocyanin pigments: Beyond aesthetics. In *Molecules* (Vol. 25, Issue 23). MDPI AG. https://doi.org/10.3390/molecules25235500

Bassolino, L., Buti, M., Fulvio, F., Pennesi, A., Mandolino, G., Milc, J., Francia, E., & Paris, R. (2020). In silico identification of myb and bhlh families reveals candidate transcription factors for secondary metabolic pathways in cannabis sativa L. *Plants*, *9*(11), 1–19. https://doi.org/10.3390/plants9111540

Bassolino, L., Fulvio, F., Pastore, C., Pasini, F., Gallina Toschi, T., Filippetti, I., & Paris, R. (2023). When Cannabis sativa L. Turns Purple: Biosynthesis and Accumulation of Anthocyanins. *Antioxidants*, *12*(7). https://doi.org/10.3390/antiox12071393

Chaves-Silva, S., Santos, A. L. dos, Chalfun-Júnior, A., Zhao, J., Peres, L. E. P., & Benedito, V. A. (2018). Understanding the genetic regulation of anthocyanin biosynthesis in plants – Tools for breeding purple varieties of fruits and vegetables. In *Phytochemistry* (Vol. 153, pp. 11–27). Elsevier Ltd. https://doi.org/10.1016/j.phytochem.2018.05.013

Dubos, C., Stracke, R., Grotewold, E., Weisshaar, B., Martin, C., & Lepiniec, L. (2010). MYB transcription factors in Arabidopsis. In *Trends in Plant Science* (Vol. 15, Issue 10, pp. 573–581). https://doi.org/10.1016/j.tplants.2010.06.005

Elshire, R.J., J.C. Glaubitz, Q. Sun, J.A. Poland, K. Kawamoto, et al. 2011. A Robust, Simple Genotyping-by-Sequencing (GBS) Approach for High Diversity Species. PLoS One 6(5): 19379. doi: 10.1371/JOURNAL.PONE.0019379.

Falcone Ferreyra, M. L., Rius, S. P., & Casati, P. (2012). Flavonoids: Biosynthesis, biological functions, and biotechnological applications. In *Frontiers in Plant Science* (Vol. 3, Issue SEP). Frontiers Research Foundation. https://doi.org/10.3389/fpls.2012.00222

Glaubitz, J.C., T.M. Casstevens, F. Lu, J. Harriman, R.J. Elshire, et al. 2014. TASSEL-GBS: A high capacity genotyping by sequencing analysis pipeline. PLoS One 9(2). doi: 10.1371/journal.pone.0090346.

Grassa, C. J., Weiblen, G. D., Wenger, J. P., Dabney, C., Poplawski, S. G., Timothy Motley, S., Michael, T. P., & Schwartz, C. J. (2021). A new Cannabis genome assembly associates elevated cannabidiol (CBD) with hemp introgressed into marijuana. *New Phytologist*, *230*(4), 1665–1679. https://doi.org/10.1111/nph.17243

Grassa, C. J., Wenger, J. P., Dabney, C., Poplawski, S. G., Motley, S. T., Michael, T. P., Schwartz, C. J., & Weiblen, G. D. (2018). *A complete Cannabis chromosome assembly and adaptive admixture for elevated cannabidiol (CBD) content*. https://doi.org/10.1101/458083

Haynes, W., Dubitzky, W., Wolkenhauer, O., Cho, KH., Yokota, H. (eds). 2013. Bonferroni Correction. Encycl. Syst. Biol. https://doi.org/10.1007/978-1-4419-9863-7_1213.

Jaakola, L. (2013). New insights into the regulation of anthocyanin biosynthesis in fruits. Trends in Plant Science, 18(9), 477-483.

Jones, C. M., Mes, P., & Myers, J. R. (2003). Characterization and Inheritance of the Anthocyanin fruit (Aft) Tomato. *Journal of Heredity*, *94*(6), 449–456. https://doi.org/10.1093/jhered/esg093

Kallam, K., Appelhagen, I., Luo, J., Albert, N., Zhang, H., Deroles, S., Hill, L., Findlay, K., Andersen, Ø. M., Davies, K., & Martin, C. (2017). Aromatic Decoration Determines the Formation of Anthocyanic Vacuolar Inclusions. *Current Biology*, *27*(7), 945–957. https://doi.org/10.1016/j.cub.2017.02.027

Khusnutdinov, E., Sukhareva, A., Panfilova, M., & Mikhaylova, E. (2021). Anthocyanin biosynthesis genes as model genes for genome editing in plants. In *International Journal of Molecular Sciences* (Vol. 22, Issue 16). MDPI. https://doi.org/10.3390/ijms22168752

Kliebenstein, D. J., Lim, J. E., Landry, L. G., & Last, R. L. (2002). Arabidopsis UVR8 regulates ultraviolet-B signal transduction and tolerance and contains sequence similarity to human Regulator of Chromatin Condensation 1. *Plant Physiology*, *130*(1), 234–243. https://doi.org/10.1104/pp.005041

Koo, Y., & Poethig, R. S. (2021). Expression pattern analysis of three R2R3-MYB transcription factors for the production of anthocyanin in different vegetative stages of Arabidopsis leaves. *Applied Biological Chemistry*, *64*(1). https://doi.org/10.1186/s13765-020-00584-0

Kundan, M., Gani, U., Fayaz, M., Angmo, T., Kesari, R., Rahul, V. P., Gairola, S., & Misra, P. (2022). Two R2R3-MYB transcription factors, CsMYB33 and CsMYB78 are involved in the regulation of anthocyanin biosynthesis in Cannabis sativa L. *Industrial Crops and Products*, *188*. https://doi.org/10.1016/j.indcrop.2022.115546

Kim, J., Lee, W. J., Vu, T. T., Jeong, C. Y., Hong, S. W., & Lee, H. (2017). High accumulation of anthocyanins via the ectopic expression of AtDFR confers significant salt stress tolerance in Brassica napus L. *Plant Cell Reports*, *36*(8), 1215–1224. https://doi.org/10.1007/s00299-017-2147-7

Kovinich, N., Kayanja, G., Chanoca, A., Riedl, K., Otegui, M. S., & Grotewold, E. (2014). Not all anthocyanins are born equal: distinct patterns induced by stress in Arabidopsis. *Planta*, *240*(5), 931–940. https://doi.org/10.1007/s00425-014-2079-1

Langmead, B., and S.L. Salzberg. 2012. Fast gapped-read alignment with Bowtie 2. Nat. Methods 9(4): 357–359. doi: 10.1038/nmeth.1923.

Li, H., Li, Y., Deng, H., Sun, X., Wang, A., Tang, X., Gao, Y., Zhang, N., Wang, L., Yang, S., Liu, Y., & Wang, S. (2018). Tomato UV-B receptor SlUVR8 mediates plant acclimation to UV-B radiation and enhances fruit chloroplast development via regulating SlGLK2. *Scientific Reports*, *8*(1). https://doi.org/10.1038/s41598-018-24309-y

Lin-Wang, K., Micheletti, D., Palmer, J., Volz, R., Lozano, L., Espley, R., Hellens, R. P., Chagnè, D., Rowan, D. D., Troggio, M., Iglesias, I., & Allan, A. C. (2011). High temperature reduces apple fruit colour via modulation of the anthocyanin regulatory complex. *Plant, Cell and Environment*, *34*(7), 1176–1190. https://doi.org/10.1111/j.1365-3040.2011.02316.x

Lipka, A.E., F. Tian, Q. Wang, J. Peiffer, M. Li, et al. 2012. GAPIT: Genome association and prediction integrated tool. Bioinformatics 28(18): 2397–2399. doi: 10.1093/bioinformatics/bts444.

Liu, Y., Lin-Wang, K., Espley, R. v., Wang, L., Yang, H., Yu, B., Dare, A., Varkonyi-Gasic, E., Wang, J., Zhang, J., Wang, D., & Allan, A. C. (2016). Functional diversification of the potato R2R3 MYB anthocyanin activators AN1, MYBA1, and MYB113 and their interaction with basic helix-loop-helix cofactors. *Journal of Experimental Botany*, *67*(8), 2159–2176. https://doi.org/10.1093/jxb/erw014

Maeda, H., & Dudareva, N. (2012). The shikimate pathway and aromatic amino acid biosynthesis in plants. In *Annual Review of Plant Biology* (Vol. 63, pp. 73–105). https://doi.org/10.1146/annurev-arplant-042811-105439

Millard, P. S., Kragelund, B. B., & Burow, M. (2019). R2R3 MYB Transcription Factors – Functions outside the DNA-Binding Domain. In *Trends in Plant Science* (Vol. 24, Issue 10, pp. 934–946). Elsevier Ltd. https://doi.org/10.1016/j.tplants.2019.07.003

Motamayor, J. C., Mockaitis, K., Schmutz, J., Haiminen, N., Livingstone, D., Cornejo, O., Findley, S. D., Zheng, P., Utro, F., Royaert, S., Saski, C., Jenkins, J., Podicheti, R., Zhao, M., Scheffler, B. E., Stack, J. C., Feltus, F. A., Mustiga, G. M., Amores, F., … Kuhn, D. N. (2013). The genome sequence of the most widely cultivated cacao type and its use to identify candidate genes regulating pod color. *Genome Biology*, *14*(6). https://doi.org/10.1186/gb-2013-14-6-r53

Naing, A. H., & Kim, C. K. (2021). Abiotic stress-induced anthocyanins in plants: Their role in tolerance to abiotic stresses. In *Physiologia Plantarum* (Vol. 172, Issue 3, pp. 1711–1723). Blackwell Publishing Ltd. https://doi.org/10.1111/ppl.13373

Neveu, V., Perez-Jiménez, J., Vos, F., Crespy, V., du Chaffaut, L., Mennen, L., Knox, C., Eisner, R., Cruz, J., Wishart, D., & Scalbert, A. (2010). Phenol-Explorer: an online comprehensive database on polyphenol contents in foods. *Database : The Journal of Biological Databases and Curation*, *2010*. https://doi.org/10.1093/database/bap024

Panche, A. N., Diwan, A. D., & Chandra, S. R. (2016). Flavonoids: An overview. In *Journal of Nutritional Science* (Vol. 5). Cambridge University Press. https://doi.org/10.1017/jns.2016.41

Singh, S., Kalia, P., Meena, R. K., Mangal, M., Islam, S., Saha, S., & Tomar, B. S. (2020). Genetics and Expression Analysis of Anthocyanin Accumulation in Curd Portion of Sicilian Purple to Facilitate Biofortification of Indian Cauliflower. *Frontiers in Plant Science*, *10*. https://doi.org/10.3389/fpls.2019.01766

Smeriglio, A., Barreca, D., Bellocco, E., & Trombetta, D. (2016). Chemistry, Pharmacology and Health Benefits of Anthocyanins. In *Phytotherapy Research* (pp. 1265–1286). John Wiley and Sons Ltd. https://doi.org/10.1002/ptr.5642

Tossi, V. E., Regalado, J. J., Iannicelli, J., Laino, L. E., Burrieza, H. P., Escandón, A. S., & Pitta-Álvarez, S. I. (2019). Beyond arabidopsis: Differential UV-B response mediated by UVR8 in diverse species. In *Frontiers in Plant Science* (Vol. 10). Frontiers Media S.A. https://doi.org/10.3389/fpls.2019.00780

UniProt Consortium. (n.d.). Entry Q9LR73 - Interleukin-18 receptor 1. UniProtKB. Retrieved March 29, 2024, from https://www.uniprot.org/uniprotkb/Q9LR73/entry

Xu, W., Dubos, C., & Lepiniec, L. (2015). Transcriptional control of flavonoid biosynthesis by MYB-bHLH-WDR complexes. In *Trends in Plant Science* (Vol. 20, Issue 3, pp. 176–185). Elsevier Ltd. https://doi.org/10.1016/j.tplants.2014.12.001

Xu, Z. S., Yang, Q. Q., Feng, K., Yu, X., & Xiong, A. S. (2020). DcMYB113, a root-specific R2R3-MYB, conditions anthocyanin biosynthesis and modification in carrot. *Plant Biotechnology Journal*, *18*(7), 1585–1597. https://doi.org/10.1111/pbi.13325

Zhang, P., & Zhu, H. (2023). Anthocyanins in Plant Food: Current Status, Genetic Modification, and Future Perspectives. In *Molecules* (Vol. 28, Issue 2). MDPI. https://doi.org/10.3390/molecules28020866

Zhou, L., He, Y., Li, J., Liu, Y., & Chen, H. (2019). CBFs Function in Anthocyanin Biosynthesis by Interacting with MYB113 in Eggplant (Solanum melongena L.). *Plant and Cell Physiology*, *61*(2), 416–426. https://doi.org/10.1093/pcp/pcz209